5-2015

Groundwater and Surface Water Contributions to Metals Loading in Bayhorse Creek at the Abandoned Ramshorn Mine Site Near Bayhorse, Idaho

Hannah L. McDonough
Utah State University

GROUNDWATER AND SURFACE WATER CONTRIBUTIONS TO METALS LOADING IN BAYHORSE CREEK AT THE ABANDONED RAMSHORN MINE SITE NEAR BAYHORSE, IDAHO

by

Hannah L. McDonough

A thesis submitted in partial fulfillments
of the requirements for the degree of

MASTER OF SCIENCE

in

Geology

Approved:

_____	_____
Thomas E. Lachmar Major Professor	William J. Doucette Committee Member
_____	_____
Peter T. Kolesar Committee Member	Mark R. McLellan Vice President for Research and Dean of the School of Graduate Studies

UTAH STATE UNIVERSITY
Logan, UT

2015

ABSTRACT

Groundwater and Surface Water Contributions to
Metals Loading in Bayhorse Creek at the
Abandoned Ramshorn Mine Site near Bayhorse, Idaho

by

Hannah L. McDonough, Master of Science

Utah State University, 2015

Major Professor: Dr. Thomas E. Lachmar
Department: Geology

Many abandoned mines in the United States are littered with waste metals that leach into watersheds and degrade habitats. Although metals-laden waters may appear pristine, fish bioaccumulate high concentrations of metals in their tissues, which create health risks if consumed by humans. This study examines the source and fate of metals in Bayhorse Creek near the abandoned Ramshorn mine outside of Challis, Idaho. In 2003, the U.S. Geological Survey found high levels of arsenic, cadmium, chromium, copper, lead, silver, and zinc in soils adjacent to the tailings pile. The Idaho Department of Environmental Quality authorized remediation to begin in summer 2011 without fully comprehending the source and fate of contaminants into the creek.

Metals loads were determined along the reach of Bayhorse Creek adjacent to the mine by measuring the flow rates of streams and groundwater seeps, and collecting water samples for chemical analysis. The chemical controls on metals mobility and attenuation in the surface and groundwater at the site were determined by computer modeling, a diffuse double-layer surface complexation model and the geochemical program PHREEQC.

Dissolved and suspended arsenic, copper, iron, manganese, lead, and zinc load the creek. The lowest site along the creek consistently measured as the highest load. Arsenic, copper, and lead loads were relatively insignificant compared to iron and manganese. The results indicate that 47% or more of the iron and manganese travel as metal-oxides, and arsenic and zinc tend to sorb to ferrous oxides. Large metals fluxes between SW-1 and SW-5 and at SW-8 suggest tailings and waste rock located between SW-1 and SW-5 and the slag pile adjacent to SW-8 are the main sources of metals contamination. Concentrations below the EPA drinking water standards and the absence of acidic pH indicate that the main metals loading consists of safe levels of iron, manganese, and zinc.

(180 pages)

PUBLIC ABSTRACT

Groundwater and Surface Water Contributions to
Metals Loading in Bayhorse Creek at the
Abandoned Ramshorn Mine Site near Bayhorse, Idaho

The U.S. Forest Service (USFS) and the Idaho Department of Environmental Quality (IDEQ) purchased property encompassing the abandoned Ramshorn mine to develop a state park. Because the abandoned copper-lead-silver mine was a potential hazard to the local creek and sediment, the IDEQ conducted several assessments to identify environmental risks. Between 2003 and 2006, the IDEQ completed a number of basic soil and water investigations in the location of mine waste. The IDEQ received investigation and cleanup funds through the EPA Comprehensive Environmental Response, Compensation, and Liability Act (CERCLA) program.

The USFS allocated $10,000 toward a two-year master's level project to determine a more complete analysis of the metals impact from the abandoned mine. I visited the project site for the extent of one flow season (July to October) to assess the metals concentrations within a creek that flows over the mine waste.

Water and sediment samples were collected and analyzed for metals content to isolate the main constituents and source of metals. The loads of metals entering the creek were calculated and used to identify the chemical behavior of the metals. The toxicity of the metals was evaluated from the chemical state and interpreted for human health issues.

Hannah McDonough

DEDICATION

In honor of Maggie Baker

for her vigor, intelligence, and appreciation for mining geology.

ACKNOWLEDGMENTS

I would like to express gratitude to my thesis advisor, Dr. Thomas E. Lachmar, for his guidance, persistence, and endurance in supporting me through this great endeavor. I would also like to thank Dr. Kolesar for his encouragement and geologic advice along the way. I would like to thank Dr. Doucette for providing me with a better understanding of aquatic chemistry and aiding with geochemical calculations.

I would also like to extend my thanks to the faculty and staff members, undergraduate, and graduate students in the Department of Geology. Multiple faculty and staff members provided me with logistical support. My peers assisted with sample processing and other technical support. I could not have done this without the help from the Utah State University Geology family.

Finally, I wish to thank my parents and sister for their support and encouragement throughout my study.

Hannah McDonough

CONTENTS

Page

LIST OF TABLES

LIST OF FIGURES

INTRODUCTION

Problem Statement

Environmental regulatory agencies, such as the U.S. Environmental Protection Agency (EPA), recognize abandoned mine lands as a common environmental problem. Toxic waste remaining from the mining process, including remnant ore and chemicals used in the mining process, contaminates the groundwater, surface water, soil, and atmosphere. The topic of mine remediation has been researched thoroughly by Alpers and Blowes (1994), Evangelou (1995), Salomons (1995), Evangelou and Zhang (1995), Gray (1996), Jambor and Blowes (1994, 1998), Banks et al. (1997), Nordstrom and Alpers (1999), and Keith and Vaughan (2000). Despite their work, effective remediation is yet to be implemented in many mines across the western U.S.

During hard rock mining, ore is extracted from vein pockets deep below the ground surface, exposing many toxic metals to open air. Once a mine is abandoned, groundwater pumping may also cease and water may fill into the mine workings (Banks et al., 1997). Water and oxygen interact with the minerals in the rocks at depth, commonly pyrite (FeS_2), thereby enhancing surface weathering processes (Motsi, 2010) and allowing metal ions to dissolve and acids to form (Langmuir, 1997). Metals display cationic behavior or are bound to an oxygen, which make them soluble in acid (Smith, 2007). The pH of groundwater decreases as the metals oxidize and sulfuric acid is produced, which increases the solubility of the metals in the natural water system. Tailings piles left behind from mining often contain high concentrations of heavy metals

and prolong the formation of acidic and toxic water. Although this occurs naturally, mining processes intensify and speed the reactions.

In addition to the lowering of the surface water pH, these non-biodegradable metals – including arsenic, cadmium, copper, iron, manganese, lead, and zinc – bioaccumulate to different degrees in fish species residing in surface waters that interact with contaminated mine waste. High concentrations of such toxic trace elements violate the Clean Water Act and pose a health risk to humans and damage the environment (Burk, 2004; Lachmar et al., 2006). Macroinvertebrates ingest the heavy metals, which become absorbed in their tissues. Higher species on the food chain become endangered after consuming the macroinvertebrates. Humans who consume fish or drink contaminated water may suffer chronic effects. While some metals such as chromium, cobalt, copper, iron, manganese, molybdenum, nickel, and zinc are essential to life and only toxic at high concentrations, other metals are non-essential and toxic at low concentrations (cadmium, lead, mercury) (Smith, 2007).

The EPA estimates that 40% of the headwaters in the U.S. have been degraded due to hard rock mining (USEPA, 2000). Under the National Environmental Protection Act (NEPA) regulations 43 CFR 3802 and 43 CFR 3809, mining companies must create a clean-up plan during the project proposal stage. However, hundreds of mines in the western U.S. were abandoned before remediation plans were required (Tordo et al., 2000). The EPA has listed many abandoned mine sites under the “Comprehensive Environmental Response, Compensation, and Liability Information System” (CERCLIS), which requires a site analysis and an assessment of the need for clean-up.

The Ramshorn mine site near Challis, Idaho was listed on the CERCLIS by the EPA in 2003 due to concerns of contamination in Bayhorse Creek, which runs along the toe of the tailings pile. The site was recommended for a "no further remedial action planned" (NFRAP) under the federal Superfund program after a Preliminary Assessment conducted by the Idaho Department of Environmental Quality (IDEQ) in July 2003 because water sampling did not exceed water quality standards indicating a non-immediate hazard. However, the site still falls under IDEQ regulations and shall be remediated accordingly with funding from the EPA Clean-Up Grant to insure public safety (IDEQ, 2003).

The Ramshorn mine was a silver mine that operated between 1868 and 1930, then intermittently until 1960, when the L & B Investment Company produced 275 tons of jig concentrate from mining waste (IDEQ, 2003). Activities ceased by 1978. Resulting slag and tailings piles, roughly 72,500 cubic yards in volume, slope down into Bayhorse Creek (IDEQ, 2003). Because the mine falls on state, federal, and private lands, the EPA and U.S. Forest Service (USFS) agreed to perform a collaborative Removal Site Evaluation (RSE) in 2009. The findings from the 2009 study show high concentrations of arsenic, lead, and other heavy metals within the tailings, which exceed the drinking water Regulatory Levels of 0.01 and 0.15 mg/L, respectively. Bayhorse Creek runs along the toe of the tailings pile and at least two groundwater seeps emerge from it and flow into the creek, further contributing to heavy metal pollution.

Three main Probable Points of Entry (PPE) for contaminant sources were identified by the IDEQ (Terragraphics, 2005). These PPEs include the tailings pile, slag (a mixture of metal oxides and silica) piles at the Bayhorse mill site, and a groundwater

adit drainage. These locations were sampled in my study. In the summer of 2009, the USFS relocated the creek to circumvent the tailings pile, therefore decreasing the surface water contamination that endangers Chinook salmon, steelhead trout, and Westslope cutthroat trout. However, a road leading up to a frequented campground nearly 3.2 km west of the mine site cuts through the tailings and poses danger to motorists and campers. Motorcycle and all-terrain vehicle tracks were observed on the tailings pile. Under EPA dictate, the USFS completed an in situ re-grading and cap remediation by August 2011.

Purpose and Objectives

This study of the abandoned Ramshorn mine examines the extent of contamination sourced from metals loading of groundwater and surface water in locations above and below the tailings pile. Determining the sources and concentrations of metals contamination helps to assess the effectiveness of, or necessity for, remediation; implementation of appropriate remediation requires knowledge of contaminants present and targeting point or non-point sources. Appropriate remediation may improve remediation efficiency and lower costs. Ultimately, the goal of this study is to determine the nature of the groundwater – surface water interactions and the potential influence of groundwater on contamination in Bayhorse Creek. These interactions are determined from the following studies:

1. Surface water discharge measurements of Bayhorse Creek and its tributary, Juliette Creek;
2. Surface water and groundwater hydrochemical analyses;
3. Tailings sediment mineralogical analyses;

4. Heavy metal analysis of creek bed sediments;

5. Geochemical modeling of water as it flows through the site and mixes with Bayhorse Creek.

Three factors influence the level of contamination from the metals loading in the creek: the mass loading, the toxicity, and the form of the metals. The toxicity of the metals is known; however, the mass loading and the metal speciation within the groundwater and surface water were not studied in great depth. The product of discharge (Q) times the metal concentration (C) equals the mass loading. The following measurements aided in mass loading calculations:

1. Measuring the surface water discharge rates at the upper and lower ends of the reach of Bayhorse Creek adjacent to the Ramshorn mine site, and all tributaries that flow into that reach.
2. Determining the rate of groundwater inflow or outflow by subtracting the discharge rates of the tributaries from the net change in the discharge rate of Bayhorse Creek.
3. Measuring the concentrations of metals in water samples taken at the surface water and groundwater discharge measurement sites.

My intentions are to determine the main source of metals loading into Bayhorse Creek; whether it is the groundwater flowing through the tailings pile, or the surface water that flows over the tailings and drains into the creek. Discharge and water sample analyses were needed to determine the source of metals.

Geochemical modeling, specifically the program PHREEQC (Parkhurst and Appelo, 2000), used these data to model metals speciation, one-dimensional transport

calculations involving reversible reactions, and inverse modeling to account for differences seen in water composition along the length of the study site. Surface water discharge measurements were taken upstream, downstream, and adjacent to the tailings pile. Groundwater discharge measurements were taken from at least two perennial seep locations. Dissolved and total metals concentrations were measured from surface water and groundwater seeps to determine the mass loading.

Data from water and soil samples taken by others in 2010 aided in an analysis of the changes in water chemistry after capping. Understanding the chemical and physical properties influencing the metal toxicity greatly improved the conceptual model of the Bayhorse Creek contamination. This study determines the effectiveness of cap remediation for this site, which may eventually be applied to other abandoned mine sites.

BACKGROUND

Location

The Ramshorn mine is located above the historic Bayhorse town site located at 44.406954N -114.363189W in the Salmon-Challis National Forest near Challis, Idaho. The upper workings of the Ramshorn mine lie at an elevation of 2,800 meters (9,200 feet) above mean sea level (amsl). Figure 1 shows the location of the Ramshorn mine within the state of Idaho.

Climate and Vegetation

The Bayhorse area does not possess climate records, but Challis, Idaho has climate records back to 1895. The region experiences a semi-arid climate, with high temperatures in July and August averaging 30° C (85° F), and with lows in December and January averaging -12° C (10° F). Such temperatures restricted mining activity to the summer months. The average annual snowfall recorded over the last 100 years amounts to 43 cm (17 in) with the highest accumulation rates during January and February. The average annual rainfall amounts to 20 cm (8 in) with the highest precipitation during May and June (WRCC, 1996). I expect to see high discharges in Bayhorse Creek during the spring and then decreasing discharges during the late summer and early fall.

Pine and aspen trees dominate the vegetation along the slopes near the field site. Hydrophilic plants, such as cottonwood trees and cattails, line the creeks. Meadows dotted with wildflowers that only bloom in late spring and early summer lie between the riparian zone and the steep talus slopes that form the sides of the valley.

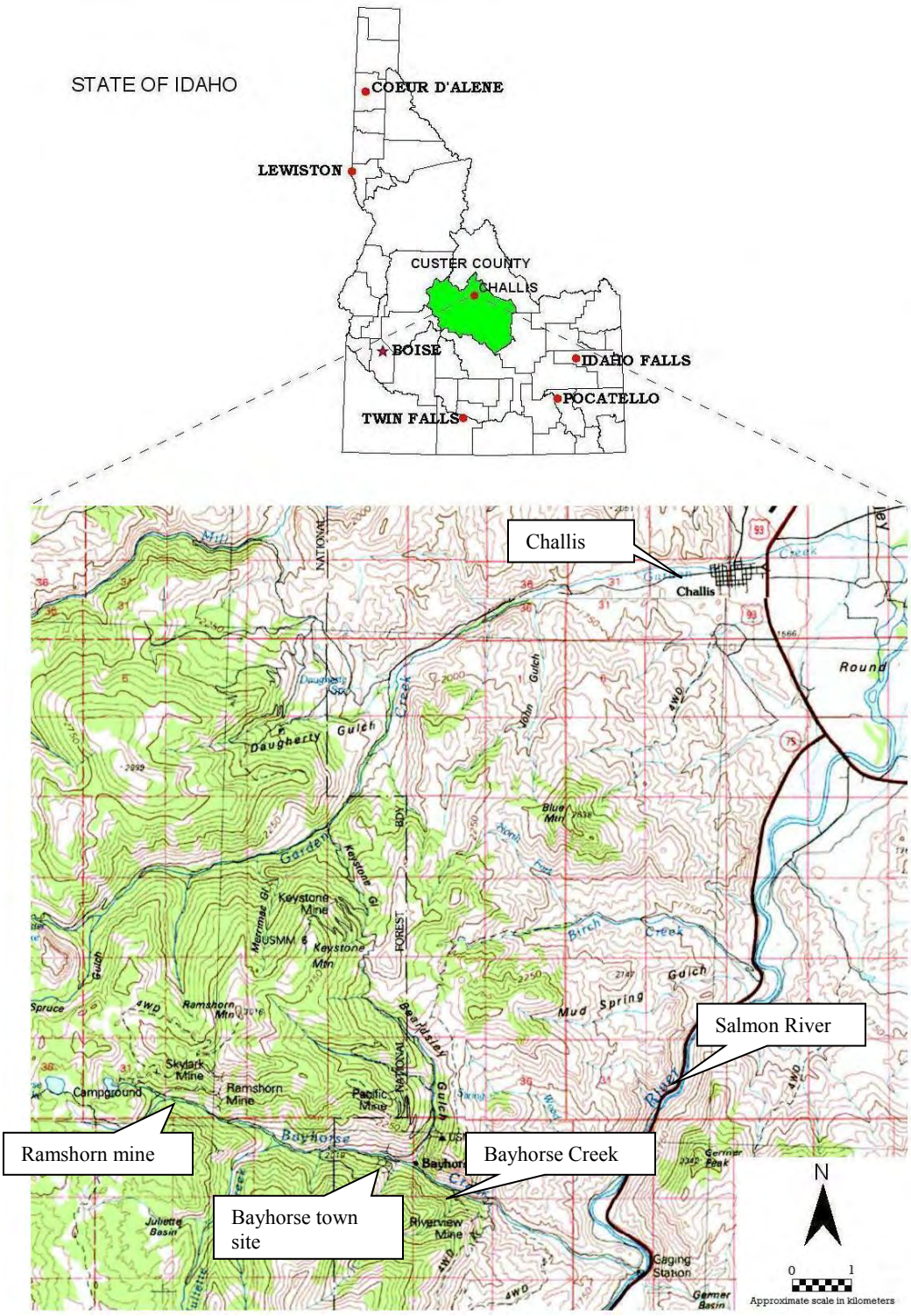

Figure 1: Location of the Ramshorn mine near Challis, Idaho (IDEQ, 2003).

An aerial photo (Figure 2) shows the relative abundance of vegetation on the north and south facing slopes of the mine site.

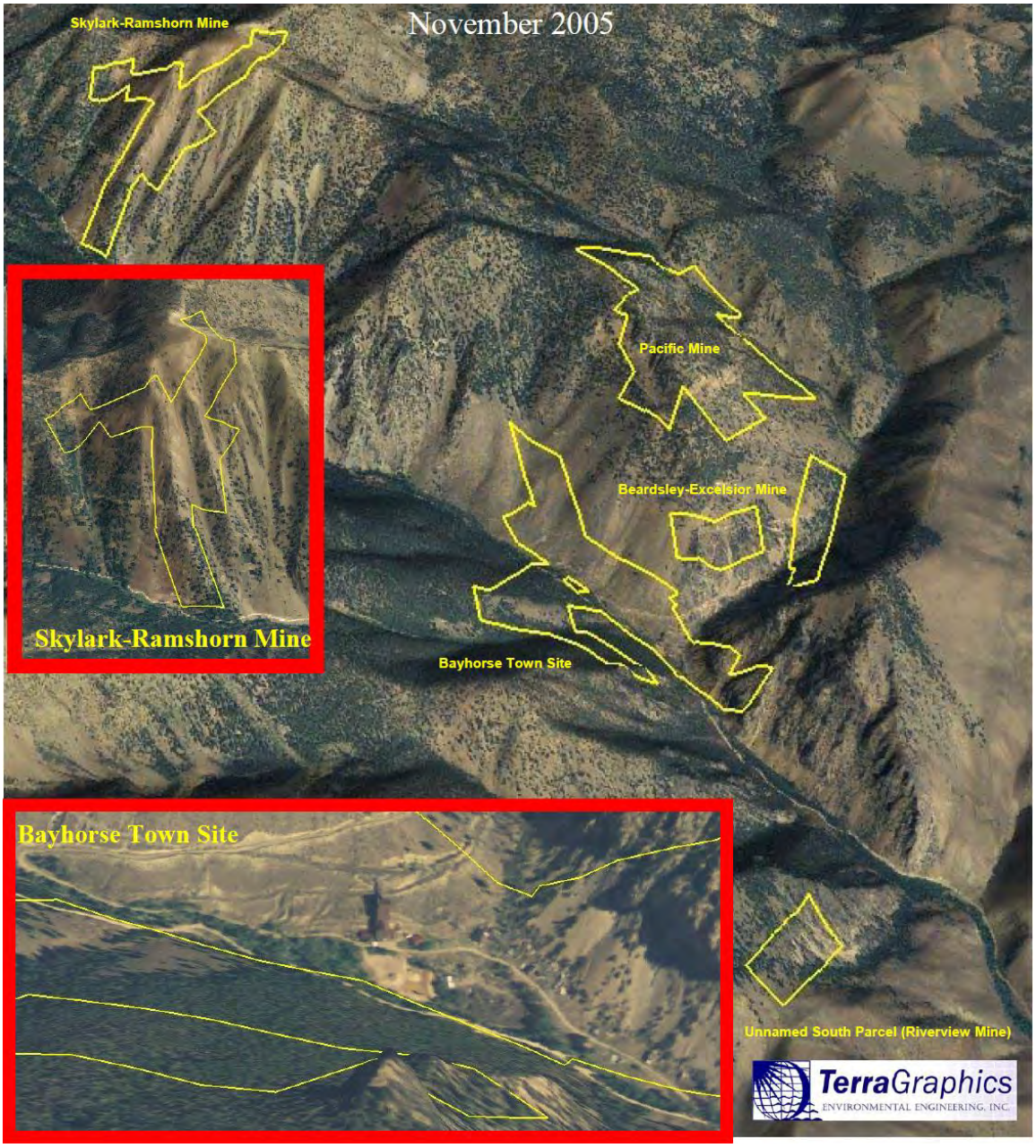

Figure 2. Aerial photo of the mine sites in the Bayhorse area, showing the relative abundance of vegetation (Terragraphics, 2005).

Geologic Setting

A large region of central Idaho is included in the Cordilleran fold and thrust belt and the Basin and Range province. The Bayhorse mining district falls in a region to the east of the Idaho batholith and the trans-Challis fault zone within the Sevier fold and thrust belt hinterland. The study area lies to the west of the Idaho-Wyoming fold and thrust belt, to the northeast of the Sawtooth Mountains in central Idaho, and to the north of the Snake River Plain.

Localized sedimentary strata were deposited directly onto the Wyoming craton during the Mesoproterozoic and the Neoproterozoic when modern Idaho existed as an intracratonic rift basin (Link and Janecke, 1999). Carbonate banks covered the region through most of the Paleozoic, during which the Antler orogeny formed basins and domes. More deformation occurred during the Pennsylvanian and Permian as the orogeny producing the ancestral Rockies activated inversion tectonics (Link and Janecke, 1999). Early Mesozoic Cordilleran deformation caused northeast vergent thrust faulting and folding, and was followed by the Cretaceous Sevier orogeny that caused shortening in an east-northeast to west-southwest orientation (Link and Janecke, 1999).

With the initiation of a subduction zone on the west coast, large reservoirs of magma formed at lower crustal depths, later cooling and crystallizing into the late Cretaceous Idaho batholith (100 Ma). The Idaho batholith causes much of the rugged topography in the region and extends nearly 320 km north to south and 120 km east to west. The batholith is made up of two main lobes: a northern lobe, called the Bitterroot lobe, and a southern lobe known as the Atlanta lobe. Heat and pressure from this granitic intrusion metamorphosed pre-existing Paleozoic sedimentary rock.

During the Eocene, the subducting Farallon plate steepened, which caused extension and thinning of the continental lithosphere and allowed volcanic activity to occur closer to the foreland (Coney, 1987; Wernicke, 1992). Numerous rifts and fissures in central Idaho allowed for the eruption of the Eocene Challis Volcanics. The magma that did not erupt lithified into the Casto pluton (50 Ma). Much of the mineralization seen within domes, faults, fractures, and plutons in this area is associated with the foreland volcanic activity (Link and Janecke, 1999). Fluid inclusion and stable isotope dating indicates that mineralization and intrusive activity were contemporaneous. Carbon dioxide-rich brines cooled and released CO_2 to form mineralized deposits (Seal and Rye, 1992).

The Salmon River, which flows over the Challis Volcanics, classifies as youthful because it has a steep gradient, steep tributaries and a V-shaped profile. It is believed to have begun incision at 2 Ma and it follows fault lines, which are at least 50 Ma. The canyon has been more recently shaped by Pleistocene glaciation.

Stratigraphy

The basal unit is the Cambrian Bayhorse Creek Dolomite (Ꞓd), overlain by the later Cambrian Garden Creek Phyllite (Ꞓg), which grades up into the upper Cambrian – lower Ordovician Bayhorse Dolomite (OꞒb). The Bayhorse Dolomite is divided into six smaller units that delineate six depositional environments. The dolomite is overlain unconformably by a thick unit of slate known as the Ordovician Ramshorn Slate (Or).

Both the Ramshorn and Skylark mines are located within the >600 m (2,000 ft) thick Ramshorn Slate unit. The slate is composed of metamorphosed shales, siltstones,

sandstones, and locally developed conglomerates (Seal and Rye, 1992). The slate contains roughly 40-60% quartz, 5-40% chlorite, and 30-40% muscovite, with lesser amounts of potassium feldspar. Biotite, cordierite, and andalusite are also important constituents of the Ramshorn Slate (Seal and Rye, 1992). Table 1 shows detailed unit descriptions of the stratigraphic column in the Bayhorse quadrangle (modified from Ross, 1937).

The Cambrian Bayhorse Creek Dolomite is very light gray to medium gray, fine to very fine grained, mostly massively bedded, with the thickness varying from 18-60 m (60-200 ft) where found along Bayhorse Creek. The dolomite grades up into the Garden Creek Phyllite. The type location is Garden Creek, which flows through Challis. The formation is confined only within the walls of the inner gorge of the creek. It shows a dark grey to black phyllite with abundant silvery sericite on cleavage surfaces. Bedding is crenulated and slightly calcareous. The formation is soft and weathers easily into flakes, which often form mobile talus piles.

The Bayhorse Dolomite sits above the phyllite. The formation crops out along the flank and crest of the local Bayhorse anticline. The dolomite is only found within the Bayhorse quadrangle and it disappears below the Challis Volcanics in the outward reaches of the quadrangle. Most of the formation is composed of a cliff-forming, thickly bedded dolomite. It displays a light creamy gray color but weathers into a darker rusty yellow. Some parts are more calcareous than others, while some parts contain nodules of dark chert that resembles pistolites. Much of the formation is comprised of a pure to fine crystalline dolomite with few calcite grains. The dolomite on the eastern flank of the anticline is interbedded with quartzite that contains fragments of dolomite. Some beds are

Table 1. Stratigraphic column (Ross, 1937).

Age	Formation	Description	Thickness (meters)
Recent	Landslides	Coarse and fine detritus	
Recent and Pleistocene	Alluvium	Sand, silt, and gravel	0 to hundreds
Wisconsinan	Late glacial deposits	Sand and gravel	Tens
Nebraskan	Early glacial deposits	Gravel	Locally tens to hundreds
Early Miocene or late Oligocene	Challis Volcanics	Germer tuffaceous member, with Yankee Fork rhyolite member in part interbedded with and in part overlying it, and basalt and basic andesite interbedded with and locally displacing it.	0 to several hundreds
		Latite-andesite member (where present, forms the lower part of the formation).	0 to several hundreds
Pennsylvanian	Wood River Fm	Impure quartzite, argillaceous and calcareous, and some limestone. A little conglomerate near the base.	2,500 ±
Upper Mississippian	Brazer Limestone	Generally dolomitic, rather massive; some chert. Local conglomerate.	600+
Mississippian and older	Milligan Fm	Argillite and argillaceous quartzite with impure dolomitic beds. Local beds of coarse grit to fine conglomerate. Most of the formation is characterized by much carbonaceous matter.	900±
Upper Devonian	Grand View Dolomite	Moderately dark with portions of light-colored well-bedded dolomite, in part quartzitic.	210

Table 1 (Cont.)

Age	Formation	Description	Thickness (meters)
Middle Devonian	Jefferson Dolomite	Dark dolomitic limestone	350
Middle Silurian	Laketown Dolomite	Moderately light colored dolomite. Locally a quartzite member thick enough to be mapped separately.	762±
	Trail Creek Fm	Brownish-gray calcareous argillite; some quartzite.	Neither top nor bottom exposed; probably several hundred
Upper Ordovician	Saturday Mtn Fm	Dark massive dolomite interbedded with argillite and shaly dolomite, in part carbonaceous.	1,500±
Middle Ordovician	Kinnikinic Quartzite	Massive light- colored quartzite with local lenses of dolomite and dolomitic shale, separately mapped; some conglomerate.	1,050±
Lower Ordovician	Ramshorn Slate	Dark thin-banded slate predominates, with argillite and argillaceous quartzite in the south.	600+
Cambrian	Bayhorse Dolomite	Generally massive thick-bedded dolomite, oolitic.	305+
	Garden Creek Phyllite	Intensely sheared and metamorphosed argillaceous rock.	No base exposed; at least several hundred
	Bayhorse Creek Dolomite	Light gray, massive, fine-grained dolomite.	18-60

up to 100 m (328 ft) thick and have fucoid markings. The places that show fucoidal quartzite may indicate the beach of a shallow marine environment. The depositional environment may have been inhabited by algae and similar organisms.

The Ramshorn Slate is the main formation that contains the Ramshorn mine. It extends roughly 3 to 8 km (2 to 5 mi) in width from Mill Creek to south of Clayton. The rock type consists of a thinly bedded argillaceous slate with well developed slaty cleavage that cuts through at high angles. The unit is underlain by a conglomerate that exceeds 150 m (500 ft) in thickness. The conglomerate contains fairly well rounded pebbles roughly 7 cm (3 in) in diameter of quartz and quartzite that sit within a siliceous matrix. A few interbeds of slate and quartzite cut through, although in thicknesses too small to be represented in a stratigraphic column. The slate ranges from a green to purple color with conspicuous bands nearly 1 cm (0.5 in) thick. Calcareous material creates a locally lighter color. All of the slate shows a well-defined slaty cleavage. The mineral make-up includes quartz, chlorite, serpentine, biotite and other micaceous minerals. Contact metamorphism has produced chiastolite and andalusite in several places. The slate has metamorphosed into a coarse-grained gray to black rock on weathered surfaces and is found on both sides of Juliette Creek. Umpleby (1917) estimated that the slate thickens up to 1,200 m (4,000 ft) in the thickest section based on an average dip of 35 degrees.

The Ramshorn Slate is overlain by the Kinnikinic Quartzite, which gradually grades up from a calcareous shale within the Ramshorn Slate into a sandy calcareous shale and finally into a true quartzite. The Kinnikinic Quartzite is found near Clayton, nearly 32 km (19 mi) south of Bayhorse. Most masses of the quartzite flank and crown

the major Bayhorse anticline along its course northward until the anticline becomes buried under Challis Volcanics. It is a well-bedded and nearly pure quartzite. While a few beds have a distinctive lavender color, the quartzite appears mostly white. Some outcrops are colored a bright red from the oxidation of flakes of specularite due to hydrothermal alteration. The rock is composed mainly of a mosaic of detrital quartz grains roughly 0.1 to 0.5 mm in diameter, which have been slightly enlarged due to formation of secondary silica. The grains are contained in a matrix of sericite. The calcareous beds are more argillaceous than the other bed types in the formation. The unit also contains lenticular lenses of impure dolostone. The beds are very irregular and show crenulation. Below the mouth of Bayhorse Creek, contorted quartzite beds dip at an average of 20 degrees. It is possible that the Kinnikinic Quartzite may be correlated to the Swan Peak Formation in northern Utah and southeastern Idaho.

The Saturday Mountain Formation is a black shaly dolomite that contains much carbonaceous material. Some beds contain rounded pebbles of quartzite, likely derived from the Kinnikinic Quartzite. Ripple marks are present in shaly beds in a few locations. The section shows a thickness of nearly 1,500 m (5,000 ft), but this is exaggerated due to crumpling and close folding. The unit contains 60-90 m (200-300 ft) zones of fissile calcareous shale. A fossil coral was discovered by Cook and Ehlers (1927), which indicates an upper Ordovician age. The horizon is equivalent to the Fish Haven dolomite in Utah and southeastern Idaho. The graptolite species found within the interbedded shales are upper Ordovician and dated earlier than any of the fauna found within the dolomite beds.

The Trail Creek Formation can be found in Malm Gulch, and presents a brownish gray calcareous argillite that breaks into thin slabs parallel to bedding. The calcite grains range from 0.02 to 0.05 mm in diameter and can be found among grains of quartz and plagioclase. Small chert lenses parallel bedding and veinlets of calcite extend several centimeters in width.

The Laketown Dolomite crops out on Lone Pine Peak, although small patches may also be seen near the Challis Volcanics Germer member. Most of the rock is a thickly bedded bluish gray dolomitic limestone, which weathers into a rusty color. Some beds have been oxidized into a bright red shade. Some of the dolomite is sandy and locally some shale beds are present. Quartzite is interbedded with some of the dolomite. Fossil records suggest that this formation is equivalent in age to the type locality of the Laketown Formation.

The Jefferson Dolomite has a name derived from the Jefferson Limestone in Montana, which shows similar features. The rock is a dolomite, and is best exposed along Grand View Canyon where it is believed to be a buildup of reefs. Most of the beds are a dark blue to gray colored dolomite with no calcite. The formation includes a few coarser sandy beds and a few lighter colored beds. It is distinguishable because of its blue color and it crops out with an abundance of digitate favosites. Its thickness is roughly 350 m (1,150 ft).

The Grand View Dolomite is found in Grand View Canyon, which lies to the southeast of Challis, ID. The Grand View Dolomite is upper or middle Devonian in age. Its thickness ranges up to 210 m (690 ft) with light colored beds in the upper 200 m (660 ft). It consists of thick dolomite beds that range in color from dark microgranular grey to

light colored sandy intervals and overlies the Jefferson Dolomite. In places, the Jefferson contains 210 m (690 ft) of a lithology indistinguishable from the Grand View Dolomite. These formations have been classified together by Hobbs et al. (1991).

The Milligan Formation was first identified in the Wood River region, and crops out in the Bayhorse quadrangle. The formation is broken up by Challis Volcanics, but similar lithologies allow for correlation. Most of the unit is a black carbonaceous argillite. It is moderately soft and cleaves into thin plates parallel to bedding. Little of the carbonaceous material has been metamorphosed. Interbedded quartzite and limestone account for a small percentage of the thickness of the formation. A thickness of roughly 900 m (3,000 ft) has been estimated, but deformation and size variations between outcrops make accurate measurements difficult. The age has been recorded as Mississippian, with the possibility of extending back into the Devonian.

The Brazer Limestone is a massive magnesian limestone that is dark gray, but in some places nearly white, while in others nearly black. Chert nodules, bands and lenses occur in the lower part of the formation. The limestone is crenulated and shows many structural irregularities. The thickness is roughly 600 m (2,000 ft) in the Bayhorse quadrangle. Umpleby (1917) estimated that similar beds in the area may have thicknesses of 1,800 m (6,000 ft). The fossils support the idea that the formation is upper Mississippian and it has been postulated by Ross (1937) that the Madison Formation, which occurs abundantly to the east, may be equivalent to the Brazer.

The Wood River Formation, unlike many of the others found in the Bayhorse quadrangle, correlates well with the stratigraphy in the Stanley basin. Some of the rocks in this formation have undergone contact metamorphism. The less metamorphosed rocks

are a gray to black quartzite with carbonaceous material mostly contributing to the color. The quartzite is mostly argillaceous with thinly spaced shaly textured layers in between. Many of these beds appear massive; however, closer inspection reveals faint cross-bedding and finer banding. A small percentage of the formation includes limestone beds. Conglomerate occurs in several localities at or near the base of the Wood River Formation. The pebbles are mostly quartz and quartzite, and the matrix is somewhat impure and is less resistant to weathering. Wollastonite and diopside occur in metamorphosed areas. Individual beds range from a few centimeters to 4.5 m (15 ft) thick. Fossils found in the unit confirm its age as Pennsylvanian.

The Permian Casto Volcanics are thought to be older than the Challis Volcanics because they have been altered by intrusive Tertiary granite. They extend laterally for about 500 km^2 (180 mi^2), and are thought to correlate with the Permian Phosphoria unit found in other parts of the northwest.

The Mesozoic section is entirely missing from the Bayhorse quadrangle because of the intrusions from the Idaho batholith during this era.

Challis Volcanics comprise a thick and widespread formation that varies laterally, but contains diagnostic features characteristic only of itself, which implies one common magma source. Three different members can be distinguished; the latite-andesite member, the Germer member, and the Yankee Fork rhyolite member.

The latite-andesite member is the oldest and lowest of the Challis volcanic flows. It is more abundant than the Germer or Yankee Fork members in most locations other than the Bayhorse quadrangle, where it is less prominent than the Germer member. It is composed of breccias, flows, and ignimbrite.

The Germer member overlies the latite-andesite member and dominates in the Bayhorse region. These are basaltic and andesitic flows that intercalate with tuffaceous layers. Most of the flows are fine-grained, light colored, and studded with small phenocrysts. The color is sometimes a shade of purple or lavender. The phenocrysts are mostly oligoclase. Some of the flows are over 90 m (300 ft) thick, although they may be absent in other locations. Some tuff layers show a water-sorted grading, though most are massive. The tuff shows remnants of vegetation such as wood fragments, logs, stumps, and leaves of trees that were covered by the volcanic ash. The preserved trees are larger than any modern-day trees, suggesting a milder climate during the Eocene. Basalt and locally interbedded calcic andesite are more abundant in the Bayhorse quadrangle than in any other area of the Challis Volcanics.

The Yankee Fork rhyolite member lies above the basaltic layer within the Germer member and can be seen in the Casto quadrangle. The first flow of rhyolite includes phenocrysts of smoky quartz within a groundmass of crystalline texture. The second flow of rhyolite is a light color with crystalline appearance and some local brecciation.

Unconsolidated clastic sediments make up the Quaternary units in the Bayhorse region. Early Pleistocene deposits related to glaciation have been reported. Thick deposits of gravel are grouped as older alluvium. The undissected and unconsolidated alluvium is referred to as younger alluvium. Landslides and talus piles are common in this region. There are numerous terrace remnants on the steep slopes near the Salmon River, depicting older river channels. A thicker cover of soil and vegetation lies on the south side of Bayhorse Creek than on the north side. Travertine, Pleistocene in age, covers a small portion of the Bayhorse quadrangle.

Structure

The Ramshorn mine sits within a north-northwestward trending anticline, which folds lower Paleozoic carbonates and pelites (Seal and Rye, 1992). According to Ross (1937), the Bayhorse anticline is "the largest and longest anticline in the northern part of Idaho." Figures 3 and 4 show geologic units displayed in a map view and geologic cross section, respectively.

Within the Bayhorse anticline, the Paleozoic rocks in the Bayhorse quadrangle show secondary folds that are double-kink folds. The folds are disturbed by granitic intrusions from the Idaho batholith and a thrust fault near Clayton. There are at least two other anticlines to the southeast. The Bayhorse anticline extends from the east fork of the Salmon River southeastward to the Hailey quadrangle. It is a broad, gentle fold with a nearly flat top that exposes the oldest rocks in the area. Both the Bayhorse Dolomite and the conglomerate overlying the fold strongly conform and dip steeply. Ross (1937) interprets the unusual rectangular geometry of the Bayhorse anticline as pinning of the top as compression acted on the flanks. Pinning by a magma body during the intrusion of the Idaho batholith could create such a mechanism. However, more recent interpretations suggest a double-kink fold within the weaker shale and phyllite units.

The Ramshorn Slate near Juliette Creek has been much disturbed due to contact metamorphism from granodiorite and tends to conform in strike to the shape of the intrusion. In the southern part of this region, dolomite shows brecciation due to sharp overturning of the fold.

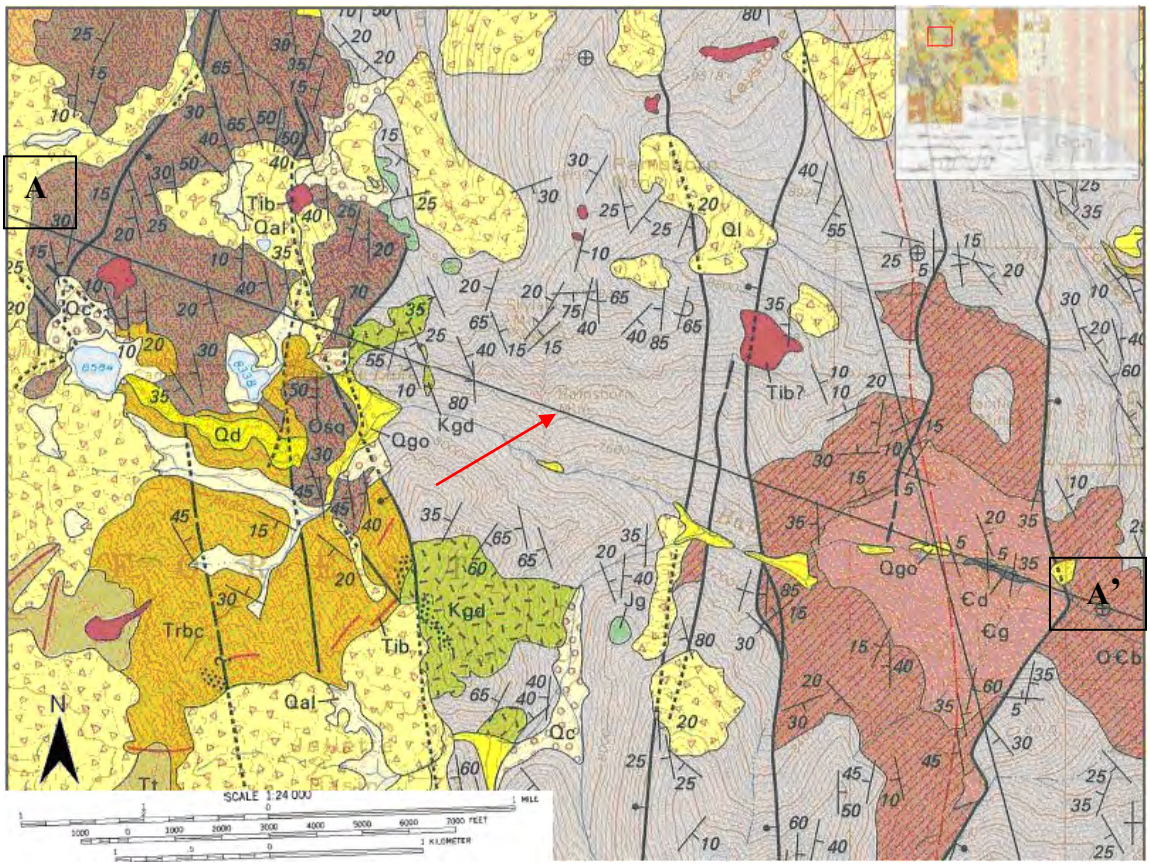

Figure 3. Geologic map showing the Ramshorn mine, indicated by the red arrow (Hobbs et al., 1991).

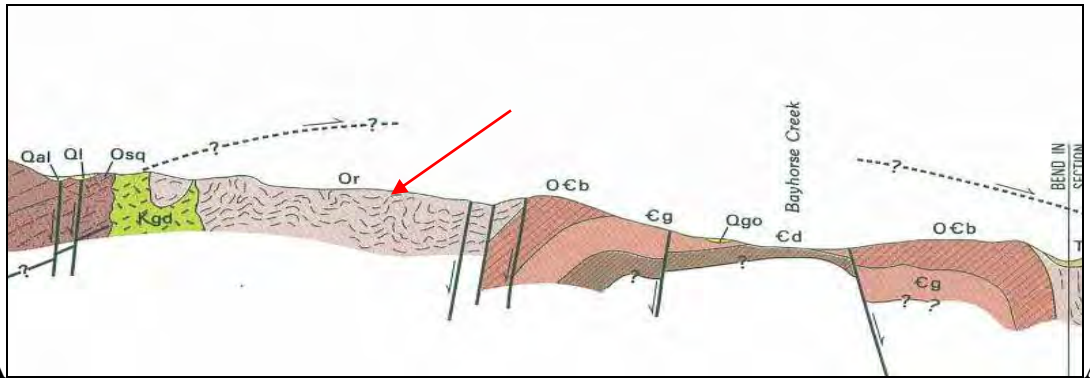

A A'

Figure 4. Geologic cross section showing the Ordovician Ramshorn Slate, indicated by the red arrow (Hobbs et al., 1991).

As seen in Figures 3 and 4, most of the normal faults on the north side of Bayhorse Creek have been downthrown to the west. Towards the south, the fault directly east of the Ramshorn mine bifurcates, with opposite dip directions allowing a block of the Ramshorn Slate to drop. Farther to the east, there is another normal fault that dips to the east and has an eastward-dipping down-dropped hanging wall. Little slate remains between the quartzite and the dolomite, indicating a large throw on the fault. Faulting may extend farther to the south as well, but has been difficult to map. In this area, later stage thrusting caused a common superposition of younger rocks above older rocks in a folded sequence, rather than the usual reverse arrangement. There is evidence that the Paleozoic strata in the Bayhorse quadrangle were deformed before they were intruded by the Idaho batholith. The doming of the structures at Juliette Creek confirm the order of tectonic events.

Ore Bodies

The carbonate rocks in the upper unit of the Cambrian Bayhorse Creek Dolomite host deposits of arsenic, copper and lead, and to a lesser extent zinc. However, ore deposits found within the Ramshorn Slate are the most valuable. They form elongated lenses or ovoid pipe-like bodies, as veinlets, disseminations, breccia fillings, and as massive or discontinuous replacements (Worl et al., 1989).

It is believed that mineralization and intrusive activity occurred simultaneously during the Cretaceous period (Seal and Rye, 1992) when granites from the Idaho Batholith intruded pre-existing sedimentary rocks (Skipp, 1987). Fluid inclusion and stable isotope data indicate that mineralization formed from hot and CO_2-rich brines.

Vein orientations strike north-south and dip to the west at angles of 40-70°. They can be up to 2 m (7 ft) in length. Many of the veins were filled with oxidized ore, which was mostly exploited between 1880-1897. North-south striking, westward dipping veins within the Ramshorn mine are composed of siderite and tetrahedrite mineralization. They are the primary sources of copper, iron, and silver ore within the Ramshorn and Skylark mines.

The principal ore minerals are siderite and tetrahedrite, though galena was also mined, and both are argentiferous. Pyrite, arsenopyrite, chalcopyrite, and sphalerite are also found in small traces associated with the veins, though siderite is the primary gangue mineral (IDEQ, 2003).

History

W.A. Norton and S.A. Boone discovered significant mineralization in the Bayhorse mining district in 1872 after a lone prospector, traveling with two bay horses, identified the mineral potential of the area in 1864 (Wells, 1983). Tom Cooper and Charley Blackburn discovered and purchased the property of the Ramshorn mine in August of 1877, and commenced mining development soon thereafter. Ramshorn Mining Co., Clayton Mining & Smelting Co., and the Beardsley Mining Co. established the mining activity between 1880 and 1898 (Mitchell, 1999).

A railroad brought high-grade ore to Salt Lake City before 1882, after which a 30-ton stamp mill and smelter were constructed in Bayhorse. Also by 1882, charcoal kilns had been built to supply coal for the smelter because importing coke from Pennsylvania was too expensive. Forty men worked in the kilns and soon the town grew to 300 people due to the prosperous mine. Men of all trades were drawn to the town, including

businessmen, bankers, cooks, and builders. Any young women that moved to the town were well attended to and quickly married.

The mine produced over $300,000 worth of silver in 1883. Unfortunately the high-grade lode ran out by 1884, requiring ore to be shipped in from Ketchum, a town southwest of Challis. Transportation and dropping silver prices limited productivity in 1889, and further, a fire that destroyed several buildings in 1889 halted mining until 1901 (Mitchell, 1999). Because of the remaining lower grade ore, a 10-ton per day mill was built on the hillside of the Ramshorn mine in 1917 and used until 1925. By the mid-1930s a second mill had been built by the Pacific mine, which lies just to the north of the Bayhorse town site.

In 1939, W.B. Swigert of Challis leased the mine and employed 15 men. The mill was dismantled and sold, and the ore was sent away to be processed. Production continued steadily until 1950. Bayhorse Mines, Inc. bought the mine and began construction on a 100-ton per day mill, which was completed in 1951. By 1959 Umont Mining Company had entered into the lease and reconstructed roads, completed geologic mapping and sampling, but lost interest by 1962. Inspiration Development Company leased the mine in 1979 for a diamond drilling operation but discontinued the operation in 1980. Currently, Kirk Hansen mines the slate outcrop above the tailings pile for the Rock Works Company.

In total, the mine produced 46,503 tons of ore and produced 25,050 tons of tailings between the years 1877 and 1978. Of this total there were 152.05 oz of gold, 2,442,085 oz of silver, 1,065,439 lb of copper, 5,976,862 lb of lead, and 37,196 lb of zinc (Mitchell, 1999).

Mine Workings

The mine originally consisted of 17 tunnels and intermediate levels accounting for 10.5 km (6.3 mi) of workings with a vertical extent of approximately 520 m (1,700 ft) (Ross, 1937). According to the current lessee, Kirk Hansen, exploration activities conducted by Inspiration Development Corp. from 1979 through 1981 obliterated the surface expression of most of the early workings (IDEQ, 2003). Today, only three collapsed adits reach the surface.

The lower workings of the Ramshorn mine include the three adits, a tailings pile, ponding on the tailings pile roughly 480 m^2 (5,200 ft^2) at its greatest extent, a small decrepit portal shed, a tramway ore loading station, and a tramway terminus ore shed

The upper Ramshorn workings include one collapsed adit whose portal is faced by an ore sorting shed, a boarding house and the upper tram loading station. Although the Ramshorn's loading operations ceased at this level, the tramway continued uphill to the Skylark Mine, where the ore shipment could access the tramway. Four additional adits were driven above these workings, though their exact location could not be determined due to the lack of surface expression. Topographic maps locate the uppermost adit at an elevation of 2,700 m (8,950 feet) amsl. Figure 5 shows a diagram of the original mine workings.

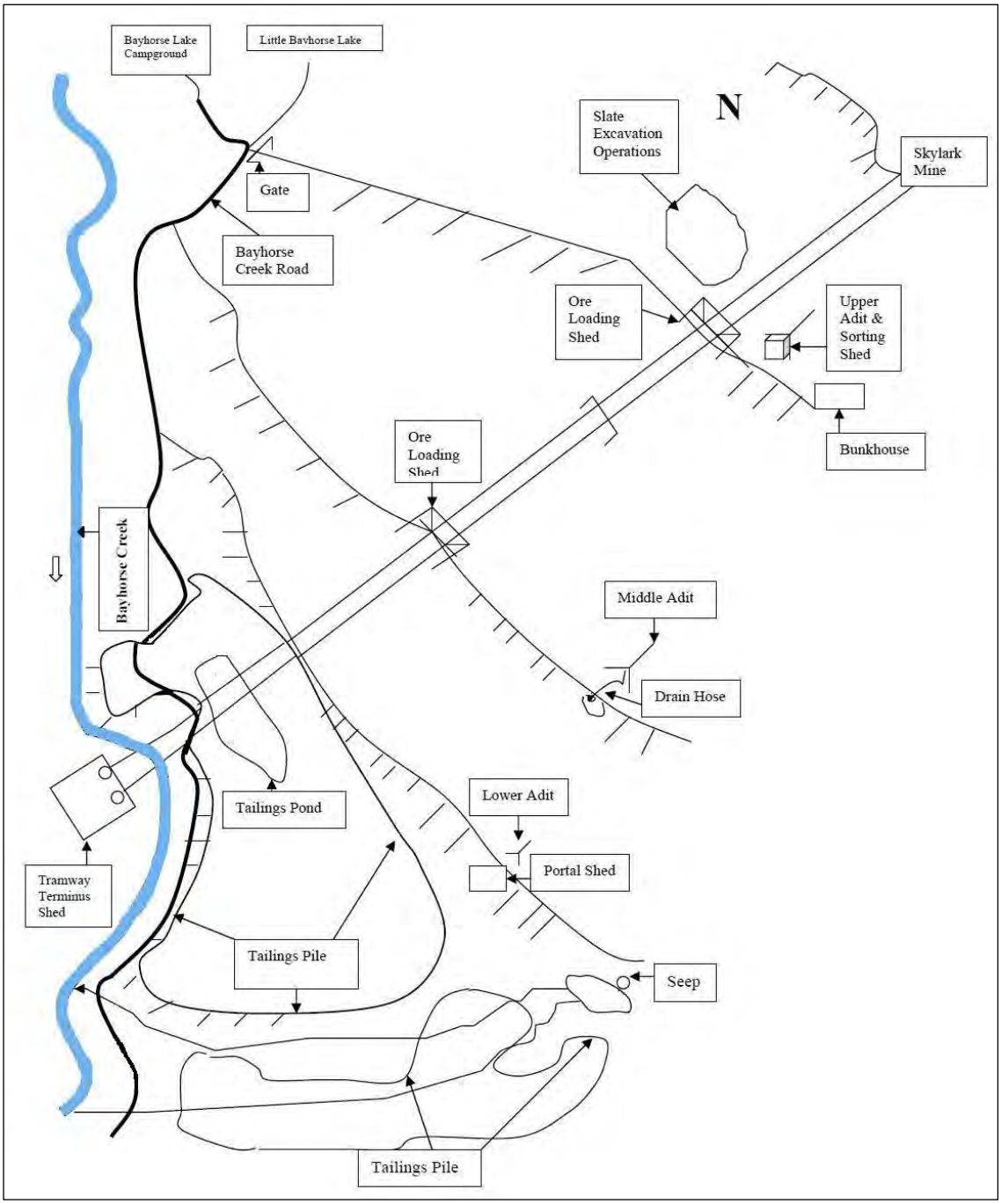

Figure 5. Diagram showing the layout of the mine workings (modified from IDEQ, 2003).

Environmental Contamination

The most damaging environmental effect from mining is heavy metal contamination of soils, sediments, groundwater, lakes and streams, although mining also emits antimony, arsenic, cadmium, copper, lead, and zinc into the atmosphere (Nordstrom and Alpers, 1999). As discussed earlier, the ore bodies deep below the earth's surface, which are normally under anoxic conditions, become exposed to surficial conditions containing abundant oxygen and water. The iron and other metal-bearing sulfide minerals within the ore bodies weather according to the following reactions (Drever, 1997):

$$2FeS_2 + 7O_2 + 2H_2O = 2Fe^{2+} + 4SO_4^{2-} + 4H^+ \quad [1]$$

$$4Fe^{2+} + O_2 + 10H_2O = 4Fe(OH)_3 + 8H^+ \quad [2]$$

Thiobacillus ferrooxidans catalyze the first reaction (Brierley, 1982), sometimes increasing the rate by several orders of magnitude (Nordstrom and Alpers, 1999). The sulfur from pyrite becomes oxidized and ferrous iron, sulfate and protons (acid) are produced. In the second reaction, the ferrous iron becomes oxidized further and is precipitated as ferric hydroxide and more acid is created. Ferric hydroxide is a visible solid that appears along sediments under surface waters as a yellow-orange color, colloquially known as "yellow boy." The acid in the solution causes the oxide film on the iron to dissolve and leaves behind a free metal ion. Metals become much more toxic and mobile when they are in the free metal ion form.

The reactions are difficult to stop without a source of alkaline water to neutralize the acid. Calcite and dolomite are common mineral sources of alkalinity (Banks et al., 1997). If the pH of the water rises sufficiently, the metals will no longer remain dissolved

and instead will precipitate out of solution (Stumm and Morgan, 1996). The metal hydroxide complex that forms when metals are precipitated from solution has a large surface area to volume ratio and acts as an adsorption surface, which then associates with other metals. The metal complexes contaminate surface water either in the form of a dissolved fluid constituent, where the water can carry the metals far from their origin, or in the form of a ferric hydroxide, where the complex will settle and possibly be ingested by macroinvertebrates.

Figure 6 characterizes various fates of dissolved metals in circum-neutral pH systems (taken from Smith, 2007). The fate of metals depends on the geochemical conditions and the thermodynamic state of the system. Some of the dissolved metals will associate with other constituents in the water such as humic acids, fulvic acids, metal-hydroxides, and clay particles (Burk, 2004; Lachmar et al., 2006). Dissolved metals in the surface water can enter the groundwater system if the surface water body is losing water to the groundwater system, and dissolved metals in the groundwater system can enter the surface water system if groundwater is flowing into the surface water system.

According to Pichler et al. (2001) milling processes that produce high arsenic concentrations will "generally precipitate As as a stable phase that will withstand the physico-chemical conditions that exist in shallow groundwater regimes" (p. 495). The relatively high detection limit of XRD analysis (~5%) negates the detection of minor constituents, such as secondary arsenic minerals in bulk tailings material (Pichler et al., 2001). Thus, the XRD analysis must be evaluated carefully for the arsenic phase.

Four physical processes in streams control transport of these constituents: advection, dilution, dispersion, and sedimentation (Salomons, 1995). The chemical processes that control transport include solution reactions, precipitation, coprecipitation and adsorption onto bed load or suspended particles (Salomons, 1995). Adsorption of metals onto the surface of particulate matter in the water column can determine its toxicity and mobility. Discharge, dissolved oxygen, and pH also determine the availability of a metal in the stream environment.

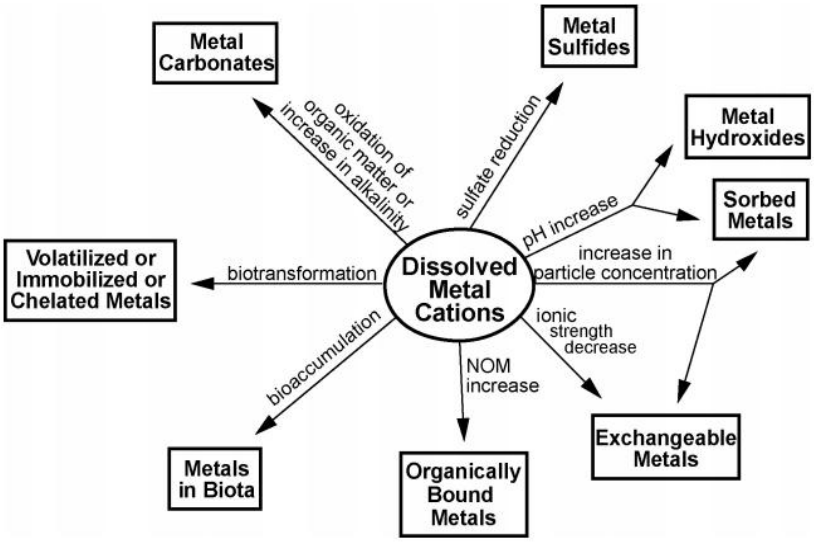

Figure 6. Various pathways for the fate of dissolved metals. NOM refers to natural organic matter (Smith and Huyck, 1999, cited in Smith, 2007).

Iron exists in the ferrous (Fe^{+2}) state under reducing conditions. In surface water iron is rarely found in concentrations above 1 mg/L. When exposed to oxygen, iron will hydrolyze to form insoluble hydrated ferrous oxide. Sometimes iron will sorb to colloidal organic matter in the water column in either a ferric (Fe^{+3}) or ferrous (Fe^{+2}) form.

Manganese commonly is present in the soluble divalent ionic form. Because of the absence of oxygen in groundwater, high limits are imposed on acceptable water systems because it is present at low concentrations and is not as toxic as other elements (APHA, 1995).

Zinc is an essential element with allowable drinking water concentrations between 0.06 mg/L and 7.0 mg/L (APHA, 1995). Copper is essential to humans at a daily requirement of about 2.0 mg.

Arsenic commonly occurs from mineral dissolution in concentrations less than 10 μg/L, although concentrations of 100 μg/L have been detected. Natural waters rarely contain concentrations of lead greater than 20 μg/L.

Summary of Consultant's Report

Ecology and Environment, Inc. (2010), acting as the Superfund Technical and Response Team (START), performed in-field X-ray fluorescence (XRF), pH, and electrical conductivity on soil samples, creek sediment samples, and surface water samples during the summer of 2010. START aimed to determine the severity of heavy metal contamination in and around the main tailings pile of the Ramshorn mine site. Other analyses such as TAL (target analyte list) metals, hardness, nitrate/nitrite, and sulfate were performed by the off-site laboratory, GEL Laboratories, LLC of Charleston, South Carolina.

START collected two background soil samples from an area west of the main tailings pile and seven surface soil composite samples from soil borings and test pits in the main tailings pile and immediate surroundings. TAL metals were measured in the

field using a portable field XRF (EPA SW-846 method 6200). Fifteen surface water samples were collected from the adit drainage, seeps, flowing well discharge, and from Bayhorse Creek both up- and down-gradient from the flowing well. Water samples were analyzed for TAL metals, pH, electrical conductivity, hardness, nitrate/nitrites, and sulfates. Thirteen sediment samples were taken from Bayhorse Creek and measured for TAL metals.

The START analyses show high levels of arsenic and lead throughout soil, sediment, and water samples. The drinking water standards for inorganic metals include arsenic at 0.01 mg/L, cadmium at 0.005 mg/ L, chromium at 0.1 mg/L, copper at 1.3 mg/L, iron at 0.3 mg/L, lead at 0.015 mg/L, manganese at 0.05 mg/L, and zinc at 5 mg/L.

The Initial Default Target Level (IDTL) and Regional Screening Level (RSL) for arsenic are both 0.39 mg/kg. The IDTL and RSL for lead are 50 mg/kg and 400 mg/kg, respectively. Their results are shown in Tables 3-2, 3-3, 3-5, and 3-6 in Appendix A.

Background samples ranged from 30 to 54 mg/kg for arsenic and from 23 to 34 mg/kg for lead (Table 3-2). In the upstream portion of the tailings, arsenic levels were found at 6.83 and 20.5 mg/kg and lead was detected at concentrations of 7.32 and 12.7 mg/kg (Table 3-6), all falling below the background sample values. In the western seep samples, arsenic was measured at 1,910 mg/kg and lead at 1,760 mg/kg, and in the eastern seep samples arsenic was found at 3,160 mg/kg and lead was found at 4,060 mg/kg (Table 3-6). In the sediment samples taken from the adit drainage channel, arsenic ranged from 84.4 to 5,530 mg/kg; lead ranged from 62.4 to 3,070 mg/kg (Table 3-6). The samples collected downstream of the tailings pile had arsenic concentrations from 37 to 1,100 mg/kg and lead concentrations of 21 to 338 mg/kg (Table 3-6).

Both the surface water samples from the creek upstream of the tailings pile and in the creek adjacent to the tailings showed insignificant levels of arsenic and lead. The water samples taken from the outfall and downstream of the adit discharge had arsenic levels ranging from 13.5 to 26.9 μg/L and lead levels ranging from <4.21 to 33 μg/L (Table 3-5). These data present an increase of arsenic and lead levels in Bayhorse Creek above the levels in the draining adit, indicating greater surface water contamination is caused by the tailings than by the draining adit.

Cadmium, copper, mercury, nickel, silver, and zinc were all found at concentrations above Regional Sediment Evaluation Team (RSET) screening levels (Table 3-6). Antimony, cobalt, copper, iron, manganese, mercury, nickel, selenium, silver, and thallium were found in concentrations greater than the IDTL or RSL (Table 3-3).

The pH ranged from 6.73 at the adit discharge to 9.17 at the eastern seep (Table 3-5), which indicates a lack of acid mine drainage. The National Water Quality Criteria allows for a pH between 5 and 9. The conductivity ranged from 44 to 512 microSiemens, hardness ranged from 25.7 to 254 mg/L, nitrate/nitrite ranged from 0.058 (estimated) to 0.64 mg/L, and sulfate ranged from 1.12 to 95.1 (both estimated) mg/L. Due to these results, the EPA proposed three possible site remediation actions, of which in-place capping was chosen to begin in July of 2011.

Capping Procedure

The USFS provided oversight for the capping remediation of the tailings pile beginning in July of 2011. The tailings were re-graded into less steep slopes, then

covered with 2/3 m (1.2 ft) of waste rock. Grading altered the current slope of 1.3H:1V to 1.8H:1V and included 2-3 m (6-10 ft) wide benches at a vertical spacing of 12 to 15 m (40-50 ft) for access and drainage control. Waste rock cap material was taken from a local site. Due to funding limitations, vegetative remediation did not occur.

METHODS

Sample Locations

The map in Figure 7 presents the study area. Eleven water sampling sites are indicated on the map. Discharge measurements were made at ten of these sites. I sampled five groundwater outflows and six surface water sites, and measured discharges at all of them except one surface water site (SW-4). I visited the field site on four occasions for data acquisition to account for seasonal effects: on July 8, August 5, September 1, and October 1 of 2011.

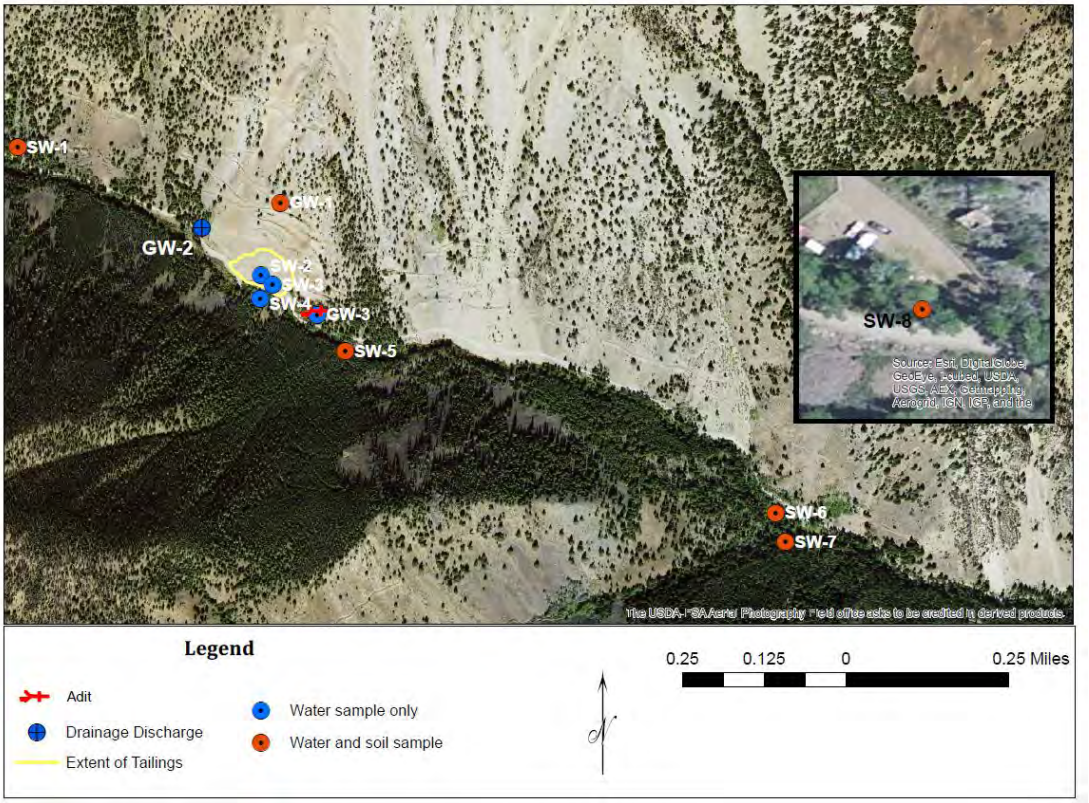

Figure 7. Map of the Ramshorn mine study area showing locations of discharge measurements in red circles, sample only measurements in orange circles, sediment samples in black triangles (overlying red circles), and tailings sample in an yellow triangle (topographic base from USGS Bayhorse 7 1/2-minute quadrangle, 1991).

Surface water samples were collected from Bayhorse Creek upstream of the tailings (SW-1), downstream of the draining adit (SW-5), and upstream of the confluence with Juliette Creek (SW-6) (Figure 7). To determine the contribution of Juliette Creek, I also collected a sample from it upstream of its confluence with Bayhorse Creek (SW-7). I collected one sample from below the Bayhorse historic town site (SW-8) to determine the impact of potential contamination from the mill site at the very easternmost portion of my study area.

Groundwater sample GW-1 (Figure 7), was taken from a seep upslope of the mine waste that emerges from the Ramshorn Slate. This sample documents the quality of the groundwater before it infiltrates through the mine waste. A groundwater sample (GW-2) was collected from a flowing well just to the west of the tailings pile to determine the quality of the groundwater in the western portion of my study area. The third groundwater sample, GW-3, was taken from the draining adit to the east of the tailings pile to determine the groundwater quality at that location. Water samples were also taken from two seeps emerging from the toe of the tailings pile, SW-2 and SW-3, and from an ephemeral pond on the southern side of the road (SW-4) that was fed by SW-3. These last three locations were only sampled in July, as they were eliminated as a result of the capping remediation that was initiated later that month.

A tailings grab sample from the base of the tailings pile (SS-2) and a sediment sample from the uppermost groundwater sample site (GW-1 SS) were collected on the first site visit on July 8. Stream sediment samples were collected adjacent to four stream water sample collection sites (SW-1 SS, SW-5 SS, SW-6 SS, and SW-8 SS) during the

third site visit on September 1, though not all were processed in the lab analyses. A rock sample was also collected from the uppermost groundwater sample site (GW-1 ROCK).

Discharge Measurements

The Ramshorn and Skylark mines lie at the upper end of the reach of the creek along which surface water discharge rates were measured. The upper boundary is located just upstream of the disturbed mining and tailings area along upper Bayhorse Creek. The lower boundary is just below the Bayhorse town site and the confluence of Bayhorse Creek with Beardsley Gulch. Bayhorse Creek flows roughly west to east in this reach. One perennial tributary, Juliette Creek, flows into Bayhorse Creek from the south.

Measurements of surface water discharge rates of Bayhorse Creek and its tributary, Juliette Creek, at five locations (SW-1, SW-5, SW-6, SW-7, and SW-8) helped determine how much water Bayhorse Creek is gaining from or losing to the groundwater system along this reach during the study period. If surface water is flowing into the groundwater system (groundwater recharge), then the summed discharges from the upper stream boundary and tributaries will be greater than the discharge at the lower boundary, and Bayhorse Creek is a losing stream. Conversely, if groundwater is flowing into the surface water system (groundwater discharge), then the summed discharges of the upper boundary and tributaries will be less than the discharge at the lower boundary, in which case Bayhorse Creek is a gaining stream. In order to calculate the groundwater recharge or discharge rates, surface water discharge rates must be measured.

Discharge measurements were made during each field data acquisition period, producing a total of four sets of discharge measurements. Discharge measurements were made along a cross section of the creek that runs perpendicular to the flow direction. The current velocity was measured in 30-cm (1-ft) width increments using a Marsh McBirney Flo-mate 2000 current meter with a top-setting wading rod using the 6/10-depth method for determining mean velocity (USGS, 1980). The stream width was determined using a fiberglass measuring tape strung above the river from each bank, and the depth was measured with the wading rod. The flow through the cross section was calculated using the simple average method to determine discharge (USGS, 1980), which uses the same principles as estimating the area under a curve. The area of individual trapezoids is multiplied by the average water velocity through each individual trapezoid, and then the individual flows associated with each trapezoid are added together.

Discharge measurements were calculated by the trapezoidal method at six locations, which are shown in Figure 7. These include five stream locations, specifically the reach of Bayhorse Creek above the tailings pile (SW-1), the creek downstream of the draining adit (SW-5), Bayhorse Creek above the confluence with Juliette Creek (SW-6), Juliette Creek (SW-7), and downstream of the Bayhorse town site (SW-8), as well as the draining adit located immediately east of the tailings (GW-3).

Discharges were also measured for four groundwater outflows. The four sites are located at the seep upslope of the tailings pile (GW-1), the flowing well (GW-2), the culvert under the road for the western seep at the toe of the tailings pile (SW-2), and the eastern seep at the toe of the tailings pile (SW-3). The discharges for these sources of water to Bayhorse Creek were determined by the volumetric method (USGS, 1980). The

volumetric method involves timing how long it takes to fill a container of known volume. Multiple measurements were made until five comparable times were achieved, and the times were averaged to estimate the discharge.

Hydrochemical Analyses

Water Sampling

Water samples are required to determine the composition and metals concentrations for use in the metals loading rate calculations and for geochemical modeling. Water samples were collected from each of the ten surface and groundwater discharge measurement sites, and from one other ephemeral site, specifically ponded water on the tailings pile (SW-4). This pond is south of SW-3.

Certain hydrochemical parameters were measured in the field during sample collection prior to filtering and acidification, including water temperature, electrical conductivity, pH, dissolved oxygen, and alkalinity. These were measured using a YSI 85 temperature, salinity, and conductivity meter, a Hanna HI 9143 dissolved oxygen meter, an Orion 203A pH meter, and a Hach field alkalinity kit.

Filtered acidified samples were collected from all eleven sampling sites for determination of dissolved inorganic constituents. Unfiltered acidified water samples were only collected from sites SW-1, SW-2, SW-5, SW-6, SW-7, SW-8, and GW-3, which have the potential to contain suspended sediments. Discharge measurements were made for determination of total and dissolved metals loading rates at ten of these eleven locations. No discharge measurement could be made for sample SW-4 because it was collected from an ephemeral pond. Appropriate samples were filtered in the field with a

0.45-micron filter. All water samples were acidified to a pH ≤ 2 with trace-metal grade nitric acid and stored in 60-mL HDPE bottles.

Laboratory Analyses

The filtered samples were analyzed for Al, B, Ba, Ca, Cd, Co, Cr, Cu, Fe, K, Mg, Mn, Mo, Na, Ni, P, Pb, S, Si, Sr, and Zn by Utah State University Analytical Laboratory (USUAL) using ICP (Inductively Coupled Plasma) analysis. Chloride concentrations were determined by USUAL using a Lachat flow injector analyzer, which is an automated colorimeter. However, chloride was not detected in any of the samples collected in July, so the samples collected in August, September, and October were not analyzed for chloride.

ICP-MS (Inductively Coupled Plasma – Mass Spectrometry) at the Utah Veterinary Diagnostic Laboratory (UVDL) was used to analyze the unfiltered and selected filtered water samples for total and dissolved concentrations, respectively, of Ag, Al, As, B, Ba, Be, Ca, Cd, Co, Cr, Cu, Fe, K, Li, Mg, Mn, Mn, Mo, Na, Ni, P, Pb, Sb, Se, Si, Sn, Sr, Tl, U, and Zn. The unfiltered samples were digested with trace-metal grade nitric acid using method 3030 E (APHA, 1995) prior to ICP-MS analysis. All unfiltered water samples were analyzed at the UVDL ICP-MS because the ICP cannot analyze unfiltered samples. Additionally, selected filtered water samples were run on the UVDL ICP-MS because the detection limits for the USUAL ICP instrument were too high to detect the trace levels of contaminants at the Ramshorn mine site. These included: GW-3, SW-1 and SW-2 collected on July 8, 2011, and GW-2, GW-3 and SW-1 collected on August 5.

Sediment Sample Analyses

One tailings soil grab sample (SS-2) was collected with a shovel, placed in a Ziploc© bag, and analyzed for potential mineral contaminants using X-ray diffraction (XRD). The tailings sample was pressed into an aluminum holder using the Philips XRD instrument in the Geology Department at Utah State University (USU). The XRD utilizes Cu K-alpha radiation ($\lambda = 1.5404$ angstroms), which passes through a crystal monochrometer. The current was set to 15 mA, the voltage was set to 35 kV, the 2-theta scanning interval was set to 3-63 degrees, the step interval was 0.05 degrees, and the scan speed was set for 2 degrees per minute. The sample ran for one hour while the X'pert program recorded peaks, correlated to signature wavelengths and heights that are specific to certain minerals. The X'pert search matches the recorded peaks to a reference database of mineral peaks then calculates a score based on the match. Dominant minerals were chosen based on scores above 18.

Five stream sediment samples were also collected at four of the locations where water samples were collected (SW-1 SS, SW-5 SS, SW-6 SS, and SW-8 SS). These samples also were collected with a shovel and placed in Ziploc© bags, and then were analyzed for heavy metals using X-ray fluorescence (XRF). Sediment samples collected from the stream bottom at each of the four locations ranged in grain size from clay to cobble. Because the samples were a heterogeneous mix of clast sizes, a representative sample was obtained from each Ziploc bag by sorting the sample into smaller proportionate piles using an aggregate soil sample splitter from the Optically Stimulated Luminescence (OSL) laboratory. Then the samples were oven dried and crushed for one minute in a rock pulverizer. These samples were analyzed by XRF to determine major

ion ratios. They were mixed with three to five drops of polypropylene film in a mortar and pestle. The sample was transferred into an aluminum pellet cup then crushed using a force of 1,000 kg in a manual press. The solid pellet was dried overnight and run on the Philips© XRF for trace metals and oxide compounds.

A sample of the country rock, Ramshorn Slate (GW-1 ROCK), was collected for XRF analysis to determine the elemental composition of the local bedrock through which the groundwater flows. This aids in identifying mineral phases for use in geochemical modeling.

Sediment samples SS-2 (tailings), SW-1 SS, SW-5 SS, and GW-1 ROCK were also sent to the UVDL to be processed and analyzed on the ICP-MS. The samples were weighed to 0.5 gram and mixed with 5 mL of concentrated nitric acid. The mixture was heated at 120-130 ºC for 14-16 hours and then hydrogen peroxide was added and the sample was diluted to 50 mL. For analysis of minor and trace components, the solution was further diluted by a 1:9 ratio (Soil & Plant Analysis Laboratory, 2005)

Geochemical Modeling

Determining the phase of metals in surface water can be a difficult analytical procedure (USGS, 1980). Because of this, chemical modeling often is used to describe the chemical nature of the water based on parameters such as temperature, pH, total dissolved solids (TDS), alkalinity, dissolved oxygen content, Eh, and other easily measured field parameters. I used PHREEQC (Parkhurst and Appelo, 2000) to interpret the chemical processes and reactions that occur as water flows through the mine site and mixes with Bayhorse Creek. Elemental composition, speciation, and saturation indices

were used to determine potential phases and oxidation states of the metals within the system. Mixing calculations were performed along with surface sorption modeling in order to describe the chemical reactions that occur when Bayhorse Creek mixes with contaminated water, and to determine the extent to which metals are adsorbed onto ferric oxides, hydroxides, oxy-hydroxides and/or oxy-hydrates during mixing. Hydrous ferric oxide (HFO) was assumed as a surface for metal sorption. First, HFO was equilibrated with each water sample, and then it was equilibrated with the mixed water sample. The surface sorption parameters were obtained from Dzombak and Morel (1990). The default parameters used were 600 m^2/g for the specific surface area, 0.005 mol/mol Fe for the strong site density, and 0.2 mol/mol Fe for the weak site density. The default input parameter was pe = 4.0 as the redox potential.

Three water sample chemical analyses (SW-1, GW-2, and GW-3 from August) were mixed and modeled using PHREEQC. This was the only sampling period when mixing could be calculated because this was the only period when Bayhorse Creek was a gaining stream between SW-1 and SW-5 during the four data collection periods. Such a model tracks the dissolution and precipitation of minerals based on the measured chemistry of surface and groundwater.

RESULTS

Discharge Measurements

Discharge results are shown in Table 2. Negative values represent recharge into the groundwater system from the creek, while positive values represent discharge from the system into the creek. All values are shown in liters per second. The discharge calculations are shown in Appendix B. The raw discharge measurements for SW-1, SW-2, SW-3, SW-5, SW-6, SW-7, SW8, GW-1, GW-2, and GW-3 are also provided in Appendix B.

Table 2 shows recharge to or discharge from the groundwater system along the upper segment of the study area, which falls between SW-1 and SW-5, the middle segment, which falls between SW-5 and SW-6, and the lower segment, which falls between SW-6 and SW-8. The total loss or gain of Bayhorse Creek was determined between SW-1 and SW-8.

Table 2. Discharge values and the calculated gains and losses in L/s.

Site ID	7/8/2011	8/5/2011	9/1/2011	10/1/2011
GW-1	0.79	0.58	0.39	0.28
GW-2	0.06	0.06	0.06	0.06
GW-3	25.13	20.03	15.54	18.15
SW-1	234.91	73.91	26.26	17.93
SW-5	244.98	94.44	33.06	29.15
SW-6	379.36	138.48	59.96	50.24
SW-7	512.31	230.18	92.13	61.01
SW-8	1102.59	404.23	199.56	159.54
Upper Segment	-15.06	0.50	-8.73	-6.93
Middle Segment	134.38	44.04	26.90	21.09
Lower Segment	210.92	35.56	47.47	48.29
Net Gain/Loss	330.24	80.10	65.63	62.45
Stream Type	Gaining	Gaining	Gaining	Gaining

The discharge in July showed a gain in all segment locations except in the upper segment. SW-8 had the highest discharge of all stream sample locations and SW-1 had the lowest discharge of all stream sample locations, resulting in an overall gaining stream. GW-3 had the highest groundwater discharge and GW-2 had the lowest rate of all groundwater discharge measurement locations.

The discharge in August showed gaining segments for all reaches of the creek. As in July, SW-8 had the highest discharge of all locations, indicating a gaining stream. August was the only month in which the upper segment was a gaining stream. This was the only month where groundwater may have contributed to metals contamination in the creek.

During September, all discharge values, except for GW-2, decreased significantly from those in August. The upper segment was a losing stream in September as it was in July. Again, the discharge at SW-8 was the highest of all the values, indicating a gaining system overall.

The discharge in October decreased slightly from the values measured during the September sampling period as expected due to seasonal effects. The value for site GW-3 increased slightly between September and October, which may be a result of a field measurement error.

Field Analyses

Results of field analyses are shown in Tables C.1, C.2, C.3, and C.4 of Appendix C. The groundwater samples, GW-1 and GW-2, are not shown in Figures 7 through 11 because they are do not discharge into the stream.

Alkalinity

Alkalinity (mg/L of $CaCO_3$) throughout the four collection months is shown in Figure 8. For the most part, the alkalinity values at each sampling site remained steady throughout the four data collection periods. GW-2 (Table C.1) had the highest alkalinity during all four data collection periods, which may reflect a longer residence time for the groundwater at that location. The water in the flowing well likely has longer exposure to carbonate rocks, which lie stratigraphically beneath the Ramshorn Slate. GW-1 had the lowest alkalinity of all the sampling sites throughout the four data collection periods. GW-1 sits topographically and stratigraphically higher than any other sampling location, where the absence of carbonate rocks and shorter residence times might contribute to lower alkalinity values. All other water samples (SW-1, SW-5, SW-6, SW-7, SW-8, and GW-3) fell between these two values.

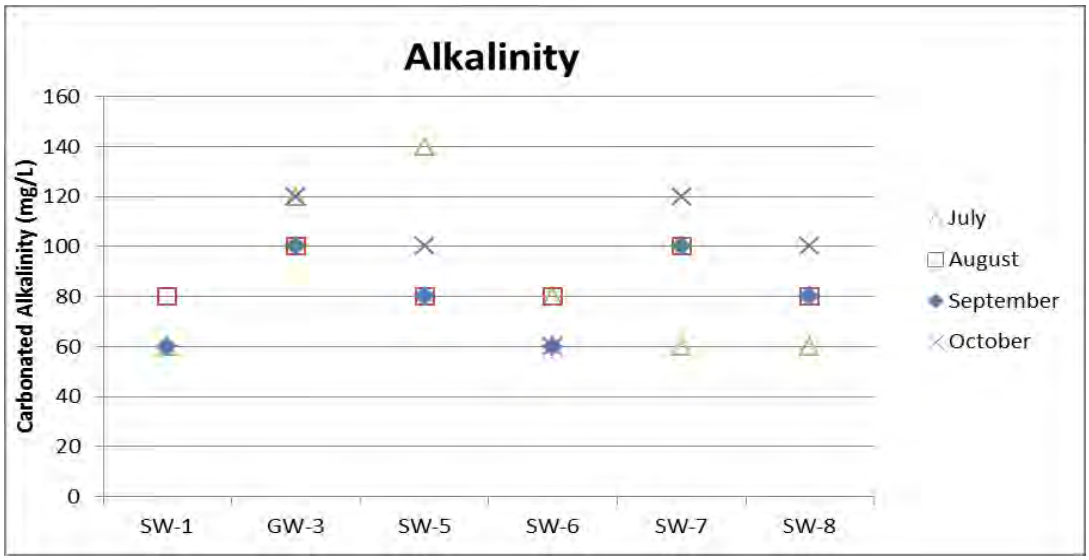

Figure 8. Alkalinity values (mg/L) for each sample site. SW-1 was not measured in October.

The highest alkalinity measured for any surface water samples was at SW-5 in July. This probably reflects the influence of the tailings pile, as one of the water samples collected from the two seeps emerging from its toe (SW-3) also had a measured high alkalinity (see Table C.1).

Electrical Conductivity

Changes in electrical conductivity (EC) from June to October are shown in Figure 9. A similar pattern can be seen with EC as with alkalinity; the water sample with the highest EC came from GW-2, while the lowest value was found at GW-1 (see Table C.1). Most of the values remained constant throughout the four data collection periods.

SW-5 had an abnormally high EC of nearly 500 µS in July. This may be due to a field measurement or recording error. However, it possibly reflects the influence of the tailings pile, as the EC of the water seeping from it at SW-3 was 570 µS (see Table C.1).

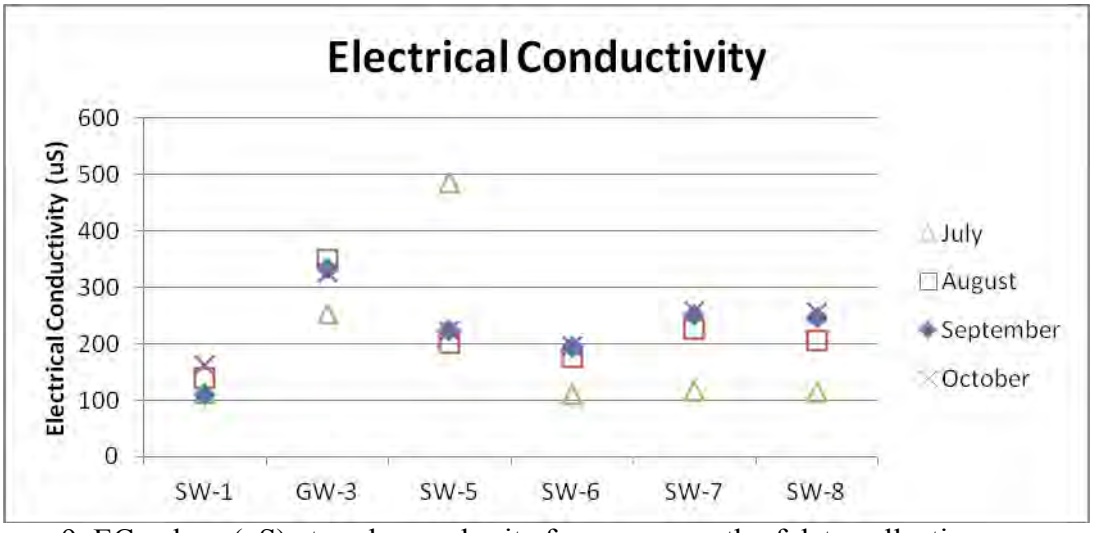

Figure 9. EC values (uS) at each sample site for every month of data collection.

Dissolved Oxygen

Dissolved oxygen was only measured for the August, September, and October sampling events because of a delay in equipment delivery. The lowest values were measured at site GW-3 (Figure 10). The dissolved oxygen content in most of the samples generally decreased from September to October, although GW-1, SW-1, and SW-7 all remained constant or increased slightly. Surface water samples ranged from 8 to 13 mg/L. Based on these dissolved oxygen measurements, all of the sulfur was assumed to be in the form of sulfate. In August the values between SW-1 and SW-8 hovered around 11 mg/L and then in September they hovered around 12 mg/L.

The values in October were much more variable between SW-1 and SW-8. Perhaps the values earlier in the summer were sourced from surface runoff, while the flows later in the fall were fed by the groundwater baseflow, which showed much more variation between sites based on the local bedrock composition.

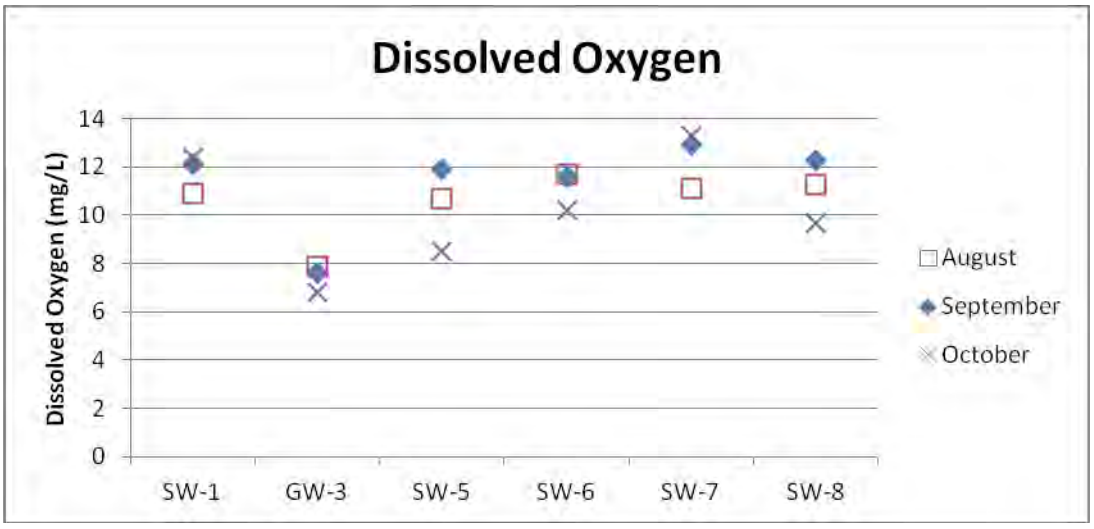

Figure 10. Dissolved oxygen measurements (mg/L) at each sample site. July was not measured.

A healthy biological value of dissolved oxygen ranges from 5 to 9 mg/L, however the temperature impacts the effect of dissolved oxygen and the values will cycle throughout one day. To account for variations in temperature, the percent saturation value is calculated. Percent saturation values were calculated using the monogram accompanying Tables C.2, C.3, and C.4 in Appendix C, by drawing a line between the measured dissolved oxygen value and the temperature, and then observing the value in which the line falls over the percent saturation. Values between 80 and 120% are considered healthy, while percent saturations above or below this range are considered unhealthy. All samples fell within the healthy range for each month, except for sample GW-3, which consistently showed a saturation value between 60 and 70%.

Temperature

Figure 11 shows that the temperatures ranged between 5 and 18ºC. Most of the temperatures remained relatively constant or decreased between July and August, except for SW-1. GW-2 consistently had the highest temperature values of the three groundwater samples. SW-5 had the highest temperature measurements of all water samples, especially during July.

pH

The pH range of all the samples was between 6 and 10, as shown in Figure 12. Most of the samples displayed a neutral or slightly alkaline pH throughout the study period. The lowest pH values were found in GW-1 and GW-3 for each sampling month. GW-2 had the highest pH value for all the groundwater samples and GW-3 displayed the lowest pH of all the groundwater samples repeatedly, although GW-1 also had a

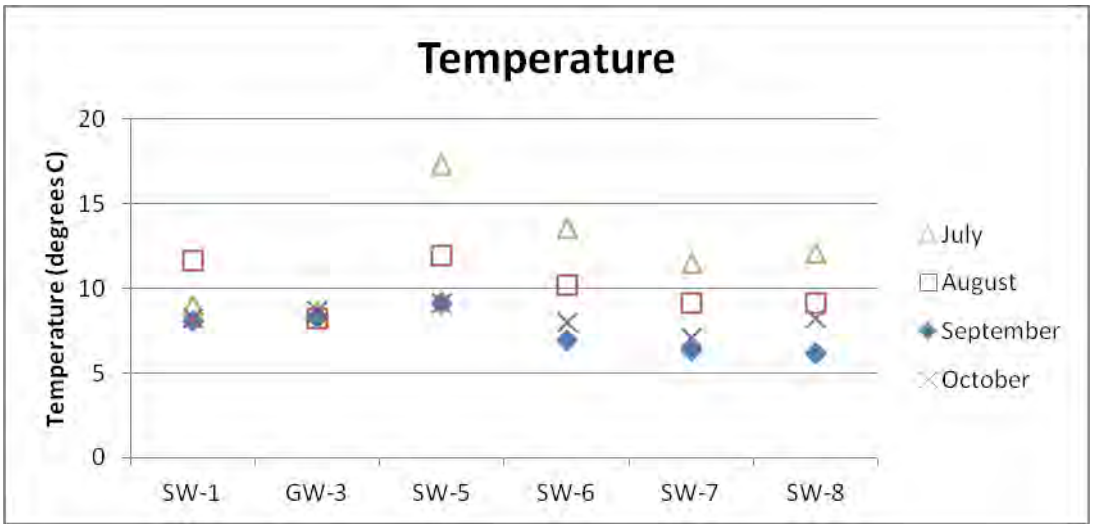

Figure 11. Field measured temperature (degrees C) by study site along the stream reach.

relatively low pH during July. GW-2 also was more alkaline than either GW-1 or GW-3. The highest pH (9.17) was measured at SW-5 in July. GW-2 and SW-6 (8.86 and 8.84, respectively) had the highest pH values in August. SW-1 and SW-8 had the highest pH values (8.6 and 8.57, respectively) during September. During October SW-7 and SW-8 had the highest pH values at 8.34 and 8.29, respectively.

Both the ground and surface waters show a slightly alkaline range throughout the study period, indicating an absence of acid mine drainage. The upper groundwater seep, GW-1, had the lowest pH throughout the field area. The adit drainage, GW-3, also had a slightly lower pH than the creek samples.

The highest pH was measured for the flowing well (GW-2), and the creek just downstream from the tailings pile (SW-5) in July. The flowing well expels water from a greater depth than the seep and draining adit, and so it may represent a deeper portion of the groundwater system, which has a longer time to interact with carbonate rocks, and

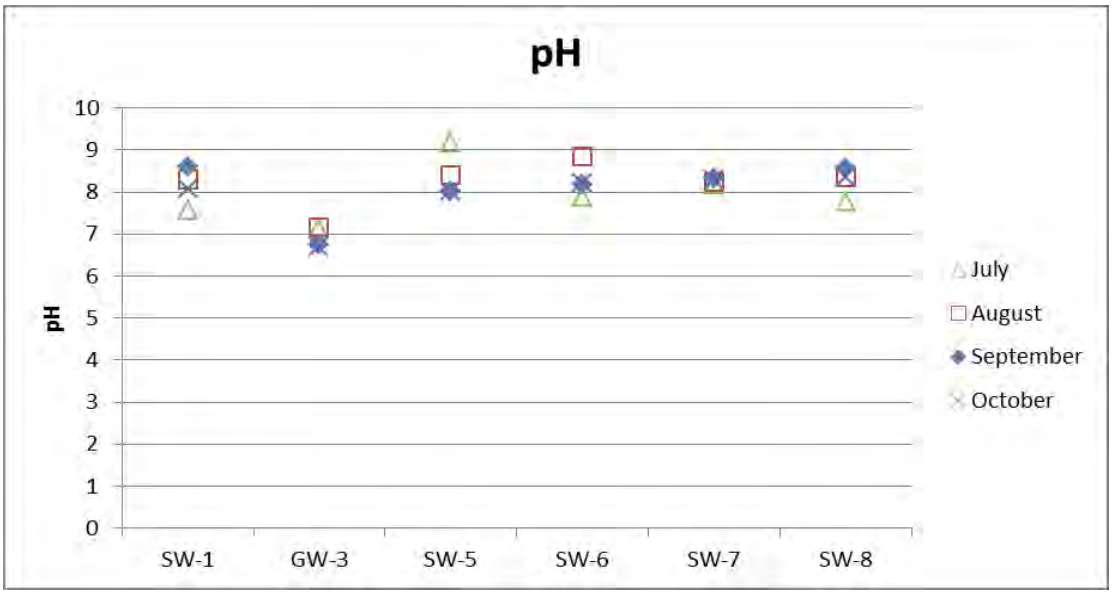

Figure 12. pH values at each site along the stream reach.

therefore has a higher pH. The surface water downstream from the tailings may have a higher pH in July than other locations in the creek because of the influence tailings pile, since the sample from SW-3 also had a high pH.

The pH values during the month of August increase slightly from July except at SW-5. This increase in pH values is probably due to the remedial capping. However, the increase was so slight that the results could be within the range of error for the pH meter. The highest pH measurements occurred at sites GW-2 and SW-6, similar to July when GW-2 and SW-5 had the highest pH values. As in July, the lowest pH values were measured at the two groundwater seeps, GW-1 and GW-3. The surface water samples may be more alkaline due to dilution of the groundwater entering the creek by the much greater quantity of surface runoff.

During September and October, the pH values decreased slightly overall from the pH in August. A greater proportion of the surface water is derived from shallow

groundwater, which happens to have lower pH values. However, the pattern may be insignificant since it occurs within the range of error for the pH meter.

Laboratory Analyses

All of the analytical results for the water samples are shown in Appendix D. Appendix D includes the results from both the UVDL and the USUAL. The detection limits for the UVDL analyses were 0.001 mg/L, were lower than the detection limits for the USUAL results, which ranged from 0.001 (Ba, Cd, and Mn) to 6 (Cl) mg/L.

Three filtered samples (GW-2, GW-3, and SW-1) from August were duplicated at the UVDL, resulting in a variance in concentration data. The variance between lab results therefore leads to discrepancies between my total and dissolved metals concentrations, since all filtered samples were analyzed by USUAL using an ICP and all unfiltered samples were run by UVDL using an ICP-MS. The variance could be attributed to the inconsistency between analytical techniques using different labs and different instruments. The UVDL ICP-MS is a more precise and accurate instrument than the USUAL ICP. Dissolved metals concentrations greater than total metals concentrations could be explained by the variance in detection limits and accuracy of each analytical method.

The USGS GW_Chart (Version 1.23.7.0) was used to create trilinear (Piper, 1944) plots for all water samples. Piper diagrams provide a visual organization for water chemistry classification. Changes in water chemistry can be observed between water samples along a transect, such as the Bayhorse Creek surface water sample sites and the

three groundwater sample sites. A Piper diagram of all the water samples has been plotted for each of the four data collection periods, and are presented in Figures 13(a-d).

Chloride concentrations were only measured for the July samples because the concentrations were all below the detection limit of 6 mg/L. Since the actual concentration of chloride may have been anywhere within the range of zero to 6 mg/L, a value of 3 mg/L was entered into the GW_Chart as an estimate of the actual concentration for all samples.

The results from the USUAL analyses show that all of the samples plot in the bicarbonate type in all four of the Piper diagrams for each data collection month except for GW-3, and SW-2, SW-3 and SW-4 in July. SW-1 has the highest percentage of calcium and bicarbonate throughout all four samplings.

Most of the water samples plot in similar hydrochemical facies regions; specifically in the calcium-magnesium-bicarbonate facies. However, GW-3 fell within the magnesium-bicarbonate facies. SW-3 and SW-4 were magnesium-bicarbonate-sulfate, but SW-2 was calcium-magnesium-bicarbonate-sulfate.

During July, SW-2, SW-3, and SW-4 had high sulfate concentrations, which is typical of water contaminated by mine drainage and suggests a source of metals waste adjacent to these locations. The water from these locations is derived directly from the tailings pile, which likely represents the location of greatest metals contamination.

In August, GW-3 continues to plot closer to the magnesium and sulfate facies. GW-1 also tends to plot near GW-3, but the water at the GW-1 sampling location is much more dilute. SW-1 continues to plot in the calcium-bicarbonate facies in the lower corners of the triangular diagrams.

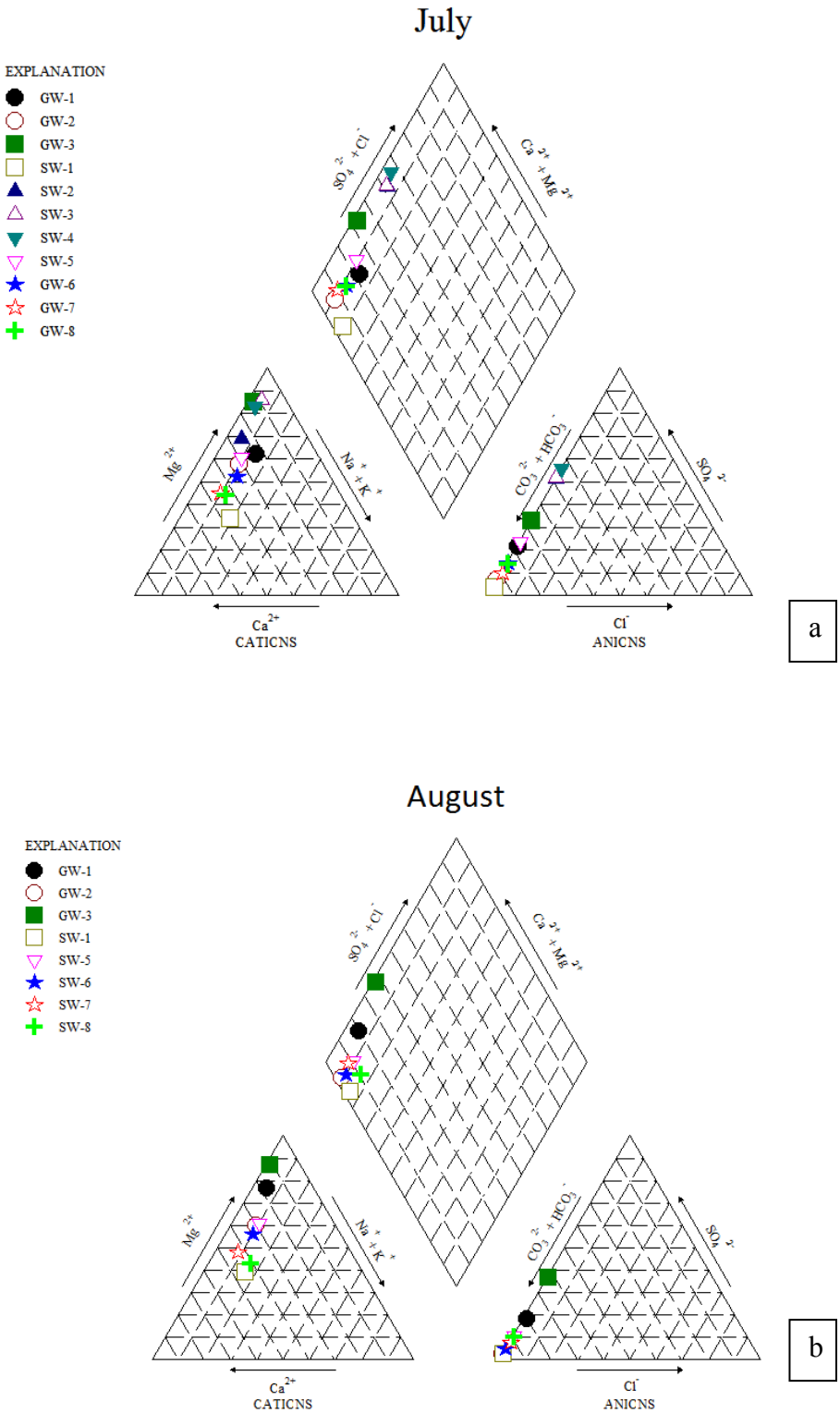

Figure 13. Piper diagram, hydrochemical facies for July (a), August (b), September (c) and October (d). (70 mg/L CaCO3 was estimated for SW-1 alkalinity since no value was recorded in October.)

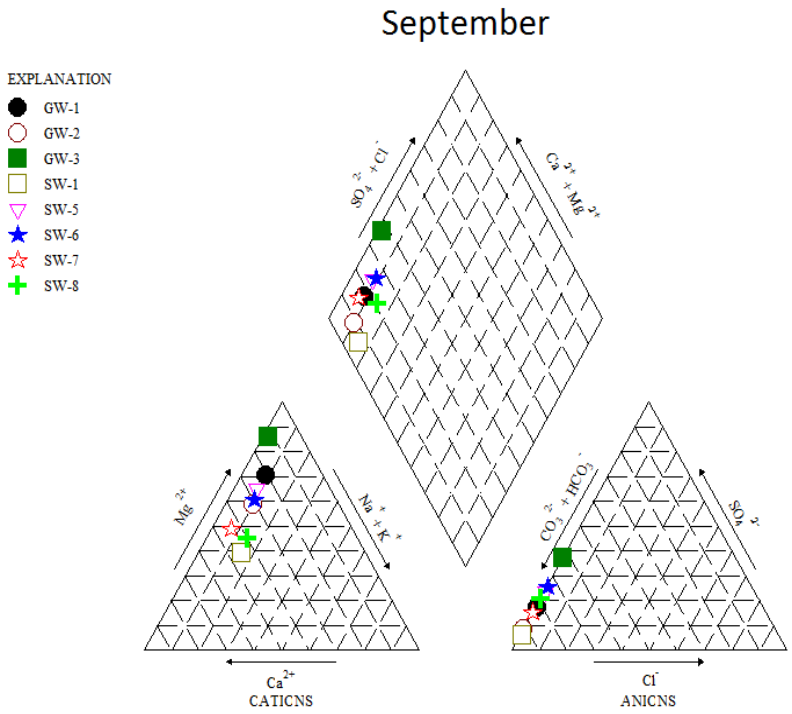

c

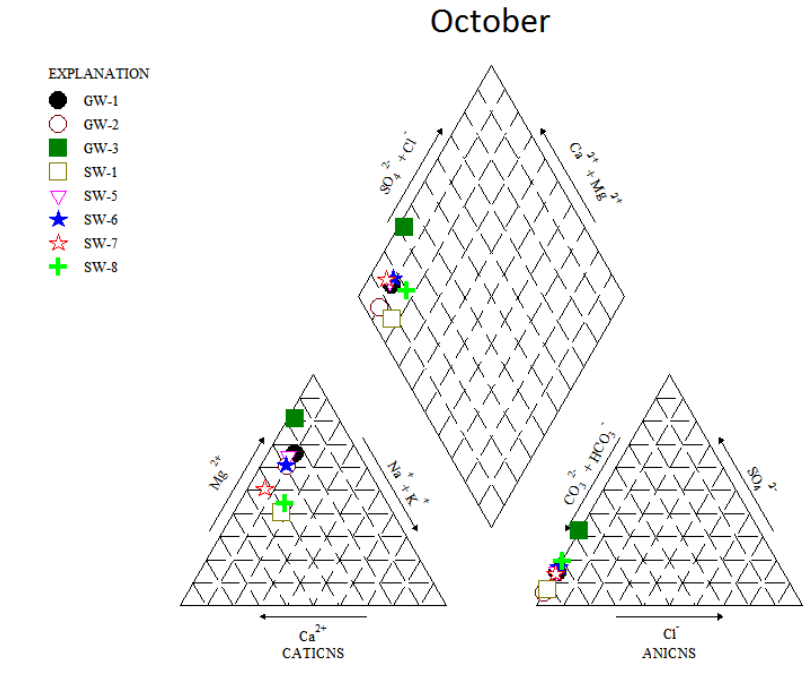

d

Figure 13 (Cont.)

In September, once again, GW-3 shows a greater abundance of magnesium and sulfate. SW-1 continues to fall in the calcium and bicarbonate corners.

The October results were very similar to August and September. The water samples are grouped closely together in the calcium-magnesium and bicarbonate type. The results in August, September, and October, are very similar to that of July except that the SW-2, SW-3, and SW-4 samples are absent due to remedial capping eliminating their flows.

Metals Loading Rates

The total, dissolved, and suspended metals loading rates for the six metals of concern (arsenic, copper, iron, lead, manganese, and zinc) were calculated for each section of Bayhorse Creek. These metals were chosen because they had the highest concentrations among the suite of metals analyzed. Dissolved and total metals loads were calculated from the concentrations measured for the filtered and unfiltered samples, respectively, which were then multiplied by the discharge rate. Suspended metals were calculated by subtracting the dissolved (filtered) load from the total (unfiltered) load. Only the UVDL analytical results were used except for filtered samples that were only analyzed by the USUAL.

Total metals concentrations should be equal to or greater than the dissolved metals concentrations, as the total metals are the sum of the dissolved metals and the suspended metals concentrations. However, water samples GW-3, SW-1, SW-2, and SW-5 in July (see Table D.1) resulted in higher concentrations of the dissolved metals of concern than in the total metals. All six metals had higher dissolved concentrations than

total concentrations for GW-3. Lead and manganese were higher in the dissolved sample than the total in SW-2 in July. Dissolved zinc was higher than the total zinc in SW-1, SW-2, and SW-5 in July. In August, dissolved iron is higher than total iron in SW-5 and dissolved zinc is higher than total zinc in SW-6 and GW-3. These could be a result of poor precision of the laboratory analyses, or a variation in analytical accuracy by the UVDL and USUAL. The calculated loads will be negative where the dissolved concentration exceeds the total concentration. This value is effectively zero, since loads cannot be negative. The remaining negative loads in Tables 3, 4, and 5 are a result of the estimated concentrations using half of the detection limit for the non detected metals. The UVDL detection limit was much smaller than the USUAL detection limit, which also contributes to negative values in Tables 3, 4, and 5.

Metals loads were determined by multiplying the metals concentrations (mg/L) by the discharge (L/s) at each location. Metals loading rates (mg/s) of total, dissolved, and suspended metals are presented in Table 3, 4, and 5 for each sample location in July, August, and October. The results for September are not shown because no unfiltered samples were analyzed by the UVDL. The load for samples with non detections were calculated using a concentration of half of the detection limit.

Iron is the metal of concern with the highest total and dissolved loads in July. Iron controls the total load of metals in the creek. The total metals load at the lowest site, SW-8, was 507.19 mg/s and the dissolved load was 241.58 mg/s. The total iron load at site SW-8 was 453.17 mg/s and the dissolved iron load was 212.14 mg/s, nearly 90% of the total and dissolved metals loads, respectively. Dissolved arsenic, copper, and lead were only detected in two groundwater seep samples (GW-3 and SW-2) and one surface water

Table 3. Loading rates of metals of concern (mg/s) in July. Zeroes indicate an insignificant value.

7/8/2011	SW-1	SW-2	GW-3	SW-5	SW-6	SW-7	SW-8
As-t	0.23	0.14	0.50	1.22	1.90	2.05	3.31
As-d	0.23	0.08	0.65	1.22	1.90	2.56	5.51
As-s	0	0.06	-0.15	0	0	-0.51	-2.21
Cu-t	1.41	0.09	0.23	0.98	1.90	2.05	6.62
Cu-d	1.41	0.04	0.28	0.98	1.52	2.05	4.41
Cu-s	0	0.06	-0.05	0	0.38	0	2.21
Fe-t	41.81	2.62	37.27	112.69	193.10	313.53	453.17
Fe-d	25.37	0.70	106.45	132.29	71.47	188.94	212.14
Fe-s	16.44	1.92	-69.18	-19.60	121.62	124.59	241.03
Mn-t	1.41	0.08	6.28	6.12	7.97	9.73	19.85
Mn-d	1.17	0.05	7.84	3.38	3.30	5.84	10.25
Mn-s	0.23	0.03	-1.56	2.74	4.67	3.89	9.59
Pb-t	0.23	0.16	0.18	0.73	1.14	1.54	3.31
Pb-d	0.23	0.02	0.20	0.12	0.19	0.26	0.55
Pb-s	0	0.14	-0.03	0.61	0.95	1.28	2.76
Zn-t	4.93	0.15	0.65	3.67	6.45	8.20	20.95
Zn-d	9.63	0.16	0.93	0.61	2.77	4.05	8.71
Zn-s	-4.70	-0.01	-0.28	3.06	3.68	4.15	12.24
Total load	50.04	3.25	45.11	125.43	212.44	337.10	507.19
Total dissolved load	38.06	1.05	116.35	138.61	81.15	203.69	241.58
Total suspended load	11.98	2.19	-71.24	-13.18	131.30	133.41	265.61

sample (SW-1) in July. Negative suspended loads are invalid and represent an error in the laboratory analyses. All negative suspended loads are assumed to have metals entirely in the dissolved form.

August loads are much decreased from the loads in July. The trends are similar to July, but on a smaller scale. As in July, iron has the highest calculated loads. Dissolved arsenic and dissolved copper were only detected in samples GW-3 and SW-1 in August, and dissolved lead was not detected at any sample location in August. The loads for the metals that were not detected were calculated using a concentration of half of the

Table 4. Loading rates of metals of concern (mg/s) in August. Zeroes indicate an insignificant value.

8/5/2011	SW-1	GW-3	SW-5	SW-6	SW-7	SW-8
As-t	0.07	0.26	0.38	0.55	0.69	0.81
As-d	0.07	0.16	0.47	0.69	1.15	2.02
As-s	0	0.10	-0.09	-0.14	-0.46	-1.21
Cu-t	0.30	0.06	0.47	0.55	2.07	0.81
Cu-d	0.07	0.05	0.38	0.55	0.92	1.62
Cu-s	0.22	0.01	0.09	0	1.15	-0.81
Fe-t	18.48	10.62	13.98	13.71	28.31	48.51
Fe-d	3.33	3.07	1.22	5.95	2.97	10.43
Fe-s	15.15	7.55	12.76	7.75	25.34	38.08
Mn-t	0.74	5.43	2.64	1.25	1.84	1.21
Mn-d	0.15	5.70	1.40	0.57	0.25	1.09
Mn-s	0.59	-0.27	1.25	0.68	1.59	0.12
Pb-t	0.15	0.02	0.09	0.14	0.46	0.40
Pb-d	0.04	0.01	0.05	0.07	0.12	0.20
Pb-s	0.11	0.01	0.05	0.07	0.35	0.20
Zn-t	1.03	0.30	1.98	2.08	5.29	4.85
Zn-d	0.81	0.45	3.78	2.31	2.60	4.24
Zn-s	0.22	-0.15	-1.79	-0.24	2.69	0.61
Total load	20.77	16.68	19.55	18.28	38.67	56.59
Total dissolved load	4.47	9.45	7.29	10.15	8.01	19.60
Total suspended load	16.30	7.24	12.26	8.13	30.66	36.99

detection limit. The total loads decrease from SW-1 to SW-6, while the dissolved loads increase, with the exception of GW-3. There is a jump in suspended and dissolved loads at the lower portion of the creek, which is mainly due to the addition of SW-7. Overall, SW-8 has the highest load values for each metal.

The metals loads in October are roughly half the magnitude of the loads in August, with the exception of the loads for the metals that were not detected and were calculated using half of the detection limit. These values would remain similar from month to month so long as the discharges remain relatively constant, because the detection limit at the lab is the same. Yet again, iron dominates the system. This time,

Table 5. Loading rates of metals of concern (mg/s) in October. Zeroes indicate an insignificant value.

10/1/2011	SW-1	GW-3	SW-5	SW-6	SW-7	SW-8
As-t	0.04	0.27	0.32	0.30	0.12	0.48
As-d	0.09	0.09	0.15	0.25	0.31	0.80
As-s	-0.05	0.18	0.17	0.05	-0.18	-0.32
Cu-t	0.05	0.05	0.20	0.15	0.06	0.48
Cu-d	0.07	0.07	0.12	0.20	0.24	0.64
Cu-s	-0.02	-0.02	0.09	-0.05	-0.18	-0.16
Fe-t	3.35	12.34	11.19	5.38	4.94	18.67
Fe-d	0.37	3.61	0.04	0.42	0.09	0.24
Fe-s	2.98	8.73	11.15	4.96	4.85	18.43
Mn-t	0.43	7.19	3.53	0.45	0.12	1.28
Mn-d	0.04	6.87	0.08	0.03	0.03	0.26
Mn-s	0.39	0.32	3.45	0.43	0.09	1.02
Pb-t	0.04	0.04	0.17	0.10	0.06	0.48
Pb-d	0.01	0.01	0.01	0.03	0.03	0.08
Pb-s	0.03	0.03	0.16	0.08	0.03	0.40
Zn-t	0.61	0.54	0.70	1.26	0.98	3.99
Zn-d	0.29	0.60	0.60	0.73	0.70	3.05
Zn-s	0.32	-0.05	0.10	0.52	0.27	0.94
Total load	4.52	20.44	16.12	7.64	6.28	25.37
Total dissolved load	0.87	11.25	0.99	1.65	1.40	5.06
Total suspended load	3.65	9.19	15.13	5.98	4.88	20.31

dissolved metals were not detected for arsenic, copper, and lead, and only detected in low concentrations, if at all, for iron and manganese.

Most of the metals remain entirely in the suspended form at the lower reach of the creek. Zinc is the only metal that has a significant dissolved load at the lower reach of the creek. Dissolved zinc loads are greatest in SW-8 in all months. It is likely that the slag waste pile presents a separate source of zinc, which contributes to SW-8. Again, SW-8 has the greatest total load of all of the locations sampled, though GW-3 and SW-5 have the next highest load contributions.

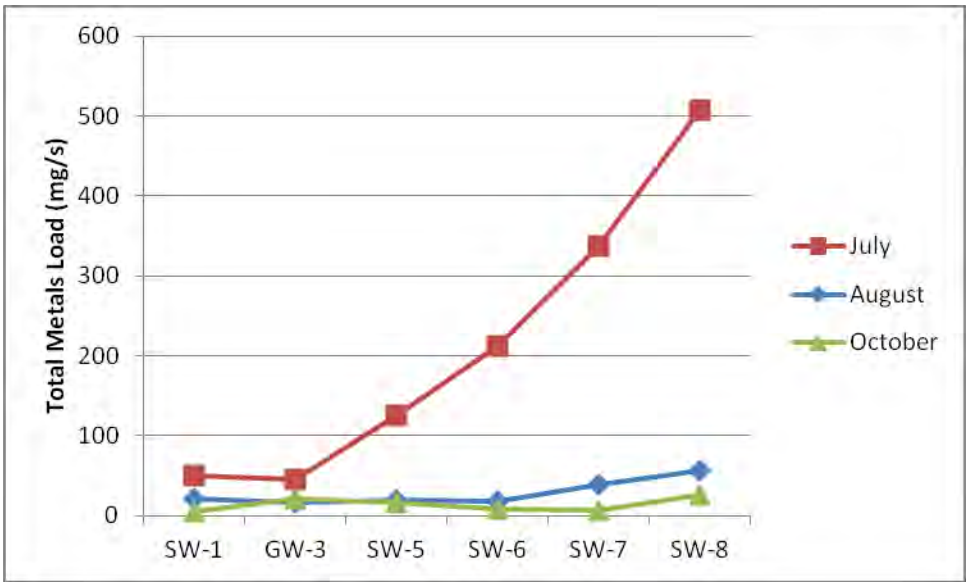

Figure 14. Total loads of metals of concern along study reach at every sampling site. Study sites are oriented from west to east, with the easternmost sites downstream.

Figure 14 shows the total loads of all six metals of concern (sum of arsenic, copper, iron, lead, manganese, and zinc) throughout the study reach for each sampling month of interest. The total loads in July showed the most drastic increase from upstream to downstream. Both August and October had similar total loads at each site, the only difference being that the August values were slightly higher because the discharge was slightly greater in August than in October.

In October, the total load at GW-3 was greater than at SW-1, SW-5, and SW-6. Downstream from the input of GW-3, SW-5 showed a slightly lower total load than SW-1 in August as well. The total load at SW-6 was less than at SW-5 in both August and October.

Sediment Sample Analyses

Sediment samples collected from the tailings pile (SS-2), four streambed locations (SW-1 SS, SW-5 SS, SW-6 SS, and SW-8 SS), the sediment at GW-1 (GW-1 SS), and the bedrock at site GW-1 (GW-1 ROCK) were dried, sorted with a 1-tier, 50 mm width steel splitter, and then crushed into a powder before processing for analysis. SS-2 and SS-2a were analyzed on the XRD for elemental results. Sample SS-2a is a duplicate sample of the tailings sample (SS-2). All samples other than the rock sample at GW-1 were analyzed on the XRF for elemental and oxide results. Four samples in the upper portion of the creek were chosen to be analyzed by the UVDL because they were adjacent to the water samples with the highest concentrations of metals. SS-2a, SW-1 SS, SW-5 SS, and GW-1 ROCK were run on the ICP-MS in order to compare the sediment and rock samples with the water samples.

XRD

The peak results are shown in Appendix E. Scores are determined from Relative Intensity percentages [Rel. Int. (%)], which are calculated by dividing the intensity of the peak at the angle indicated by the intensity of the highest peak then multiplying by 100. Both samples show similar results. As summarized in Tables 6 and 7, the dominant minerals appear to be quartz, illite, kaolinite, and siderite.

XRF

Sediment samples collected from the stream bottom at locations SW-1, SW-5, SW-6, and SW-8 show clay to cobble grain sizes. These samples were run using an XRF

to determine major ion ratios. Weight percents were normalized using the equation below:

100/X and (100-R)/SA

where X = sum percent of total weight percents, R = sum of all weight percents other than SiO_2 and Al_2O_3, and SA = raw value + SiO_2 normalized weight percent. A summary of weight percents and concentrations in ppm is presented in Tables 8 and 9. Three of the concentrations are calculated as negative values (CaO for GW-1 ROCK, and Sc for SW-5

Table 6. Mineral peak results for tailings sample (SS-2).

Visible	Ref. Code	Score	Compound Name	Displacement [°2Th.]	Scale Factor	Chemical Formula
*	00-046-1045	74	Quartz, syn	-0.026	0.852	SiO_2
*	00-026-0911	47	Illite-2M1 (NR)	0.046	0.371	$(K,H_3O)Al_2Si_3AlO_{10}(OH)_2$
*	00-058-2006	38	Kaolinite-1Ad	0.009	0.040	$Al_2Si_2O_5(OH)_4$
*	00-012-0531	29	Siderite	-0.018	0.100	$FeCO_3$
*	00-058-2025	49	Glauconite, heated	0.023	0.167	$(K,Na)(Fe,Al,Mg)_2(Si,Al)_4O_{10}(OH)_2$

Table 7. Mineral peak results for re-run of tailings sample (SS-2a).

Visible	Ref. Code	Score	Compound Name	Displacement [°2Th.]	Scale Factor	Chemical Formula
*	00-046-1045	66	Quartz, syn	-0.030	0.858	SiO_2
*	00-058-2016	54	Illite-2M2, glycolated	0.013	0.325	$(K,H_30)Al_2(Si_3Al)O_{10}(OH)_2 \cdot xH_2O$
*	00-058-2006	39	Kaolinite-1Ad	0.005	0.076	$Al_2Si_2O_5(O H)_4$
*	00-052-1044	46	Chlorite-serpentine (NR)	-0.059	0.068	$(Mg,Al)_6(Si,Al)_4O_{10}(OH)_8$
*	00-003-0746	23	Siderite	0.077	0.125	$FeCO_3$
*	00-042-1425	18	Selenium	0.227	0.039	Se

SS and SW-8 SS). This is a feature of the analytical program when the detections are below the limit of the instrument. The instrument attempts to give a value to the element even though the value is too small to detect and below the standard value. I will take these values to indicate that the element is not present in my sample.

Table 8 presents the weight percent of oxides found in each sediment sample. Silicon and aluminum oxides dominate the sediment and rock samples. This suggests the dominant composition of minerals found in the sediments and bedrock are silicates such as quartz and muscovite, which correlates well with the known Ramshorn Slate mineralogy and XRD results. Iron and manganese oxides are present in lower weight percents.

The concentrations in ppm of certain metals found within the sediment samples are displayed in Table 9. Sample SW-8 SS has an elevated concentration of zinc, 2,228 ppm, almost ten times greater that the zinc concentrations found in the sample with the second highest concentration (SW-5 SS). The sulfur concentration found in the creek

Table 8. XRF results for soil and rock samples taken during September collection period as weight percents. Majority of sample percents dominated by SiO_2 and Al_2O_3 after correction factor applied.

Sample	SW-1 SS	SW-5 SS	SW-6 SS	SW-8 SS	GW-1 SS	GW-1 ROCK
Al_2O_3 wt %	20.926	21.231	25.003	24.208	26.357	30.665
CaO wt %	1.214	1.399	0.645	1.699	0.012	-0.013
Fe_2O_3 wt %	4.952	8.317	6.691	9.608	9.404	5.216
K_2O wt %	3.232	3.863	3.536	3.409	3.148	4.576
MgO wt %	0.876	1.279	1.440	1.549	2.192	1.671
MnO wt %	0.059	0.350	0.126	0.308	0.078	0.040
Na_2O wt %	1.007	1.353	1.427	1.170	0.937	1.184
P_2O_5 wt %	0.184	0.157	0.110	0.141	0.142	0.064
SiO_2 wt %	66.848	61.359	60.246	57.182	56.950	55.582
TiO_2 wt %	0.701	0.691	0.778	0.725	0.778	1.015
Sum wt%	100.000	100.000	100.000	100.000	100.000	100.000

Table 9. Concentrations of trace elements on XRF in parts per million.

	Ba	Ce	Cr	Cu	La	Nb	Ni	Rb	S	Sc	Sr	V	Y	Zn	Zr
SW-1 SS	814	60	81	16	55	18	23	100	18	15.7	217	73	22	68	199
SW-5 SS	1015	72	105	1729	47	15.9	36	115	1360	-266.7	273	76	27	256	173
SW-6 SS	847	66	191	40	66	16.8	41	153	13	6.8	210	112	38	133	197
SW-8 SS	714	55	109	257	45	11.5	41	104	465	-13.2	173	100	50	2228	160
GW-1 SS	504	51	149	73	68	12.3	45	150	261	3.7	90	114	38	129	173
GW-1 ROCK	692	64	183	10	66	14.8	24	228	331	11.3	135	132	47	68	221

sediment sample directly downstream from the tailings pile (SW-5 SS) is 1,360 ppm, nearly triple the next highest sample concentration, which is found in the town site creek sediment (SW-8 SS). Copper in SW-5 SS is 1,729 ppm, which is almost seven times the concentration in the next highest sample (SW-8 SS), which had a concentration of 257 ppm.

ICP-MS

The four sediment and rock samples shown in Table 10 were also run through the UVDL ICP-MS for additional metals concentration data. The samples at the upper end of the study reach were chosen for analysis on the ICP-MS as a fine-tuned examination of the elements in the sediments and rock samples near the highest sources of potential contamination. The upper reach was the area of greatest concern based on the analytical results from the water samples, as well as the location of the chemical modeling. The sediments at the lower end of the reach did not seem to be as pertinent to the study at the time the analyses were run.

The sediments found in SS-2a, SW-1 SS, SW-5 SS, and GW-1 ROCK show similar results to those found in the water samples in that iron occurs in the highest

Table 10. ICP-MS analysis of sediment and rock samples in mg/L.

	As	Cu	Fe	Mn	Pb	Zn
SW-1 SS	13	10.95	19516.49	299.99	17.97	46.74
SS-2a	2868.38	328.3	64307.72	4233.93	1383.41	510.23
SW-5 SS	714.47	1898.08	38797.34	2470.02	278.25	227.78
GW-1 ROCK	3.27	8.83	24340.61	219.7	2.09	42.88

concentrations. Manganese is not found in as high concentrations as iron. Arsenic, copper, lead, and zinc occur in high concentrations in SS-2a and SW-5 SS, but not in SW-1 SS or GW-1 ROCK.

Metals Phase and Oxidation State

PHREEQC results for August samples GW-3 and SW-1 are shown in Appendix F. The calculated elemental compositions are listed before the saturation indices. Solution 1 represents SW-1, the upstream portion of the creek, solution 2 represents GW-2, the flowing well, and solution 3 represents GW-3, the draining adit at the lower end of the tailings pile. Mix 1 represents the mix of 99% SW-1 and 1% of GW-2, as these reflect the relative discharges of surface water inflow and groundwater baseflow into the creek. GW-2 and SW-1 are mixed because GW-2 is derived from groundwater directly upstream of the mine tailings pile, which may represent groundwater that mixes with the creek downstream of SW-1 but upstream of GW-3. Mix 2 represents the mix of 79% Mix 1 and 21% GW-3 based on the contribution of the draining adit to the discharge of the creek.

Chemical inputs based on averages with Piper (1944) diagrams (Wanty et al., 2004) were used to compare the chemical results from the model mixes. I compared the

results from Mix 2 to SW-5 as a way to check that the chemistry was a result of mixing between Mix 1 and GW-3.

The values shown in Tables F.1 through F.5 of Appendix F are molalities for elements and saturation indices for mineral phases. Higher molalities indicate a greater concentration in the elemental makeup of the system. The mineral phases with the highest saturation indices are highlighted in bold in Appendix F.

A positive, zero, or negative saturation index reflects supersaturation, equilibrium, or undersaturation, respectively, of the mineral in question. Only positive values are listed in Appendix F because they indicate the likelihood of precipitation of metals, which will transfer them from the dissolved to the suspended state. The larger the saturation index value, the more supersaturated the mineral; however, molal values are not calculated for minerals in PHREEQC. It should also be noted that a positive saturation index value does not necessarily indicate mineral precipitation, because kinetics control the rate of mineral precipitation.

Certain minerals associate with metals. They are usually insoluble or have components also found in mine waste (Smith, 2007). A list of minerals that control metal concentrations was created by Nordstrom and Alpers (1999). The minerals include alunogen ($Al_2(SO_4)_3 \cdot 17H_2O$), anglesite ($PbSO_4$), basaluminite ($Al_4(SO_4)(OH)_{10} \cdot 5H_2O$), calcite ($CaCO_3$), cerussite ($PbCO_3$), chalcanthite ($CuSO_4 \cdot 5H_2O$), epsomite ($MgSO_4 \cdot 7H_2O$), ferrihydrite ($Fe^{3+})_2O_3 \cdot 0.5H_2O$), gibbsite ($Al(OH)_3$), goslarite ($ZnSO_4 \cdot 7H_2O$), gypsum ($CaSO_4 \cdot 2H_2O$), halotrichite-pickeringite ($(Fe,Mg)Al_2(SO_4)_4 \cdot 22H_2O$), manganese oxides ($Mn_nO_n$), melanterite ($FeSO_4 \cdot 7H_2O$), otavite ($CdCO_3$), rhodochrosite ($MnCO_3$), schwertmannite ($Fe_8O_8(OH)_6(SO_4) \cdot nH_2O$ or

$Fe^{3+}_{16}O_{16}(OH,SO_4)_{12\text{-}13}\cdot 10\text{-}12H_2O$), scorodite ($FeAsO_4\cdot 2H_2O$), siderite ($FeCO_3$), microcrystalline silica (SiO_2), smithsonite ($ZnCO_3$), and witherite ($BaCO_3$).

Bixbyite, birnessite, cupricferrite, hausmannite, hematite, maghemite, magnesioferrite, magnetite, nsutite, and pyrolusite are especially supersaturated in solution 1 (Table F.1). The minerals with the highest saturation indices are highlighted in bold. These compounds are iron, manganese, and copper oxides. The remaining compounds with positive saturation indices are predominantly iron, manganese, copper, and aluminum hydroxides, oxides, or oxyhydroxides.

Solution 2 has supersaturation results of bixbyite, birnessite, cupricferrite, hematite, hausmannite, maghemite, magnesioferrite, magnetite, nsutite, and pyrolusite (Table F.2). The remaining minerals are predominantly aluminum, calcium, copper, iron, magnesium, and manganese oxides, hydroxides or oxyhydroxides.

Solution 3 shows high saturation indices for bixbyite, birnessite, cupricferrite, hematite, maghemite, magnetite, nsutite, and pyrolusite (Table F.3). These are iron and manganese oxides. The remaining minerals are aluminum, copper, iron, and manganese oxides, hydroxides or oxyhydroxides.

As expected, the mix of solution 1 and solution 2 shows that this mixture is nearly identical chemically to solution 1 (Table F.4). The chemistry appears to be similar to SW-5. Mix 1 has large positive saturation indices of the manganese oxides birnessite, bixbyite, hausmannite, manganite, nsutite, and pyrolusite. The iron oxides consist of cuppricferrite, hematite, maghemite, magnesioferrite, and magnetite. These results indicate that iron and manganese are the metals most likely associated with precipitated solids in Mix 1.

Mix 2 (Table F.5) has very similar results to mix 1. Manganese oxides (birnessite, bixbyite, hausmannite, nsutite, and pyrolusite) and iron oxides, hydroxides, and oxyhydroxides (cupricferrite, hematite, maghemite, magnesioferrite, and magnetite) dominate the saturation indices. The modeling suggests that iron and manganese are more likely to precipitate out of solution in the water samples, with a smaller presence of aluminum, calcium, magnesium, and silicon oxides, hydroxides, and oxyhydroxides.

Speciation distribution calculations are shown in Appendix G. They quantify the molality for various species of metal complexes. The higher molality values indicate a higher presence of individual metal speciation, which indicates the oxidation state and the mobility of the metal. Using pre-existing knowledge of metals speciation mobility, the likelihood of transport can be predicted from these values.

Most elements in my results only occur in one oxidation state, but metals such as arsenic, copper, and iron may occur in two or more oxidation states based on their chemical structure. The speciations are modeled in the PHREEQC program for sites SW-1, GW-2, and GW-3 in August. Because of the spatial and temporal constraints on the data, only these sites are compared to understand the upstream surface water, groundwater, and their mixed speciation. Molalities smaller than 10^{-5} are disregarded in species identification. Percentages of each oxidation species have not been calculated because the majority of species were the only species present.

Based on results in Tables G.1, G.2, G.3, G.4 and G.5, arsenic occurs exclusively in the form As^{5+} in mix 1 and mix 2. Arsenic in the form As(5) is about 60 times less toxic than in the form As(3) (Jain and Ali, 2000; from Ferguson and Gavis, 1972). The

model shows that iron occurs as Fe^{3+}, and manganese and zinc occur only in the +2 oxidation state in both mix 1 and mix 2.

Table H.1 shows the results for surface sorption at strong and weak HFO sites. According to Table H.1, the strong binding sites of HFO are most available for arsenic, lead, and zinc when reacted with mix 1 and mix 2. The weak binding sites of HFO also mostly react with arsenic as shown in Table H.1. Since there was very little chemical difference between mix 1 and mix 2, it is expected that the HFO sorption sites would look quite similar for the two mixes.

DISCUSSION

Ramshorn Mine Site Hydrology

The peak flow of Bayhorse Creek occurred in the month of June, as evidenced by a road wash-out on June 24, which prevented access to the study site. By the time of the first site visit on July 11, few snow patches remained on the peaks and spring run-off was mostly complete. No snow remained below the study area. A peak flow during the month of June along the Salmon River demonstrated the month delay of Idaho spring runoff in 2011 (NRCS, 2012).

Discharge values were greatest in all stream and tributary channels during the July data collection period and successively decreased throughout the following three months (Table 2). The creek segment SW-1 to SW-5 lost 15.06 L/s to infiltration, but then gained 345.30 L/s between sites SW-5 and SW-8 from groundwater inflow. GW-3 contributed 25.13 L/s of flow to the total discharge at SW-5. SW-7 contributed 512.31 L/s of flow to the total discharge at SW-8. Therefore, tributaries contributed a total of 537.44 L/s to the total flow of 1102.59 L/s and the system had a net gain of 330.24 L/s from groundwater inflow. However, the upper segment of the study reach, SW-1 to SW-5, lost water to the groundwater, eliminating that pathway for metals to enter the stream. In July minor discharges were measured for the upper tailings pile seep (GW-1) and for the flowing well (GW-2) at 0.79 L/s and 0.06 L/s, respectively.

The second data collection period occurred on August 5, 2011. The total flow of Bayhorse Creek had decreased by more than half its flow in July (from 1102.59 L/s to 404.23 L/s). The two tributaries GW-3 and SW-7 contributed 250.21 L/s to the total flow.

Between SW-1 and SW-5 Bayhorse Creek gained 0.50 L/s. During this acquisition period, much of the land surrounding the creek was completely saturated with groundwater seepage, indicating a significant contribution of groundwater into the creek. This was observed when field boots sank into nearly a foot of mud. August was the only month that could be modeled for groundwater-surface water mixing because it was the only month that the upper segment of the creek was a gaining stream.

During the third data collection period on September 1, the creek lost 8.73 L/s to the groundwater system between SW-1 and SW-5, but gained 74.37 L/s between SW-5 and SW-8. The loss of surface water to groundwater between SW-1 and SW-5 may be attributed to a lowering of the water table due to a decrease in snow runoff saturating the ground at higher elevations. GW-3 contributed 15.54 L/s to the discharge at SW-5. GW-3 and SW-7 contributed 107.67 L/s to the total discharge at SW-8 of 199.56 L/s during September.

The creek lost 6.93 L/s of flow to the groundwater system between SW-1 and SW-5 on October 1, during the fourth and final collection period. As expected, surface water continued to infiltrate into the groundwater system as the water table dropped throughout the dry summer season. GW-3 contributed 18.15 L/s to the discharge at SW-5. Tributaries GW-3 and SW-7 contributed 79.16 L/s to the total discharge at SW-8 of 159.54 L/s during October.

The discharge at site GW-1 decreased each month. The discharge at GW-2 remained constant at 0.06 L/s for the entire field season. The discharge at GW-3 decreased consistently between July, August, and September, and then slightly increased

in October. The slight increase in October may reflect the actual fluctuation of the flow within the draining adit during base flow, or it may be a field measurement error.

The general decrease in the discharges at GW-1 and GW-3 indicates a decrease in infiltration as the water table dropped, resulting in a smaller amount of water flowing through the mine waste. A similar decrease in discharge was measured for the surface water system. A loss in groundwater discharge throughout the dry summer months suggests that the shallow groundwater system is directly affected by spring runoff. The shallow groundwater that interacts with the mining waste has a low residence time, and will not produce the amount of dissolved metals that groundwater with a longer residence would be able to produce.

Chemical Results

Dissolved Oxygen

The groundwater sample GW-1 showed some of the highest levels of dissolved oxygen (Tables C.2, C.3, and C.4 in Appendix C). This suggests that the water seeping through the fractures in the rock are in an oxidizing environment. GW-2 also showed high dissolved oxygen levels indicating an oxidizing environment at an unknown depth. GW-3 had the lowest dissolved oxygen values indicating a reducing environment. GW-3 also had some of the highest metals concentrations.

Dissolved oxygen in surface water samples followed the trend to remain constant or decrease throughout the study period. The samples in August remained around 11 mg/L while September surface water samples measured closer to 12 mg/L. October values drop for sites SW-5, SW-6, and SW-8, but the values at sites SW-1 and SW-7

remain roughly the same. The decrease in dissolved oxygen for sites SW-5, SW-6, and SW-8 may be explained by a decrease in water sourced from snowmelt runoff and an increase in groundwater baseflow. SW-1 and SW-7 may remain at similar dissolved oxygen values from July to October because they are not affected by the mine site.

pH

Overall the pH values were neutral to slightly alkaline (Figure 12). This suggests the absence of acid mine drainage and the influence of a neutralizing chemical reaction such as carbonate dissolution. The Bayhorse Dolomite contains an abundance of carbonate, which provides bicarbonate to the water and would buffer acidic metals reactions. Another possibility is that there are no oxidation reactions taking place in the groundwater system to create excess protons and reduce the pH. Although dissolved oxygen results suggest that the groundwater seeps (except GW-3) are sourced from an oxidizing environment, the kinetics of the reaction may be too slow to run in the short residence time that the groundwater remains at depth. As suggested by the dissolved oxygen values in the flowing well at GW-2, the groundwater may not be anoxic at depth, indicating that there is a source of oxygen in the subsurface.

Piper Diagrams

Piper (1944) diagrams were created using the sample results to characterize the hydrochemical facies of all the sample locations. The results show similar values for most of the surface and groundwater samples, which plot in the calcium-magnesium-bicarbonate facies. This may reflect the influence of local rock types, which consist mainly of slates and carbonates. However, SW-2, SW-3, and SW-4 plotted closest to the

magnesium-sulfate facies type, which suggests a source of metals likely from the tailings pile where these samples were collected.

In Figures 13(a-d), GW-3 plotted in the magnesium-bicarbonate facies, indicating the highest proportion of magnesium of any sample except SW-2, SW-3 and SW-4. SW-1 plots in the lowest corner, indicating the highest proportion of calcium and bicarbonate. Based on appearance and previous sampling, the creek upstream of the tailings was expected to contain the lowest sulfate and magnesium proportions. GW-1 and GW-3 both tend to plot at a higher ratio along the sulfate axis, which is more typical of acid mine water. GW-1 and GW-3 are the samples with the highest metals concentrations, and are more like mine waters than any other water samples other than SW-2, SW-3 and SW-4. GW-1 may indicate a source of metals contamination from a higher location than the waste rock slope.

The calcium-magnesium-bicarbonate type water, indicated by the Piper diagrams, is expected because the pH values range mostly from 7-9, and thus in an open system bicarbonate should be the dominant carbonate species.

GW-3 may interact with the uncontaminated upper portion of the creek (SW-1) to create an intermediate facies type, as SW-1 and GW-3 appear to mix to create the water type found at SW-5. SW-6, SW-7 and SW-8 all appear to have similar chemistries because they are located downstream of the mine workings, reflecting the influences of dilution by both surface and groundwaters and of the bedrock in that area.

Ore Classification

Figure 15(a) shows the general locations of water sample metals concentrations plotted against pH as recorded by Plumbee and Nash (1995; reprinted in Smith, 2007).

The values of mine water and natural water are plotted on these axes, and are used to classify the type of hard rock contamination based on the location of the values. The y-axis displays the summation of cadmium, copper, cobalt, lead, nickel, and zinc concentrations in unfiltered water samples on a log scale, and the x-axis plots the corresponding pH values. Cadmium, cobalt, and nickel did not appear in any of my water samples and do not contribute any value to my concentrations.

Figure 15(b) was created to show how my samples look when plotted along the axes of Figure 15(a). The pattern indicates that the samples classify as either pyrite-sphalerite-galena-chalcopyrite veins in rocks with high carbonate contents or in rocks altered to contain carbonate minerals, or pyrite-poor sphalerite-galena veins and replacements in carbonate-bearing sedimentary rocks. Large samples of galena were collected from the mine site, which would support either type of mineral assemblage. Although carbonate minerals (calcite, aragonite, dolomite) were not observed within the immediate bedrock, carbonate rocks do appear above and below the Ramshorn Slate in the Bayhorse anticline, and Piper diagrams show a predominance of bicarbonate in most samples. Furthermore, although the bedrock is not considered carbonate-bearing sedimentary rocks, the dominant ore bodies were taken from a low-grade metamorphosed slate formation containing carbonate units.

Pyrite only occurs in trace amounts within the ore mineralization in the Bayhorse region (Seal and Rye, 1992), suggesting that the ore at the Ramshorn mine classifies as

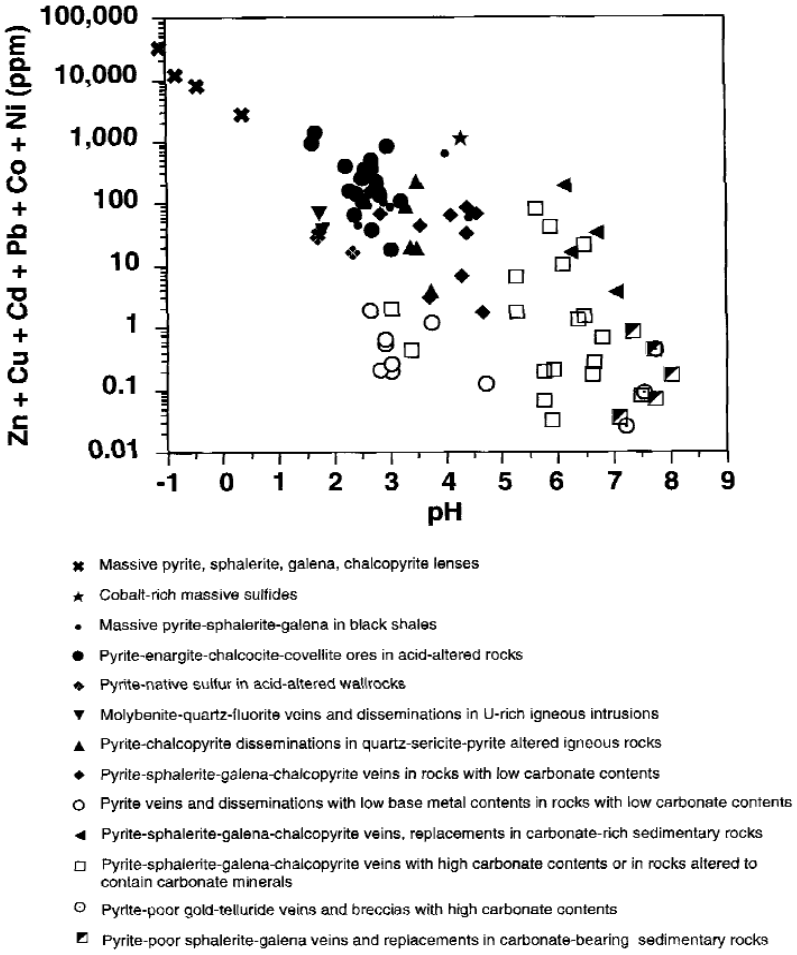

a

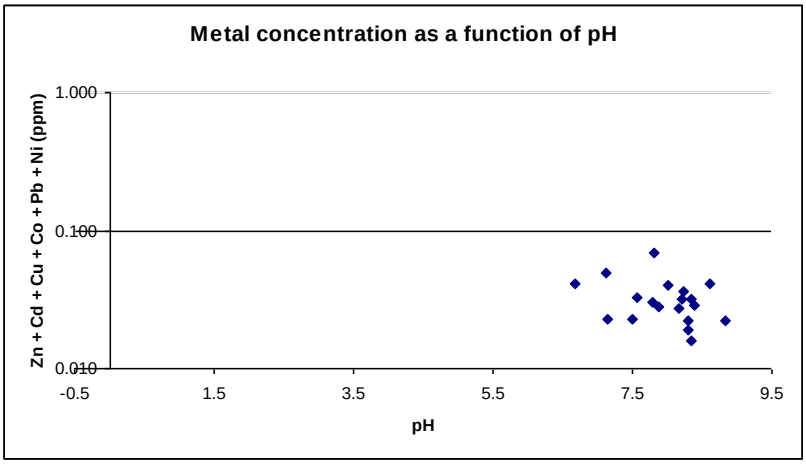

b

Figure 15(a). Metals concentrations as a function of pH for all water samples (Plumlee and Nash, 1995). Variations in aqueous base metal concentrations (given as the sum of base metals zinc, copper, cadmium, cobalt, nickel, and lead) as a function of pH for water draining various types of mineralized rock in diverse sites within Colorado. Figure 15(b) shows Ramshorn samples plotting in the pyrite-poor sphalerite-galena type veins.

pyrite-poor sphalerite-galena veins. The lack of pyrite in the rock and ore explains the absence of acid production in the ground and surface waters, since the dissolution of pyrite is the primary source of excess protons.

Metals Loading Rates

The metals loading rates shown in Tables 3, 4, and 5 indicate that loads tend to increase from SW-1 to SW-8 during July. August and October loads do not show as large an increase from SW-1 to SW-8. These patterns are also shown graphically in Figures 14 and 16(a-c).

Figure 16(a) shows that suspended and dissolved iron dominate metals loads in July. A large increase in dissolved and suspended iron – and to a lesser degree manganese and zinc – can be seen from SW-1 to SW-8. All other metals occur in loads too small to generate any noticable patterns.

Suspended and dissolved iron, manganese, and zinc also dominate metals loads during August. Suspended iron decreases from SW-1 to SW-6, but increases again at SW-8. Suspended iron at site SW-8 far exceeds the load of any other metal. The mix of SW-7 with SW-6, appears to equal the level at SW-8. The level of iron in SW-7 suggests that the mine tailings and waste pile are not the sole contributor of iron to the creek.

The metals loads in October are much lower than the loads during July and August, and there is less variance between the dissolved and suspended loads. In fact, the suspended iron load at GW-3 exceeds the load at SW-6. Again, suspended iron dominates the metals loads at SW-8 and, as seen in July and August, both suspended iron and suspended zinc have the largest increases between SW-1 and SW-8.

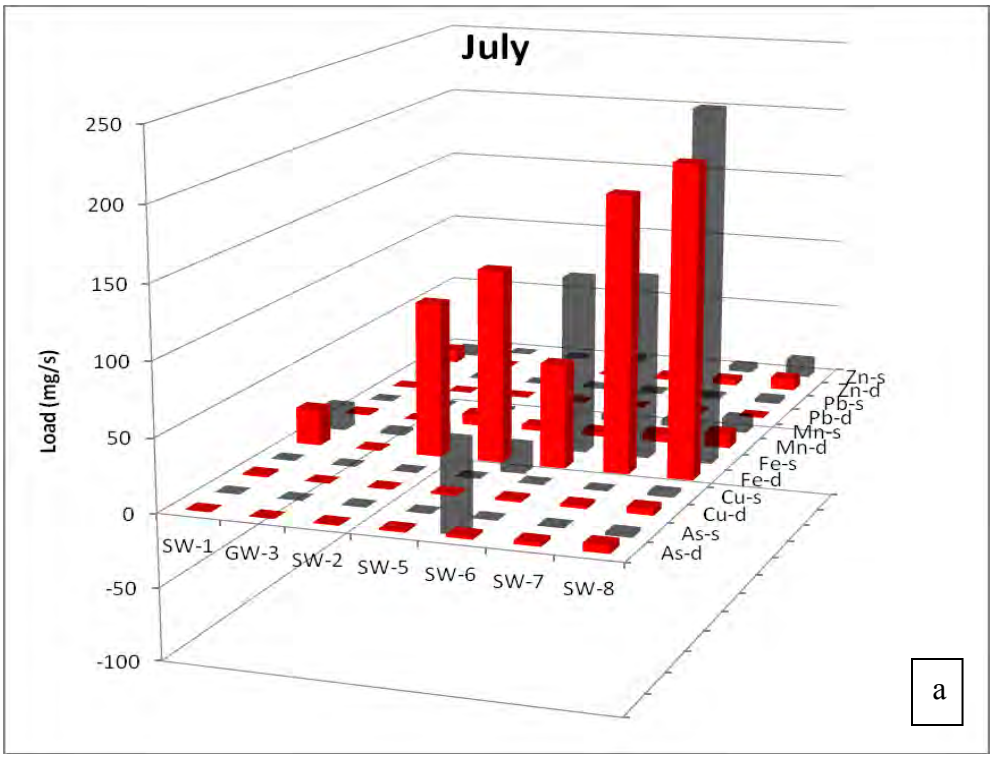

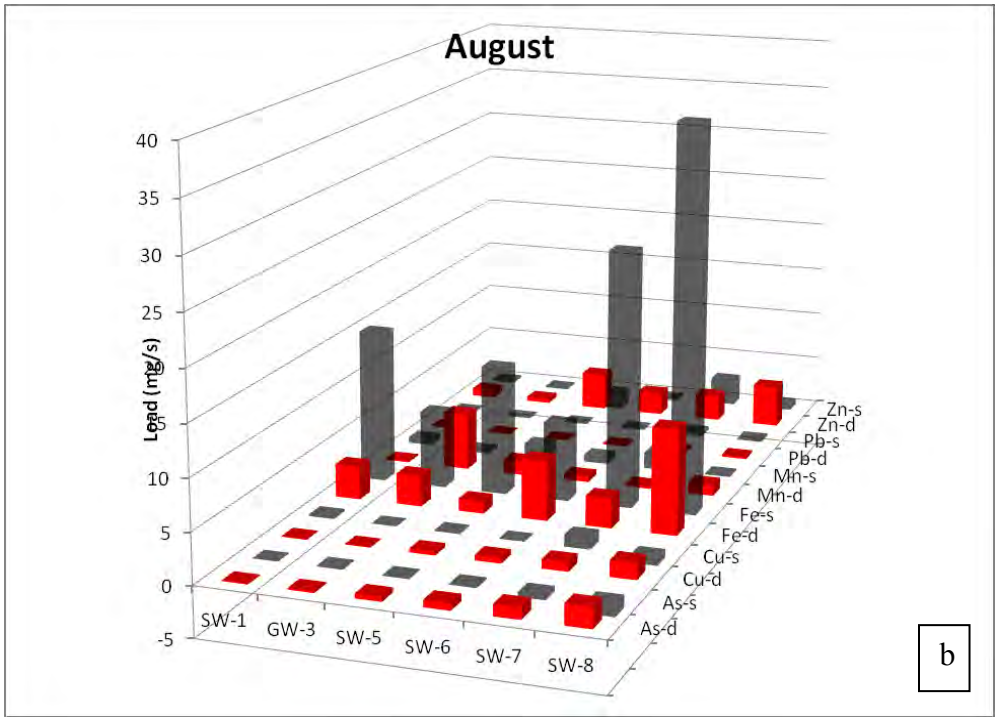

Figure 16. Loads (mg/s) from suspended (black) and dissolved (red) metals from water samples GW-1, SW-1, SW-5, SW-6, and SW-8 for July (a), August (b), and October (c). Note changes on the y-axis scale.

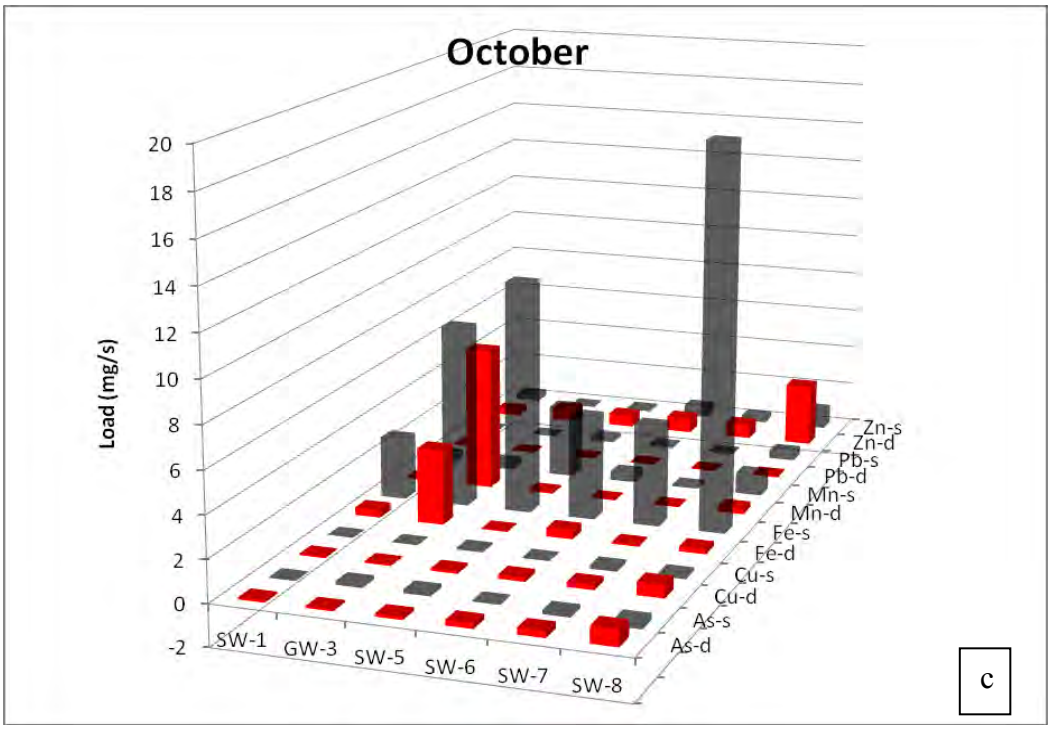

Figure 16 (Cont.)

The loads decrease by an order of magnitude from July to August. The discharge rate decreases with a proportional decrease in metals loading. If the surrounding watershed sediments are contaminated, we should expect increased runoff to increase the load, but in Bayhorse Creek, it appears that a higher discharge would not increase the metals load (Salomons, 1995). The surrounding sediments – tailings and waste rock – may be the main contributor to the increases in the loads during high flows. The decreased discharge would explain the lower metals loads during baseflow.

The percent suspended solids have been calculated from the ICP and ICP-MS data by subtracting the dissolved loads from the total loads and then dividing by the total loads. Table 11 shows samples from August, which were modeled for metals transport along the stream reach. The values would be expected to be positive because total concentrations should be greater than dissolved concentrations, but a few of the values

are negative indicating a discrepancy between the analyses of the filtered and unfiltered samples. Arsenic, copper, and lead are not shown because the loads were not large enough to be significant.

High suspended solid percentages suggest that a metal may be sorbed to other inorganic species or to particulate matter in the water column. The presence of hydrous iron oxides creates weak and strong surface sites for metals sorption.

Oddly, dissolved manganese and zinc in August were greater than the total manganese and zinc at site GW-3, likely caused by a laboratory error. Also, dissolved zinc is greater than total zinc at sites SW-5 and SW-6.

Table 11. Percent of metals in the form of suspended solids. Arsenic, copper, and lead did not occur in high enough concentrations to calculate.

August	SW-1 %	GW-3 %	SW-5 %	SW-6 %	SW-7 %	SW-8 %
Fe	82%	71%	91%	57%	90%	79%
Mn	80%	-5%	47%	54%	86%	10%
Zn	21%	-51%	-90%	-11%	51%	13%
Total	78%	41%	69%	51%	87%	69%

In samples where dissolved loads are higher than total loads, the differences between the filtered and unfiltered concentrations may just be a result of minor variation between two similar water samples. The dissolved values that are higher than the total values are usually only greater by a few hundredths of a unit (mg/L). These discrepancies may indicate that there were no suspended sediments to increase the unfiltered concentration (i.e., due to analytical variation). For samples with a greater discrepancy between the dissolved and total load, I assume that there was an error in the analysis at

the laboratory. In all cases, it is best to assume that the metals are entirely in the dissolved form.

Net flux values (Tables 12, 13, and 14) were calculated by subtracting a downstream load from an upstream load to determine the change in loading along a stream section. In cases where the suspended load was negative due to laboratory errors, the load was calculated as zero in the flux calculations. This occurred in the upper and middle segments in July for suspended iron, the upper segment in July for suspended zinc, and the upper and middle segments in August for suspended zinc. The net flux represents the total change of metals load from the uppermost site of the Bayhorse Creek study area (SW-1) to the site directly downstream of the tailings and groundwater seep (SW-5), as well as between the two creek sites upstream and downstream of the town site (SW-6 and SW-8, respectively). Negative values indicate that metals are decreasing throughout the reach of the creek. The stream sections that pose the most likely source of metals are between SW-1 and SW-5, upstream and downstream of the tailings pile, and between SW-6 and SW-8, upstream and downstream of the slag waste at the town site.

The iron fluxes are dominant during July, and suspended iron is dominant during October, when other metals have low fluxes. The dissolved iron flux shows a large increase along the upper segment of the creek during the month of July at a rate of 106.92 mg/s. The net suspened flux is negative because of the loss of suspended iron and the minor increase of suspended zinc, manganese and lead.

All suspended and dissolved metals other than iron occur in such small quantities that their presence plays a minor role in determining the flux in the upper segment of the

Table 12. Net flux values (mg/s) between sites SW-1 and SW-5, SW-5 and SW-6, and SW-6 and SW-8 in July. Zeroes indicate metals with concentrations below detection limits.

July	SW-5 - SW-1	SW-6 - SW-5	SW-8 - SW-7 - SW-6
As-d	0.99	0.67	1.05
As-s	0	0	-1.69
Cu-d	-0.43	0.54	0.84
Cu-s	0	0.38	1.83
Fe-d	106.92	-60.82	-48.27
Fe-s	-16.44	121.62	-5.19
Mn-d	2.21	-0.08	1.11
Mn-s	2.51	1.92	1.03
Pb-d	-0.11	0.07	0.11
Pb-s	0.61	0.34	0.53
Zn-d	-9.02	2.16	1.89
Zn-s	7.76	0.62	4.41
Net dissolved flux	100.56	-57.46	-43.26
Net suspended flux	-25.16	144.48	0.91

creek. Copper and lead may occur in low amounts because they were valuable mining metals and mostly removed.

Unlike the upper reach, the middle reach of the creek gains groundwater in July, yet the dissolved iron load decreases by 60.82 mg/s. The decrease in the dissolved iron load contrasts with the increase in discharge (134.38 L/s). Dissolved iron may be lost due to precipitation. The precipitation of iron would explain the decrease in the dissolved load and the increase in the suspended load. Manganese is the only metal for which the dissolved load decreases slightly. The dissolved loads for all of the other metals increase slightly.

Both dissolved and suspended iron loads decrease along the lower reach of the creek during July. Since suspended metals fluxes are negligible along this reach, the decrease in the dissolved flux cannot be the result of precipitation or adsorption onto

suspended sediments. The creek is gaining along this reach, so the decreased dissolved load also cannot be explained by outflow of ground water from the creek. The dissolved iron may be adsorbing onto bed load.

During the month of August, the fluxes are much lower than the fluxes in July. The dissolved iron slightly decreases in the upper segment. Suspended iron also decreases in the upper segment, which means that the decrease in the dissolved iron flux cannot be the result of precipitation or adsorption onto suspended sediments, and must be the result of adsorption onto bedload. Except for manganese, all of the other suspended metals decrease in the upper segment, though to a lesser extent. Overall, the reach has a positive dissolved flux as a result of the relatively large dissolved zinc flux. The negative suspended flux is seen in all metals except for manganese and is likely due to dissolution of suspended metals other than iron into the dissolved form.

In the middle reach, where discharge is gained, dissolved iron increases and suspended iron decreases. Furthermore, all of the other suspended metals fluxes decrease, except for suspended zinc and lead. The loss of suspended metals may be the result of dissolution. However, PHREEQC results indicate that iron should precipitate rather than dissolve.

As in the middle segment of the creek, the lower segment displays a slight increase in dissolved iron. The slag waste in the lower reach may be a source of iron in the groundwater. The suspended iron also increases in this reach of the creek. Two things could contribute to this: an increase of dissolved species leads to oversaturation and precipitation, and/or the desorption of iron from bed load. Although the suspended iron

Table 13. Net flux values (mg/s) between sites SW-1 and SW-5, SW-5 and SW-6, and SW-6 and SW-8 in August.

August	SW-5 - SW-1	SW-6 - SW-5	SW-8 - SW-7 - SW-6
As-d	0.398	0.220	0.178
As-s	-0.094	-0.044	-0.614
Cu-d	0.304	0.176	0.142
Cu-s	-0.127	-0.094	-1.959
Fe-d	-2.108	4.736	1.505
Fe-s	-2.394	-5.004	4.980
Mn-d	1.250	-0.830	0.270
Mn-s	0.655	-0.568	-2.146
Pb-d	0.010	0.022	0.018
Pb-s	-0.064	0.022	-0.212
Zn-d	2.964	-1.465	-0.669
Zn-s	-2.016	1.559	-1.851
Net dissolved flux	2.819	2.860	1.444
Net suspended flux	-4.040	-4.129	-1.803

increases in the lower reach, the net suspended load decreases due to the decrease of all other metals, mainly copper, manganese, and zinc. Because all of the other metals loads are much smaller than iron during this season and segment of the creek, the iron load has the greatest impact on the overall metals loading.

In October, the upper reach is a losing stream again. The suspended iron increased along this reach but dissolved iron decreased slightly. It is likely that the dissolved iron precipitates or is adsorbed onto suspended sediment. The net dissolved flux, however, increased by a small amount, which was due to the influence of the other metals.

The middle reach is a gaining stream. The suspended iron decreased by 6.191 mg/s, but the dissolved iron increased by only 0.373 mg/s, which may be due to dissolution. The decrease in suspended iron may result from the suspended iron falling

Table 14. Net flux values (mg/s) between sites SW-1 and SW-5, SW-5 and SW-6, and SW-6 and SW-8 in October.

October	SW-5 - SW-1	SW-6 - SW-5	SW-8 - SW-7 - SW-6
As-d	0.056	0.105	0.241
As-s	0.229	-0.125	-0.186
Cu-d	0.045	0.084	0.193
Cu-s	0.105	-0.138	0.074
Fe-d	-0.329	0.373	-0.269
Fe-s	8.170	-6.191	8.618
Mn-d	0.033	-0.051	0.200
Mn-s	3.064	-3.024	0.503
Pb-d	0.006	0.011	0.024
Pb-s	0.133	-0.085	0.293
Zn-d	0.312	0.136	1.612
Zn-s	-0.223	0.420	0.144
Net dissolved flux	0.123	0.659	2.001
Net suspended flux	11.479	-9.142	9.445

out of suspension or adsorbing onto the bedload. The net loads parallel the iron loads in this segment.

During October, the lower reach is a gaining stream. Suspended iron increased in this segment of the creek and the dissolved iron decreased by a small amount. The increase in suspended iron suggests the precipitation of dissolved iron and/or desorption of iron from bed load sediments. The total net fluxes for all of the other metals all increase along the lower reach in October, as well, except for suspended arsenic.

The suspended and dissolved iron fluxes in July and the suspended iron fluxes in October are by far the largest values of all the metals, and therefore control the net fluxes in those two months. Of the other metals of concern only manganese and zinc are significant during August and October; suspended copper, manganese, and zinc cause the net suspended load to decrease in the lower segment of the creek in August. In October, the net dissolved load in the upper reach is positive despite the negative iron flux,

because every other dissolved constituent increases. In the lower reach of the creek, the net dissolved load increases due to the combined effect of all metals other than iron. It appears that the loads of the metals other than iron are only significant in the late season when the discharge has decreased nearly seven fold. The metals fluxes along Bayhorse Creek are principally impacted by the oxidation state of iron present in the groundwater and its ability to adsorb or desorb and dissolve or precipitate as it mixes with the creek.

X-ray Analysis

Results from X-ray analysis are useful for comparing the bedrock to previous studies (Seal and Rye, 1992) and assessing the parent rock of the tailings. The amount of metals present in the creek sediment samples cannot be determined from these analyses, however, due to the limited range of elements measured via XRF and XRD. The X-ray results are consistent with the local bedrock types: Bayhorse Dolomite and Ramshorn Slate (Hobbs et al., 1991). The tailings are likely mostly derived from the Ramshorn Slate because of its proximity to mining activities and the chemical makeup of the tailings.

The highest percentages in the sediment samples SW-1 SS, SW-5 SS, SW-6 SS, SW-7 SS, SW-8 SS, and GW-1 ROCK at the Ramshorn mine were of silica, aluminum and iron oxides based on the XRF analyses (Table 8). These values are to be expected in the Ramshorn Slate and may not be elevated by mining practices.

The bedrock sample, collected near the groundwater seep at the upper region of the study area, showed high concentrations of silica and aluminum (Table 8). Common minerals such as quartz, micas, and feldspars contain these elements, so it is not surprising to find them in high concentrations.

Iron oxides also were commonly present, which would reflect the breakdown of bedrock and formation of hydrous ferric oxides. The relatively large amount of ferric oxides in the bedrock may be a source of the iron transported throughout the surface and groundwater systems. Fortunately, the toxicity of both aluminum and iron requires higher concentrations than other metals such as arsenic or lead. Upon normalizing its measured percentage to its expected level in soil as compared with other metals (Lindsay, 1979), there is not a significantly greater contribution of iron in the system than any of the other metals measured.

The high concentration of zinc found in SW-8 SS (Table 6) is nearly ten times greater than the common range of soil concentrations (Lindsay, 1979). The zinc may be sourced from the slag pile which exists along the banks of the creek at the Bayhorse town site. The copper values found in sample SW-5 SS and SW-8 SS exceeded the common soil concentrations by 17 and 2.5 times, respectively. The copper may be sourced from the tailings and slag pile contamination sites, respectively.

Stream sediment sample SW-5 SS results in some of the highest concentrations of metals of all the creek bed sediments. This may be an irregularity from a more concentrated grab sample, or it may indicate that the metals leaching from the tailings pile sorb to the iron oxides and then travel downstream attached to sediment or organic matter. Metals input from GW-3 may also contribute to the metals found in SW-5 SS. The sediments may not yet have traveled downstream as far as SW-6, depending on the sedimentation rate of the creek. Creek samples from SW-8 SS also displayed high concentrations of some metals, but not as high as SW-5 SS concentrations. Since the concentrations do not accumulate steadily from SW-5 to SW-8 at the same rate as the

discharge, it appears that SW-8 SS obtains its metals load from a source other than upstream. The source may be leaching from the slag pile located at SW-8.

Table 15 lists the concentrations of the water samples taken adjacent to the sediment samples during the month of August. The only sediment samples analyzed by the UVDL on its ICP-MS were SW-1 SS, SS-2a, SW-5 SS, and GW-1 ROCK because they were the areas of most concern regarding metals loading to the creek. The full length of the creek could not be compared using these results, so the XRF sediment results were used instead, even though not all metals of concern were detected via XRF.

Arsenic and lead are not listed in Table 15 because they cannot be analyzed on the USU Geology Department XRF. However, the concentrations of arsenic and lead found in sediment samples analyzed by the ICP-MS at SW-1, SW-5, and GW-1 ROCK were relatively insignificant compared to iron and to a lesser extent manganese.

Copper and zinc were the only metals of concern that the XRF analyzed. Iron and manganese were identified in their oxide forms Fe_2O_3 and MnO, respectively, and represented as a weight percentage of the pressed powder sample. A calculation method may be used to isolate the weight percents of iron and manganese from the oxygen. The calculation is described in the equation below where A is the atomic weight, N is the number of moles in the oxide analyzed, $_C$ is the cation value, and $_O$ is the oxygen value. The final weight percent of the cation can then be multiplied by 10,000 to convert parts per hundred into parts per million.

$$A_C*N_C/((A_C*N_C)+(A_O*N_O))*\text{weight \%} = \text{weight \%}_C$$

Table 15. Comparison of metals concentrations from four sediment samples (XRF) and unfiltered water samples (ICP-MS) at adjacent sites (ppm).

	Cu	Fe	Mn	Zn
GW-1-ROCK	10	36480	350	68
GW-1-SS	73	65780	680	129
GW-1 (Aug)	<0.008	0.03	0.001	0.01
SW-1-SS	16	34630	520	68
SW-1 (Aug)	0.004	0.25	0.01	0.014
SW-5-SS	1729	58170	3060	256
SW-5 (Aug)	0.005	0.148	0.028	0.021
SW-6-SS	40	46800	1100	133
SW-6 (Aug)	0.004	0.099	0.009	0.015
SW-8-SS	257	67200	2690	2228
SW-8 (Aug)	0.002	0.12	0.003	0.012

The concentrations of copper and zinc (ppm) from XRF analyses are 1/10,000th of the weight percent. The water samples from August were chosen to remain consistent with PHREEQC and sediment analyses, thus allowing the results to be compared.

The sediment and rock concentrations of all four metals are orders of magnitude greater than the concentrations in the adjacent water samples. The highest metals concentrations in the sediment were found in the lowest portion of the study reach. The metals concentrations at each site probably are not exclusively influenced by transport from contaminated sites upstream; they are likely influenced by precipitation/dissolution and/or adsorption/desorption with the local sediments, and by groundwater inflow along gaining reaches.

Iron and manganese showed much higher concentrations in the sediment samples than copper and zinc. This may indicate a stronger sorption process for both iron and manganese, as indicated by PHREEQC. The iron and manganese concentrations may appear greater in the sediments than copper and zinc because they are typically found in higher concentrations in soils than other metals (Lindsay, 1979).

Iron concentrations in the sediment, rock, and water samples far exceed the concentrations of copper, manganese, and zinc. The highest sediment concentrations were detected in SW-8 SS at 67,200 ppm and in GW-1 SS at 65,780 ppm. The concentrations of dissolved iron in the August water samples do not align with the sediment concentrations at the adjacent location, since the highest concentration was detected in SW-1. The lowest iron concentration in the creek bed sediments was found in SW-1 SS.

Positive SI values for iron and manganese in the PHREEQC results indicate that iron has the potential to precipitate into iron oxides in the upper and middle reaches of the creek. This chemistry coincides with a decrease in the dissolved iron concentration in the upper (SW-1) and middle (SW-5) segments. It appears that the sediments and bedrock naturally contain a higher concentration of iron than any other metal of concern and that it precipitates and/or adsorbs to the bed load as it travels downstream, since the dissolved iron concentrations generally decrease and the sediment concentrations increase from SW-1 to SW-8.

Compared to iron, manganese is not found in as high concentrations in the sediments or in the water samples. As with iron, the manganese sediment concentrations are much greater than the dissolved concentrations. This is consistent with the PHREEQC results, which show the potential for manganese oxide precipitation. The highest concentrations of manganese are at SW-5, which may reflect input from the draining adit at GW-3. It is possible that the concentration of manganese present in the local bedrock has a direct relationship with the concentration of dissolved manganese at

each site, as manganese may be found in higher concentrations in the ore body near SW-5 than in the natural bedrock and sediments above and below it.

Zinc was detected at its highest concentrations in the lowest portion of the creek. The detection at SW-8 SS was 2,228 ppm, roughly ten times the next highest concentration of zinc. As with iron and manganese, the zinc sediment concentrations are higher than the dissolved concentrations at every sample location. The zinc concentrations in the sediments, though, are not as high as iron or manganese. Zinc does not show much potential to precipitate according to the PHREEQC calculations.

Copper is detected in all sediment samples analyzed on the XRF. The GW-1 ROCK sample had the lowest concentration of 10 ppm and SW-5 SS had the highest concentration of 1,729 ppm. The groundwater sample at GW-1 was below the detection limit, and SW-5 had the highest concentration of copper of any of the water samples.

ICP-MS Contributions

The results from the ICP-MS analysis support the results from the X-ray analysis. ICP-MS sediment and rock sample results are shown in Table 7. The sediment sample from the tailings pile (SS-2a) contains the highest concentrations of all metals, with the exception of copper, which is the highest in SW-5 SS. Iron and manganese are the metals that result in the highest concentrations, especially in SS-2a and SW-5 SS. GW-1 ROCK and SW-1 SS show the lowest values of each metal, though iron is found in high concentrations in both samples. Arsenic, copper, lead, and zinc are also found in higher concentrations in SW-5 SS than in SW-1 SS and GW-1 ROCK.

Zinc is readily adsorbed onto clay minerals in soil, and will associate with iron and manganese oxides (McLean and Bledsoe, 1992). As described by McLean and Bledsoe (1992), copper and lead have a strong affinity to bind to soil particles. The retention of copper in soils may be controlled by adsorption to $CaCO_3$ (McLean and Bledsoe, 1992; Cavallaro and McBride, 1978; Dudley et al., 1988, 1991; McBride and Bouldin, 1984). Lead concentrations in soil are controlled by pH; lead is not soluble at high pH (McLean and Bledsoe, 1992). This would explain why lead is seen at higher concentrations in the soil than dissolved in the water column.

PHREEQC

Three site locations from the August data collection period were run through the PHREEQC (Parkhurst and Appelo, 2000) modeling program to generate speciation distributions, saturation indices, charge balance percent error, and hydrous ferric oxide (HFO) surface complex distributions. The three water samples chosen were at the three locations and during the only time when groundwater recharged the upper segment of the surface water system. This made it possible to calculate mixed water chemistry for the groundwater influx using the chemistry of the flowing well at GW-2, and for the draining adit at GW-3 with the surface water from SW-1.

Mobile cations in neutral water with abundant iron substrates are Ca, Cd, Cl, Mg, Na, S, Sr, and Zn (Smith, 2007). The presence of metal ligands, organic substrates, and ferric oxides provides a space for these metals to bond and travel in the system in the sorbed form. Metals in the free ion form are most toxic to organisms in the creek. The metal present in Ramshorn samples in the dissolved, free-ion form was zinc.

The SI values from the PHREEQC modeling of solution 1, solution 2 and solution 3 (Tables F.1, F.2, and F.3) indicate the presence of iron oxides, hydroxides and oxyhydroxides. There are many varieties of these phases. In mix 1 and mix 2, the saturation indices indicate that iron and manganese are the metals most likely to precipitate out of solution.

Strong and weak binding sites for HFO surfaces are shown in Table H.1 of Appendix H. The strong sites are dominated primarily by OZn^{+} and secondarily by $OHAsO_4^{3-}$. The weak sites are dominated primarily by $OHAsO_4^{3-}$ and secondarily by OZn^{+}. Both sites also have minor amounts of $HAsO4^{-}$ and H_2AsO_4. These are the highest concentrations found within the HFO binding species, however, these are still relatively small concentrations as compared with other acid mine water samples (Burk, 2004).

Sources of Contamination

Iron is the metal of concern detected at the highest concentrations at the Ramshorn mine site. It is detected in concentrations above the Maximum Contaminant Level for drinking water, 0.3 mg/L, as listed by the EPA (USEPA, 2009).

Iron, manganese, and zinc occur in much greater concentrations than any other metal, though manganese and zinc are usually found at lower concentrations than iron. It is likely that they are present in the bedrock as well as in the tailings, waste rock, and slag piles.

The abundance of iron may be due in part to its presence in a wide variety of ore minerals that remain in the tailings and waste rock piles. Iron is a common element found in ore minerals such as pyrite (FeS_2), arsenopyrite (FeAsS), and siderite ($FeCO_3$). Seal and Rye (1992) studied the area extensively and identified north-south striking veins that dip to the west. The veins are dominantly composed of siderite-tetrahedrite ($Fe_{0.85}$, $Mn_{0.10}$, $Mg_{0.05}$, CO_3) but also include minor traces of pyrite, sphalerite, chalcopyrite, and arsenopyrite (Seal and Rye, 1992). The siderite-tetrahedrite veins were economically exploited during mining activities.

The background level of iron found in SW-1 may be explained by the argillaceous metasedimentary Ramshorn Slate, which may contain glauconite ($(K,Na)(Fe^{3+},Al,Mg)_2(Si,Al)_4O_{10}(OH)_2$) and other iron-bearing clay minerals.

Dissolved iron loads increase dramatically between SW-1 and SW-5 in July (Table 12). The increase in dissolved iron between SW-1 and SW-5 in July must be

attributed to a source other than the groundwater influx because the upper segment of the creek was a losing reach. The gain of dissolved iron loads can be attributed to dissolution of suspended iron.

Dissolved and suspended manganese loads both increase between SW-1 and SW-5 in July, but to a far lesser extent than iron. In fact, both the dissolved and the suspended manganese loads increase between SW-1 and SW-5 during all three sampling events (Table 12). A source of iron and manganese is likely located downstream of SW-1 and upstream of SW-5. The tailings and waste rock piles most likely account for the increases in dissolved iron and dissolved and suspended manganese loads between SW-1 and SW-5 in July. Copper and lead may occur in smaller concentrations because they were removed during mining. It is clear from the sediment samples (Table 10) that the tailings and SW-5 SS have high potential to load the creek with iron and manganese.

In July SW-1 and SW-8 have higher dissolved zinc loads than any other sites (Table 3). SW-8 SS has the highest zinc concentrations (Table 9). Zinc is known to occur with other heavy metals in slag waste and the bulk of the zinc at SW-8 likely can be attributed to the slag pile. Because there is also a low concentration of zinc in the SW-1 SS sample, naturally occurring zinc likely is present in the bedrock, which may explain the high dissolved zinc load at SW-1 during July. Zinc is primarily observed in the dissolved form (Table 11).

Arsenic was detected at GW-1 during all four sampling periods. GW-1 ROCK had an arsenic concentration of 3.27 mg/L (Table 10), which was less than the tailings sample, although the grab sample does not account for lateral and stratigraphic variation within the Ramshorn Slate. Veins were not observed during the field visits so no samples

were collected from them. It is likely that a trace amount of arsenic dissolves into groundwater as it passes through veins and the tailings pile.

The economically valuable minerals – copper and lead – have been mostly removed from the site during mining activities. Copper and lead are observed only in low concentrations and loads as dissolved or suspended metals in the creek.

Dissolved copper was only detected at low concentrations at GW-3 and SW-1 in July and August, and at SW-2 in July. Similar to the other metals, the most likely source of copper is in minerals associated with sulfide mineralization. The GW-1 ROCK and SW-1 SS samples both contained copper (Tables 9 and 10).

Dissolved lead was only detected in samples analyzed by the UVDL, but it was found at its highest concentrations in GW-3, SW-1, and SW-2 in July. Lead was also detected in samples SW-1 SS and GW-1 ROCK (Table 10). Large chunks of remnant galena on site indicate the occurrence of lead sulfide within the mine and suggest that it still interacts with the ground and surface waters.

Metal Transport Pathways

Table 11 displays the breakdown of suspended and dissolved metals during the month of August when the creek gained groundwater. Arsenic, copper, and lead loads are too small to register in the suspended solids calculations. Iron and manganese primarily travel as suspended solids throughout the entire length of the study reach, except for manganese at GW-3. Zinc is the only metal that enters in the suspended form and becomes dissolved throughout the length of the study area except at SW-7, which is the tributary, Juliette Creek, and not Bayhorse Creek itself.

Iron enters the creek primarily as a suspended solid and remains a suspended solid throughout the reach. The PHREEQC results suggest that iron, as well as manganese, should precipitate as numerous hydroxides, oxides, and oxyhydroxides in all three solutions and in both of the mixes (Appendix F). Positive saturation indices indicate the potential for iron and manganese precipitation when groundwater mixes with Bayhorse Creek. The PHREEQC results also suggest the likelihood of both iron and manganese remaining in the suspended form.

Both dissolved manganese and dissolved zinc loads at GW-3 are greater than their respective total loads in the month of August (Table 4). This may be a result of a laboratory error or the difference of values calculated from two separate labs. Regardless, this suggests that the both manganese and zinc exist primarily in the dissolved state at this location in August. It is likely that manganese enters the groundwater that drains from the adit in the dissolved form and then precipitates once it mixes with the creek.

Zinc is found primarily in the dissolved form where it enters the creek at GW-3 and SW-1. Apparently zinc stays in solution after it mixes with the creek. The PHREEQC results suggest that zinc is likely to be adsorbed onto HFO (Appendix H).

Arsenic, copper, and lead only occur in small loads in the upper portion of the creek. The PHREEQC modeling indicates that arsenic, as As(5), is present as two oxides, $HAsO_4^{2-}$ and $H_2AsO_4^-$, in solution 3 (GW-3), mix 1 and mix 2. What little arsenic loads the creek at GW-3 is mostly in this less toxic form.

Copper does not likely sorb based on PHREEQC calculations. Copper enters the creek in the dissolved state at SW-1 and GW-3, and then precipitates into suspension before reaching SW-5. Lead also is in the dissolved state where it enters the creek at SW-

1 and GW-3, and is found as a suspended solid from SW-5 to SW-8. Mining activities may have removed most of the copper and lead from the study area.

Metals Fate

Of the metals of concern, only iron, manganese, and zinc were found in significant concentrations and loads (arsenic and lead were found at concentrations just above the EPA cleanup level in a few locations). The loads of arsenic, copper, and lead have such a minor impact on the creek, that they were not included in the calculations of suspended and dissolved metals.

During the month of July, iron and manganese enter the creek between SW-1 and SW-5, iron in the dissolved form and manganese in both the dissolved and suspended forms (Table 12). The dissolved iron load decreases dramatically and the suspended iron load increases dramatically along the middle reach, likely due to dissolved iron precipitating from solution. Both the dissolved and suspended manganese and zinc loads increase in the middle reach of the creek. In the lower reach of the creek, dissolved and suspended iron both decrease, while dissolved and suspended manganese and zinc continue to increase. The manganese and zinc are likely flushed downstream out of the study area.

In the month of August, manganese enters the creek in both the dissolved and suspended form in the upper reach (Table 13), while zinc enters only in the dissolved form. Suspended iron decreases along the upper and middle reaches in August, while dissolved iron decreases along the upper reach and increases along the middle reach. This suggests that the suspended iron either settles out or dissolves along the middle reach of

the creek. Iron enters the creek in the dissolved form in the middle reach, while both dissolved and suspended manganese and dissolved zinc decrease. Dissolved and suspended iron loads increase below SW-6. Suspended manganese and dissolved and suspended zinc loads all decrease in the lower reach of the creek.

In October, the upper reach of the creek is loaded with suspended iron and manganese (Table 14). The creek loses suspended iron and manganese between SW-5 and SW-6, and then gains suspended iron between SW-6 and SW-8. Dissolved manganese decreases along the middle reach in October, but both dissolved and suspended manganese increase along the lower reach. Both dissolved and suspended zinc increase along the lower reach as well. This suggests that there is a source of metals below the middle reach of the creek. The only likely source is the slag pile, which is located adjacent to SW-8. As in July, the dissolved and suspended manganese and zinc, as well as the suspended iron, are likely flushed out of the study area.

SUMMARY, CONCLUSIONS, AND RECOMMENDATIONS

Summary

In 2008, the IDEQ, in partnership with the EPA, began cleanup at the Ramshorn mine site, which is listed as a Brownsfield property. The primary goal of the mine cleanup was to limit the amount of metals contamination in Bayhorse Creek, which runs near the mine site. The tailings pile located upstream of the former smelter posed the greatest threat of contamination to Bayhorse Creek. As part of the cleanup, the creek was rerouted to flow away from the tailings pile. Although Bayhorse Creek no longer runs directly adjacent to the tailings pile, there are still concerns that the creek is affected by the mine waste.

I conducted a study, as proposed by the USFS, of the metals loading sourced from the tailings and slag piles into Bayhorse Creek. I intended for this study to provide the USFS with an assessment of the sources and impacts of contamination. Previous reports indicate that high concentrations of arsenic, iron, manganese, and lead remain in the tailings waste. I expected these metals to flow into the creek when the groundwater was high enough to interact with the tailings pile, and then to decrease during the drier season when the water table lowered.

To determine the metals loading and transport at the Ramshorn mine site, surface water, groundwater, and sediment samples were collected and analyzed. Filtered water samples were analyzed using ICP and unfiltered water samples were analyzed using ICP-MS to quantify the concentrations of dissolved and total metals, respectively. Samples were collected from locations adjacent to suspected areas of contamination to determine the dissolved and suspended metals loads along various segments of the creek. Sediment,

tailings, and bedrock samples were also collected from the creek and mine site, and processed through X-ray analysis to determine the presence of metals in the underlying geology. Metals loads in the creek were compared to the concentrations in sediment, tailings, and rock samples to identify potential sources of contamination. I monitored metals loading one day per month for four months from July to October.

The dominant bedrock type in the area is the Ramshorn Slate. The ore characterization by Plumbee and Nash (1995) suggests that the chemistry of the hydrologic system is controlled by a pyrite-poor sphalerite-galena veins and replacements in carbonate-bearing sedimentary rocks. This aligns with the geology of the host rock and veins. The veins are dominantly composed of siderite-tetrahedrite ($FeMnMgCO_3$) and minor traces of arsenopyrite, chalcopyrite, pyrite, and sphalerite (Seal and Rye, 1992). The combination of carbonate bedrock and the absence of the protons produced by the breakdown of pyrite create an alkaline environment. Therefore, the metals generally do not dissolve into their cationic form, except for zinc.

The tailings and waste rock located between SW-1 and SW-5 are considered to be the main source of metals contamination. The slag pile near SW-8 is also considered to be an important source.

Both dissolved and suspended metals loads were highest in July (Table 3) when the stream discharge was highest and no remediation of the tailings and waste rock piles had occurred yet. For each month, the total dissolved plus suspended metals loads increased with distance downstream from the mine. The highest total metal loads were consistently found at SW-8. Suspended loads exceeded dissolved loads for iron and manganese, but not zinc, which is present predominantly in the dissolved form (Table

11). However, there were some discrepancies in the data obtained from the USUAL and the UVDL, particularly at low concentrations, as some metals had higher dissolved than total concentrations (arsenic, copper, iron, manganese, lead, and zinc at GW-3 in July, and iron at SW-5 in July).

The positive saturation indices for iron and manganese calculated by the chemical modeling program PHREEQC indicates that they will precipitate as oxides, hydroxides, and oxyhydroxides (Appendix F). The PHREEQC modeling also indicates that there are sorption sites available for arsenic and zinc (Appendix H).

Arsenic, copper, and lead are found in such small loads that they have a minimal impact on the creek. Most of the copper and lead were probably removed from the site during mining activities. Furthermore, none of these three metals was detected in the dissolved form at SW-5 or downstream of it, and they are much less harmful when they are not in the dissolved state.

Conclusions

Arsenic, copper, iron, manganese, lead, and zinc are the metals of concern at the Ramshorn mine site based on previous investigations and my analytical results. Of these six metals, iron was detected at the highest concentrations, while manganese and zinc were the only other metals detected in significant concentrations and loads; arsenic, copper, and lead were not high enough to be considered a concern.

Forty-seven percent or more of iron and manganese loads were in the suspended form at sites SW-1, SW-5, SW-6, and SW-8, except for manganese at SW-8 (Table 11). Zinc is the only metal that travels outside of my study area in the dissolved form.

The metals at the Ramshorn mine site are present in the parent bedrock, but were unleashed at unnatural levels during mining. The major sources are from the tailings and waste rock piles located between SW-1 and SW-5, and the slag pile adjacent to SW-8.

Metals loads were highest in July when the discharge of Bayhorse Creek was the highest. The metals loads were much lower in the later months of the season, undoubtedly due to the dramatic decrease in discharge.

The mineralogical composition of siderite-tetrahedrite, which is $FeMnMgCO_3$, corresponds well with the high concentrations of iron, manganese, and carbonate. As shown in Figure 15, the mineralization at the Ramshorn mine site does not appear to contain much pyrite. The ore veins consist dominantly of sphalerite and galena. Acid production would not be as prevalent in a pyrite-poor rock-water interaction. It appears that the carbonate within the rocks prevents the production of large volumes of acid by neutralizing any acid that is produced. When less acid is produced, and therefore the number of protons is fewer, there is less competition for binding sites on cation complexes. As a result, metals are less likely to remain dissolved in solution. The combination of low acid production and carbonate abundance leads to more alkaline water, which creates a neutral pH that inhibits metals from persisting in their dissolved form except for manganese and zinc, and zinc is the only metal in my study that remains in the dissolved form.

Iron, manganese, and zinc are not as toxic as other metals like arsenic and lead. Furthermore, the dilution from tributaries and by uncontaminated groundwater along any gaining reaches downstream from the study area renders the toxicity of the metals in the

creek harmless. The other three metals – arsenic, copper, and lead – are found in such small loads that they do not affect the overall metals flux. Though they may be carried into the system in the dissolved state, they will either precipitate out or, in the case of arsenic, be adsorbed downstream of SW-5. These metals are much less harmful when they are not in the dissolved state.

Suspended metals are far less of a concern to humans and biota than dissolved metals because they are too large to be absorbed into macroinvertebrate tissue and consumed at higher trophic levels. Not only are these metals less toxic to macroinvertebrates than they would be in their dissolved form, but they also are less likely to be transported for long distances. For these reasons, there is little concern of toxicity in the ground and surface waters. Instead, iron and manganese remain in the suspended form, and are likely precipitated or transported out of the system.

Although zinc remains primarily in the dissolved form in Bayhorse Creek throughout the entire study area, it was not detected in nearly as high concentrations or loads as iron. Furthermore, like iron and manganese, zinc is not as toxic as other metals. The dissolved zinc is likely transported out of the study area, where it is diluted by tributaries and/or uncontaminated groundwater along reaches where the creek is a gaining stream.

Iron, manganese, and zinc are essential metals in human metabolism and are even required in our diet. However, the relatively low levels of iron and manganese detected in the creek barely exceeded EPA drinking water standards, and then only during the month of July.

The metals from the remaining tailings and waste rock piles at the Ramshorn mine site and the slag at the Bayhorse town site do not pose a significant risk to aquatic life or human recreation. The remediation completed by the IDEQ during the summer of 2011 was effective in reducing metals loads in Bayhorse Creek.

Recommendations

Remediation in the summer of 2011 reduced the amount of groundwater infiltrating through the tailings and waste rock, and subsequently into the creek, between the months of July and August. Lesser amounts of long-term contaminants, such as iron and manganese, remain in the creek sediments, nonetheless. The level of contamination found during my summer 2011 study did not indicate highly acidic or metals-laden surface or groundwater. It was apparent that the creek had the highest metals concentrations and loads in July, resulting from either a seasonal increase in discharge, the effect of the subsequent remediation procedure, or a combination of the two. However, remediation processes are not permanent. The re-grading and capping of the tailings and waste rock piles will only prevent runoff from infiltrating and interacting with the contaminants for a period of time. To insure that long-term runoff does not cause leakages in the cap, it might be advisable to check the site on a regular basis and re-cap if contamination returns to the July 2011 levels. However, the slightly alkaline pH and absence of high concentrations of dissolved metals seem to indicate that the site was not a threat to human health or the environment even prior to remediation and may not need additional monitoring.

REFERENCES CITED

Alpers C.N., and D.W. Blowes. 1994. Environmental geochemistry of sulfide oxidation. ACS Symposium Series 550. American Chemical Society, Washington, DC.

American Public Health Association (APHA). 1995. Standard methods for the examination of water and wastewater. 19th edition. American Public Health Association, Washington, DC.

Banks D., P.L. Younger, R.-T. Arnesen, E.R. Iversen, and S.B. Banks. 1997. Mine-water chemistry: The good, the bad and the ugly. Environmental Geology 32:157-174.

Brierley, C.L. 1982. Microbiological mining. Scientific American 247:44-53.

Burk, N.I. 2004. Geochemistry of groundwater–surface water interactions and metals loading rates in the north fork of the American Fork River, Utah, from an abandoned silver/lead mine. M.S. thesis, Utah State University, Logan.

Cavallaro, N., and M.B. McBride. 1978. Copper and cadmium adsorption characteristics of selected acid and calcareous soils. Soil Science Society of America Journal 42:550-556.

Coney, P.J. 1987. The regional tectonic setting and possible causes of Cenozoic extension in the North American Cordillera. In: M.P. Coward, J.F. Dewey, and P.L. Hancock, editors, Continental extensional tectonics. Geological Society Special Publication 28. Geological Society, London, UK. p. 177-186.

Cook, C.W., and G.M. Ehlers. 1927. A possible occurrence of the Richmond formation in the vicinity of Clayton, Idaho. Papers of the Michigan Academy of Science, Arts & Letters 7:51-53.

Drever, J.I. 1997. The geochemistry of natural waters: surface and groundwater environments. 3rd ed. Prentice Hall, Upper Saddle River, NJ.

Dudley, L.M., J.E. McLean, R.C. Sims, and J.J. Jurinak. 1988. Sorption of copper and cadmium from the water-soluble fraction of an acid mine waste by two calcareous soils: column studies. Soil Science 145:147-214.

Dudley, L.M., J.E. McLean, T.H. Furst, and J.J. Jurinak. 1991. Sorption of Cd and Cu from an acid mine waste extract by two calcareous soils: column studies. Soil Science 151:121-135.

Dzombak, D.A., and F.M.M. Morel. 1990. Surface complexation modeling: Hydrous ferric oxide. John Wiley & Sons, New York.

Ecology and Environment, Inc. 2010. Draft removal site evaluation report, Ramshorn mine site, Custer County, Idaho. Idaho Department of Enivronmental Quality Contract EP-S7-06-02. Technical Direction Document 08-08-0006. Seattle, WA.

Evangelou V.P. 1995. Pyrite oxidation and its control. CRC Press, Boca Raton, FL.

Evangelou V.P., and Y.L. Zhang. 1995. A review: Pyrite oxidation mechanisms and acid mine drainage prevention. Critical Reviews in Environmental Science and Technology 25:141-199.

Ferguson, J.F., and J. Gavis. 1972. A review of the arsenic cycle in natural waters. Water Research 6:1259-1274.

Gray, N.F. 1996. Field assessment of acid mine drainage contamination in surface and groundwater. Environmental Geology 27:358-361.

Hobbs, S.W., W.H. Hays, and D.H. McIntyre. 1991. Geologic map of the Bayhorse area, central Custer County, Idaho. Miscellaneous Investigations Series Map I-1882. U.S. Geological Survey, Washington, DC. Scale 1:62500.

Idaho Department of Environmental Quality (IDEQ). 2003. Ramshorn mine preliminary assessment report Custer County, Idaho. Seattle, WA.

Jambor, J., and D.W. Blowes. 1994. Environmental geochemistry of sulfide minewastes. Mineralogical Association of Canada Short Course 22. Mineralogical Association of Canada, Ottawa, ON.

Jambor J.L., and D.W. Blowes. 1998. Theory and applications of mineralogy in environmental studies of sulfide bearing mine wastes. In: L.J. Cabri, and D.J. Vaughn, editors, Modern approaches to ore and environmental mineralogy. Mineralogical Association of Canada Short Course 27. Mineralogical Association of Canada, Ottawa, ON.

Keith, C.N., and D.J. Vaughan. 2000. Mechanisms and rates of sulphide oxidation in relation to the problems of acid rock (mine) drainage. In: J.D. Cotter-Howells, L.S. Campbell, E. Valsami-Jones, and M. Batchelder, editors, Environmental mineralogy: microbial interactions, anthropogenic influences, contaminated land and waste management. Mineralogical Series 9. Mineralogical Society, London, UK. p 117-139.

Lachmar, T., N. Burk, and P. Kolesar. 2006. Groundwater contribution of metals from an abandoned mine to the North Fork of American Fork River, Utah. Water, Air, and Soil Pollution 1-4:103-120.

Langmuir, D. 1997. Aqueous environmental geochemistry. Prentice Hall, Upper Saddle River, NJ.

Lindsay, W.L. 1979. Chemical equilibria in soils. John Wiley & Sons, New York.

Link, P.K., and S.U. Janecke. 1999. Geology of east-central Idaho: Geologic roadlogs for the Big and Little Lost River, Lemhi, and Salmon River Valleys. In: S.S. Hughes, and G.D. Thackray, editors, Guidebook to the geology of eastern Idaho. Idaho Museum of Natural History, Pocatello. p 295-334.

McBride, M.B., and D.R. Bouldin. 1984. Long-term reactions of copper (II) in a contaminated calcareous soil. Soil Science Society of America Journal 48:56-59.

McLean, J.E., and B.E. Bledsoe. 1992. Behavior of materials in soils. EPA-540-S-92-018. USEPA. Robert S. Kerr Laboratory, Ada, OK.

Mitchell, V.E. 1999. History of the mines in the Bayhorse area, Custer County, Idaho. Staff Report 99-8. Idaho Geological Survey, Moscow.

Motsi, T. 2010. Remediation of acid mine drainage using natural zeolite. Ph.D. dissertation, University of Birmingham, Birmingham, UK.

Natural Resources Conservation Service (NRCS). 2012. Streamflow comparison for central Idaho and upper Snake: Mean daily streamflow of Middle Fork Salmon River. NRCS. http://www.nrcs.usda.gov/wps/portal/nrcs/detail/id/snow/?cid=nrcs144p2_048138#2012 (accessed 3 June 2013).

Nordstrom, D.K., and C.N. Alpers. 1999. Geochemistry of acid mine waters. In: Plumlee, G.S., and M.J. Lodsdon, editors, Environmental geochemistry of mineral deposits. Reviews in Economic Geology 6A:133-160.

Parkhurst, D.L., and C.A. Appelo. 2000. User's guide to PHREEQC (version 2) –A computer program for speciation, batch-reaction, one-dimensional transport, and inverse geochemical calculations. Water-Resources Investigations Report 99-4259. U.S. Geological Survey, Washington, DC.

Pichler, T., M.J. Hendry, and G.E.M. Hall. 2001. The mineralogy of arsenic in uranium mine tailings at the Rabbit Lake in-pit facility, northern Saskatchewan, Canada. Environmental Geology 40:495-506.

Piper, A.M. 1944. A graphic procedure in geochemical interpretation of water analyses. Trans. of the American Geophysical Union 25:914–923.

Plumlee, G.S., and J.T. Nash. 1995. Geoenvironmental models of mineral deposits–fundamentals and applications. In: E.A. du Bray, editor, Preliminary compilation of descriptive geoenvironmental mineral deposit models. Open File Report 95-831. U.S. Geological Survey, Washington, DC. p. 1-9.

Ross, C.P. 1937. Geology and ore deposits of the Bayhorse region, Custer County, Idaho. Bulletin 877. U.S. Geological Survey, Washington, DC.

Salomons, W. 1995. Environmental impact of metals derived from mining activities: Processes, prediction, prevention. Journal of Geochemical Exploration 52:5-23.

Seal, B., and S.J. Rye. 1992. Stable isotope study of water-rock interaction and ore formation, Bayhorse base and precious metal district, Idaho. Economic Geology 87:271-287.

Skipp, B. 1987. Basement thrust sheets in the Clearwater orogenic zone, central Idaho and western Montana. Geology15:220-224.

Smith, K.S. 2007. Strategies to predict metal mobility in surficial mining environments. Geological Society of America Reviews in Engineering Geology 17:25-45.

Soil & Plant Analysis Laboratory. 2005. Analysis of major, minor and trace elements in soil and sediment samples with ICP-OES and ICP-MS, standard operation procedure University of Wisconsin, Madison.

Stumm, W., and J.J. Morgan. 1996. Aquatic chemistry. 3rd ed. John Wiley & Sons, New York.

TerraGraphics Environmental Engineering, Inc. 2005. Bayhorse site risk assessment and proposed risk management plan. Idaho Department of Environmental Quality and Idaho Department of Public Recreation. Seattle, WA.

Tordo, G.M., A.J.M. Baker, and A.J. Willis. 2000. Current approaches to the revegetation and reclamation of metalliferous mine wastes. Chemosphere 41:219-228

Umpleby, J.B. 1917. Geology and ore deposits of the Mackey region, Idaho. Professional Paper 97. U.S. Geological Survey, Washington, DC.

U.S. Environmental Protection Agency (USEPA). 2000. Liquid assets: America's water resources at a turning point. USEPA. http://water.epa.gov/lawsregs/lawsguidance/cwa/economics/liquidassets/index.cfm (accessed 3 June 2013).

U.S. Environmental Protection Agency (USEPA). 2009. Drinking Water Contaminants. EPA-816-F-09-004. USEPA. http://water.epa.gov/drink/contaminants/index.cfm. (accessed 3 June 2013).

U.S. Geological Survey (USGS). 1980. National handbook of recommended methods for water-data acquisition. Office of Water Data Acquisition, Reston, VA.

Wanty, R.B., P.L. Verplanck, B.A. Kimball, M.L. Tuttle, R.L. Runkel, and B.R. Berger. 2004. Resolving natural and anthropogenic sources of solutes to a watershed from historic mining. In: R.B. Wanty, and R.R. Seal II, editors, Proceedings of the 11th international symposium on water-rock interaction. Taylor and Francis, London, UK.

Wells, M.W. 1983. Gold camps & silver cities. Bulletin 22. 2nd ed. Idaho Bureau of Mines and Geology, Moscow.

Wernicke, B. 1992. Cenozoic extensional tectonics of the U.S. Cordillera. In: Burchfiel, B.C., P.W. Lipman, and M.L. Zoback, editors, The cordilleran orogen: Conterminous U.S. The Geology of North America, G-3. Geological Society of America, Boulder, CO.

Western Regional Climate Center (WRCC). 1996. Period of Record Monthly Climate Summary. WRCC. http://www.wrcc.dri.edu/cgi-bin/cliMAIN.pl?id1663 (accessed 3 June 2013).

Worl, R.G., A.B. Wilson, C.L. Smith, M.D. Kleinkopf, and R.C. Skyles. 1989. Mineral resource potential and geology of the Challis National Forest, Idaho. Bulletin 1873. U.S. Geological Survey, Washington, DC.

APPENDICES

Appendix A
Consultant Results

Table 3-2

Summary of XRF Arsenic and Lead Results
Ramshorn Mine Site
Custer County, Idaho

EPA Sample ID	Sample Date	Location ID	Sample Location	Analytical Results (mg/kg) Arsenic	Lead
Idaho IDTL (1)				0.39	50
EPA RSL-Residential (2)				0.39	400
10060001	6/2/2010	SB01SB05	Tailings Pile - Soil Boring 1	**1,524**	**1,117**
10060002	6/2/2010	SB01SB11.5	Tailings Pile - Soil Boring 1	**1,799**	**1,077**
10060003	6/2/2010	SB01SB15	Tailings Pile - Soil Boring 1	**219**	**265**
10060004	6/2/2010	SB01SB20	Tailings Pile - Soil Boring 1	**388**	**561**
10060005	6/3/2010	SB02SB02	Tailings Pile - Soil Boring 2	**1,349**	**840**
10060006	6/3/2010	SB02SB05	Tailings Pile - Soil Boring 2	**1,237**	**1,851**
10060007	6/3/2010	SB02SB10	Tailings Pile - Soil Boring 2	**1,155**	**913**
10060008	6/3/2010	SB02SB15	Tailings Pile - Soil Boring 2	**1,737**	**1,554**
10060009	6/3/2010	SB02SB20	Tailings Pile - Soil Boring 2	**2,359**	**1,306**
10060010	6/3/2010	SB02SB25	Tailings Pile - Soil Boring 2	**2,403**	**2,778**
10060011	6/3/2010	SB02SB30	Tailings Pile - Soil Boring 2	**1,330**	**866**
10060012	6/3/2010	SB02SB35	Tailings Pile - Soil Boring 2	**101**	**103**
10060013	6/3/2010	SB03SB05	Tailings Pile - Soil Boring 3	**1,547**	**1,087**
10060014	6/3/2010	SB03SB15	Tailings Pile - Soil Boring 3	**427**	**211**
10060015	6/3/2010	SB03SB20	Tailings Pile - Soil Boring 3	**364**	**333**
10060016	6/3/2010	SB03SB25	Tailings Pile - Soil Boring 3	**345**	< 6.2
10060017	6/3/2010	SB03SB30	Tailings Pile - Soil Boring 3	**154**	**84**
10060018	6/3/2010	SB03SB35	Tailings Pile - Soil Boring 3	**68**	**59**
10060019	6/3/2010	SB03SB40	Tailings Pile - Soil Boring 3	**38**	22
10060020	6/3/2010	SB04SB2.5	Tailings Pile - Soil Boring 4	**1,524**	**1,020**
10060021	6/3/2010	SB04SB11.5	Tailings Pile - Soil Boring 4	**1,555**	**821**
10060022	6/3/2010	SB04SB15	Tailings Pile - Soil Boring 4	**1,276**	**742**
10060023	6/3/2010	SB04SB20	Tailings Pile - Soil Boring 4	**1,473**	**831**
10060024	6/3/2010	SB04SB25	Tailings Pile - Soil Boring 4	**1,681**	**1,421**
10060025	6/3/2010	SB04SB31.5	Tailings Pile - Soil Boring 4	**201**	**128**
10060026	6/3/2010	SB04SB35	Tailings Pile - Soil Boring 4	**147**	**71**
10060027	6/3/2010	SB04SB40	Tailings Pile - Soil Boring 4	**614**	< 6.2
10060028	6/3/2010	SB05SB05	Tailings Pile - Soil Boring 5	**2,409**	**841**
10060029	6/3/2010	SB05SB10	Tailings Pile - Soil Boring 5	**1,342**	**2,381**
10060030	6/3/2010	SB05SB20	Tailings Pile - Soil Boring 5	**2,081**	**1,866**
10060031	6/3/2010	SB05SB25	Tailings Pile - Soil Boring 5	**779**	**484**
10060032	6/3/2010	SB05SB30	Tailings Pile - Soil Boring 5	**321**	**168**
10060033	6/3/2010	SB05SB35	Tailings Pile - Soil Boring 5	**155**	**116**
10060034	6/3/2010	SB05SB40	Tailings Pile - Soil Boring 5	**106**	**57**
10060035	6/3/2010	SC-01	Top of Main Tailings Pile	**1,636**	**885**
10060036	6/3/2010	SC-02	Waste Rock West of Main Tailings Pile	**1,466**	**1,212**
10060037	6/3/2010	SC-03	Waste Rock directly above Main Tailings Pile	**1,507**	**1,348**
10060038	6/3/2010	SC-04	Waste Rock above SC-03	**2,160**	**1,937**
10060039	6/3/2010	SC-05	Top of Waste Rock Pile from Collapsed Adit to East	**581**	**166**
10060040	6/3/2010	SC-06	Lower Portion of Tailings Pile (above road)	**2,121**	**1,260**
10060041	6/3/2010	SC-07	Lower Portion of Tailings Pile (below road)	**1,902**	**1,445**
10060042	6/4/2010	BG-1	Background Surface Soil	**54**	34
10060042 Dup	6/4/2010	BG-1 Dup	Background Surface Soil	**53**	34
10060043	6/4/2010	BG-2	Background Surface Soil	**34**	23
10060043 Dup	6/4/2010	BG-2 Dup	Background Surface Soil	**30**	26

Table 3-2

Summary of XRF Arsenic and Lead Results
Ramshorn Mine Site
Custer County, Idaho

EPA Sample ID	Sample Date	Location ID	Sample Location	Analytical Results (mg/kg) Arsenic	Lead
Idaho IDTL (1)				0.39	50
EPA RSL-Residential (2)				0.39	400
10060045	6/4/2010	SB06SB2.5	Bayhorse Creek Road - Soil Boring 6	**1,947**	**881**
10060046	6/4/2010	SB06SB05	Bayhorse Creek Road - Soil Boring 6	**1,029**	**893**
10060047	6/4/2010	SB07SB2.5	Bayhorse Creek Road - Soil Boring 7	**2,108**	**762**
10060047 Dup	6/4/2010	SB07SB2.5 Dup	Bayhorse Creek Road - Soil Boring 7	**2,006**	**797**
10060048	6/4/2010	SB07SB05	Bayhorse Creek Road - Soil Boring 7	**2,114**	**1,099**
10060048 Dup	6/4/2010	SB07SB05 Dup	Bayhorse Creek Road - Soil Boring 7	**3,935**	**1,560**
10060049	6/4/2010	SB07SB10	Bayhorse Creek Road - Soil Boring 7	**239**	< 6.2
10060050	6/4/2010	SB07SB15	Bayhorse Creek Road - Soil Boring 7	**424**	**71**
10060051	6/4/2010	SB08SB15	Bayhorse Creek Road - Soil Boring 8	**168**	< 6.2
10060051 Dup	6/4/2010	SB08SB15 Dup	Bayhorse Creek Road - Soil Boring 8	**95**	< 6.2
10060052	6/4/2010	SB08SB20	Bayhorse Creek Road - Soil Boring 8	**29**	17
10060052 Dup	6/4/2010	SB08SB20 Dup	Bayhorse Creek Road - Soil Boring 8	**30**	15
10060053	6/3/2010	REP-TP-1 (Comp.)	Repository - Test Pit 1	**63**	**57**
10060053 Dup	6/3/2010	REP-TP-1 (Comp.) Dup	Repository - Test Pit 1	**54**	45
10060054	6/3/2010	REP-TP-1 (1 ft bgs)	Repository - Test Pit 1	**3**	18
10060054 Dup	6/3/2010	REP-TP-1 (1 ft bgs) Dup	Repository - Test Pit 1	**6**	18
10060055	6/3/2010	REP-TP-1 (4 ft bgs)	Repository - Test Pit 1	**10**	29
10060055 Dup	6/3/2010	REP-TP-1 (4 ft bgs) Dup	Repository - Test Pit 1	**9**	23
10060056	6/3/2010	REP-TP-1 (8 ft bgs)	Repository - Test Pit 1	**9**	20
10060056 Dup	6/3/2010	REP-TP-1 (8 ft bgs) Dup	Repository - Test Pit 1	**8**	23
10060057	6/3/2010	REP-TP-5 (2 ft bgs)	Repository - Test Pit 5	**8**	17
10060057 Dup	6/3/2010	REP-TP-5 (2 ft bgs) Dup	Repository - Test Pit 5	**16**	48
10060058	6/3/2010	REP-TP-5 (5 ft bgs)	Repository - Test Pit 5	**5**	19
10060058 Dup	6/3/2010	REP-TP-5 (5 ft bgs) Dup	Repository - Test Pit 5	**3**	18

Notes: A **BOLD** value indicates that the result exceeds the IDTL.
A highlighted value indicates that the result exceeds the RSL.
(1) Idaho Risk Evaluation Manual (IDEQ 2004).
(2) EPA Regional Screening Levels (EPA 2010).

Key:
bgs = below ground surface
Comp. = composite
Dup = Duplicate
EPA = United States Environmental Protection Agency
ft = feet
ID = identification
IDEQ = Idaho Department of Environmental Quality
IDTL = Initial Default Target Limit
mg/kg = milligrams per kilogram
RSL = Regional Screening Level
XRF = x-ray fluorescence

Table 3-3

Summary of TAL Metal Results in Soil Samples
Ramshorn Mine Site
Custer County, Idaho

Sample ID:	Screening Levels		10060042	10060043	10060035	10060039	10060001	10060002	10060009	10060044	10060012	10060013	10060017
Sample Location:	Idaho IDTL (1)	EPA RSL Residential (2)	BG-1	BG-2	SC-01	SC-05	SB01SB05	SB01SB11.5	SB02SB20	SB02SB20-D	SB02SB35	SB03SB05	SB03SB30
TAL Metals (mg/kg)													
Aluminum	nsa	77,000	17,300	18,000	1,330	14,600	2,110	1,820	606	802	8,760	1,790	10,200
Antimony	4.8	31	1.21	1.1 U	**174**	**24.7**	**474**	**176**	**160**	**127**	**21.6**	**189**	**90.4**
Arsenic	0.39	0.39	**63.1 J**	**68.6 J**	**1,380**	**768 J**	**2,010**	**1,380**	**924**	**981**	**248 J**	**1,590**	**382**
Barium	896	15,000	185 J	131 J	7.14	121 J	8.94	78.3	5.16 U	5.22 U	38.6 J	13.6	57.3
Beryllium	1.6	160	1.15	1.59	0.492 U	1.14	0.563	0.581	0.516 U	0.598	0.494 U	0.73	0.556 U
Cadmium	1.4	70	0.588 U	0.549 U	4.92 U	0.916	5.06 U	5.31 U	5.16 U	5.22 U	0.546	5.13 U	5.56 U
Calcium	nsa	nsa	2,080 J	1,690 J	712	1,470 J	812	5,690	1,390	1,080	448 J	974	1,010
Chromium	2,135	120,000	19.8	42.6	18.4	28.7	22	20.8	38.7	16	20.1	22.6	25.3
Cobalt	nsa	23	13.4	18.2	15.4	16.4	18	20.1	24.4	18	10.1	18	22.1
Copper	921	3,100	47.8 J	94.4 J	508	193 J	**1,080**	662	302	402	82.4 J	580	294
Iron	5.8	55,000	**25,900**	**40,200**	**66,900**	**41,800**	**75,100**	**53,800**	**92,400**	**72,700**	**27,100**	**58,200**	**53,900**
Lead	50	400	37.9	28.9	**1,080**	**189**	**1,190**	**867**	**846**	**1,110**	**314**	**1,440**	**6,130**
Magnesium	nsa	nsa	3,220	5,810	3,870	6,240	5,300	4,650	7,180	8,040	4,740	5,490 J	4,920 J
Manganese	223	1,800	**980**	**875**	**3,630**	**1,570**	**4,740**	**6,980**	**6,000**	**4,270**	**634**	**3,650**	**3,500**
Mercury	0.0051	23	**0.0176 J**	0.0127 U	**0.261 J**	**0.0761 J**	**0.344 J**	**0.249 J**	**0.408 J**	**0.32 J**	**0.0538 J**	**1.22**	**0.0919**
Nickel	59	1,500	29	51.7	49.5	44.7	**61.4**	**62.9**	**90.2**	58	31.2	58.5	40.7
Potassium	nsa	nsa	2,800	6,170	258	2,410	501	442	227	272	296	424 J	2,100 J
Selenium	2.0	390	**4.22**	**6.35**	**37.8**	**6.81**	**40.2**	31.9 U	**48.8**	**38.2**	**5.11**	**26.9**	33.4 U
Silver	0.19	390	**1.44**	**1.1**	**42**	**7.25**	**114**	**32.4**	**31.3**	**26**	**7.55**	30.8 U	**82.1**
Sodium	nsa	nsa	65.1	87	24.6 U	51	28.7	43.5	25.8 U	26.1 U	39.5	32.8	52.8
Thallium	1.6	nsa	**7.6**	**9.41**	24.6 U	**13.3**	20.2 U	106 U	20.6 U	20.9 U	**5.71**	20.5 U	22.2 U
Vanadium	nsa	390	28.9	42.4	11.4	24.4	15.1	12.8	27.7	11.6	11.7	15.5	19.9
Zinc	886	23,000	104	105	737	172	851	543	612	577	136	635	120

Notes: A **BOLD** value indicates that the result exceeds the IDTL.
A highlighted value indicates that the result exceeds the RSL.
(1) Idaho Risk Evaluation Manual (IDEQ 2004).
(2) EPA Regional Screening Levels (EPA 2010).

Key:
ID = identification
IDEQ = Idaho Department of Environmental Quality
IDTL = Initial Default Target Level
EPA = Environmental Protection Agency
J = estimated value
mg/kg = milligrams per kilogram
nsa = no screening level available
RSL = Regional Screening Level
TAL = target analyte list
U = not detected (at the indicated reporting limit)

Table 3-5

Summary of TAL Metal and Water Quality Parameter Results in Surface Water Samples
Ramshorn Mine Site
Custer County, Idaho

Sample ID:		Screening Levels				10060114	10060113	10060115	10060112	10060111	10060110	10060109	10060108	10060107	10060106	10060105	10060104	10060103	10060102	10060101
						SW-06	SW-05	SW-15	SW-14	SW-13	SW-12	SW-04	SW-11	SW-10	SW-09	SW-08	SW-07	SW-03	SW-02	SW-01
Sample Location:	Units	Idaho REM - Freshwater (Criterion Continuous) (1)	Idaho REM - Human Health (Consumption of Organisms Only) (1)	National WQC Freshwater CCC (2)	National WQC - Human Health (Consumption of Organisms Only) (2)	Bayhorse Creek Upstream (0.5 miles)	Bayhorse Creek Upstream (0.25 miles)	Drainhole Discharge	Western Seep	Western Seep Outfall	Eastern Seep	Bayhorse Creek at Site	Adit Discharge	Adit Drainage	Adit Pond	Adit Discharge Outfall	Adit Discharge Outfall	Bayhorse Creek Downstream of Adit Discharge	Bayhorse Creek Downstream (0.25 miles)	Bayhorse Creek Downstream (0.5 miles)
TAL Metals																				
Aluminum	µg/L	nsa	nsa	87	nsa	2,590 J	4,050 J	200 U	446 J	2,570 J	1,370 J	323 J	180 J	152 J	121 J	261 J	107 J	11,600 J	12,300 J	7,160 J
Antimony	µg/L	nsa	4,300	nsa	640	10 U	10 U	10 U	4.94	107.5	60.5	5.47	10 U	10 U	4.11	10 U	10 U	10 U	10 U	10 U
Arsenic	µg/L	190	50	150	0.14	30 U	30 U	30 U	31.8	**236**	**437**	18.8	32	21.4	26.4	12	13.5	26.9	**51.9**	37.9
Barium	µg/L	nsa	nsa	nsa	1,000 (6)	68.4	83.3	5.98	4.83	16	10.8	20.9	11.4	11.4	13.5	6.97	5.92	179	199	**128**
Beryllium	µg/L	nsa	nsa	nsa	nsa	5 U	5 U	5 U	5 U	5 U	5 U	5 U	5 U	5 U	5 U	5 U	5 U	5 U	5 U	5 U
Cadmium	µg/L	2.05 (4)	nsa	0.25	nsa	5 U	5 U	5 U	5 U	5 U	5 U	5 U	5 U	5 U	5 U	5 U	5 U	5 U	5 U	5 U
Calcium	µg/L	nsa	nsa	nsa	nsa	7,100	6,700	23,500	7,080	7,920	9,340	8,800	8,770	8,770	9,060	8,930	8,880	9,120	9,680	8,150
Chromium (3)	µg/L	382 (4)	nsa	74	nsa	3.2	5.13	5 U	5 U	5.96	5.48	5 U	1.29	5 U	5 U	5 U	5 U	14.7	15.9	9.43
Cobalt	µg/L	nsa	nsa	nsa	nsa	1.48	1.27	5 U	5 U	3.96	4.12	5 U	2.48	1.63	1.22	5 U	5 U	5.4	6.95	4.29
Copper	µg/L	25.2 (4)	nsa	Calc. (5)	1,300 (6)	10 U	10 U	10 U	4.93	**104**	**133**	7.77	4.49	10 U	7.36	10 U	10 U	19	**32.4**	23.8
Iron	µg/L	nsa	nsa	1,000	nsa	2,700	3,640	1,420	565	8,290	8,140	455	1,560	1,060	1,300	385	282	12,000	13,800	8,380
Lead	µg/L	6.83 (4)	nsa	2.5	nsa	10 U	10 U	10 U	14.3 U	**267**	**453**	18.2 U	10 U	10 U	10 U	10 U	4.21 U	**33**	**67.2**	**46.3**
Magnesium	µg/L	nsa	nsa	nsa	nsa	3,050	3,280	30,200	11,800	20,500	62,000	13,500	40,000	40,300	40,300	39,900	39,300	5,840	5,830	4,970
Manganese	µg/L	nsa	nsa	nsa	nsa	146	131	42	23	433	537	34.3	630	452	366	143	36	523	726	513
Mercury	µg/L	0.012	0.15	0.77	0.3 (7)	0.2 U	0.2 U	0.2 U	0.2 U	0.2 U	0.2 U	0.2 U	0.2 U	0.2 U	0.2 U	0.2 U	0.2 U	0.2 U	0.2 U	0.2 U
Nickel	µg/L	346 (4)	4,600	52	4,600	3.02	3.34	1.5	5 U	10.5	11.4	5 U	8.12	8.67	9.5	2.29	5 U	11.5	14.6	9.36
Potassium	µg/L	nsa	nsa	nsa	nsa	1,320	1,680	2,980	984	1,790	2,150	969	659	648	663	670	702	3,180	3,440	2,430
Selenium	µg/L	5	nsa	5	4,200	30 U	30 U	30 U	30 U	30 U	30 U	30 U	30 U	30 U	30 U	30 U	30 U	30 U	**6.11**	30 U
Silver	µg/L	nsa	nsa	nsa	nsa	5 U	5 U	5 U	5 U	7	13.5	5 U	5 U	5 U	5 U	5 U	5 U	1.14	1.79	1.24
Sodium	µg/L	nsa	nsa	nsa	nsa	2,190	2,350	7,380	1,500	1,750	1,600	2,340	981	996	1,010	1,010	997	2,440	2,570	2,460
Thallium	µg/L	nsa	6.3	nsa	0.47	20 U	20 U	20 U	20 U	20 U	20 U	20 U	20 U	20 U	20 U	20 U	20 U	20 U	20 U	20 U
Vanadium	µg/L	nsa	nsa	nsa	nsa	4.18	5.26	5 U	5 U	3.55	1.87	5 U	5 U	5 U	5 U	5 U	5 U	16.1	17.5	10.3
Zinc	µg/L	230 (4)	nsa	120	26,000	9.7	11.2	10 U	6.3	93.8	133	10.6	10.9	10.1	13.3	3.39	3.33	46.6	62.6	41.2
Water Quality Parameters																				
pH	standard units	nsa	nsa	6.5 to 9	5 to 9 (6)	7.88	7.78	8.46	8.25	7.71	9.17	8.07	6.73	8.64	8.70	8.34	8.10	7.49	7.47	7.77
Conductivity	µs/CM	nsa	nsa	nsa	nsa	0.044	0.38	0.336	0.128	0.19	0.512	0.152	0.315	0.315	0.309	0.39	0.249	0.49	0.48	0.49
Hardness ($CaCO_3$)	mg/L	nsa	nsa	nsa	nsa	26.6	25.7	168	56.3	89.8	254	70.1	169	162	166	164	161	39.5	38.5	34.5
Nitrogen, Nitrate/Nitrite	mg/L	nsa	nsa	nsa	10,000 (6)	0.0865 J	0.0745 J	0.25 U	0.62	0.64	0.249 J	0.236 J	0.11 J	0.104 J	0.0715 J	0.064 J	0.25 U	0.086 J	0.072 J	0.058 J
Sulfate	mg/L	nsa	nsa	nsa	nsa	1.12 J	1.2 J	14.7 J	37.1 J	40.6 J	95.1 J	25.2 J	59.1 J	59.2 J	58.8 J	59.1 J	56.7 J	2.79 J	2.52 J	2.21 J

Notes:
A **BOLD** value indicates that the result exceeds one of the Idaho REM screening levels.
A highlighted value indicates that the result exceeds one of the National Water Quality Criteria screening levels
(1) Idaho Risk Evaluation Manual, Table 3-5 (IDEQ 2004). Values for fresh water - criterion continuous and human health for consumption of organisms only.
(2) National Recommended Water Quality Criteria (EPA 2006). Values for Freshwater CCC and human health for consumption of organisms only.
(3) Assumes chromium III.
(4) Calculated based on chronic screening levels and maximum hardness values detected in surface water samples.
(5) Freshwater criterion for freshwater is based on a calculation of several variables; not all variables are available for this data set.
(6) No value for consumption of organisms only; value for water + organism used.
(7) Assumes methylmercury.

Key:
CCC = Criterion Continuous Concentration
ID = identification
IDEQ = Idaho Department of Environmental Quality
J = estimated value
µg/L = micrograms per liter
mg/L = milligrams per liter
µs/cm = microsiemens per centimeter
nsa = no screening level available
REM = Risk Evaluation Manual
TAL = target analyte list
U = not detected (at the indicated reporting limit)
WQC = Water Quality Criteria

Table 3-6

Summary of TAL Metal Results in Sediment Samples
Ramshorn Mine Site
Custer County, Idaho

Sample ID:	Screening Levels		10060163	10060162	10060161	10060160	10060159	10060158	10060157	10060156	10060155	10060154	10060153	10060152	10060151
	RSET Interim Freshwater (1)		SED-06	SED-05	SED-14	SED-13	SED-12	SED-04	SED-11	SED-10	SED-09	SED-07	SED-03	SED-02	SED-01
Sample Location:	SL1 (2)	SL2 (3)	Bayhorse Creek Upstream (0.5 miles)	Bayhorse Creek Upstream (0.25 miles)	Western Seep	Western Seep Outfall	Eastern Seep	Bayhorse Creek at Site	Adit Discharge	Adit Drainage	Adit Pond	Adit Discharge Outfall	Bayhorse Creek Downstream of Adit Discharge	Bayhorse Creek Downstream (0.25 miles)	Bayhorse Creek Downstream (0.5 miles)
TAL Metals (mg/kg)															
Aluminum	nsa	nsa	4,310	7,440	3,500	2,390	4,730	2,540	908	362	7,950	6,590	5,380	9,180	5,450
Antimony	nsa	nsa	1.46 U	1.74 U	199	29.2	235	10.8	489	222	224	9.27	51.3	49.5	8.96
Arsenic	20	51	6.83	**20.5**	**1,910**	**225**	**3,160**	**46.6**	**5,530**	**1,560**	**2,710**	**84.4**	**1,100**	**446**	**137**
Barium	nsa	nsa	121	194	28.1	48.3	37.7	53.6	1200	170	245	21.6	294	243	150
Beryllium	nsa	nsa	0.729 U	0.868 U	1.16 U	0.57 U	1	0.653 U	8.18	1.39	2.65	0.632 U	1.13 U	1.17 U	0.63 U
Cadmium	1.1	1.5	0.729 U	0.868 U	**4.1**	2.85 U	7.2 U	0.653 U	33.3 U	7.28 U	**3.81**	3.16 U	1.13 U	1.17 U	0.63 U
Calcium	nsa	nsa	3,080	4,430	2,480	2,340	1,200	1,490	8,190	2,150	2,950	573	3,930	7,480	2,580
Chromium	95	100	8.94	14.2	21	11.5	28.1	8.98	66	22.2	32.8	13.9	18.5	18.6	13.1
Cobalt	nsa	nsa	4.96	8	20.3	13.9	32	4.94	634	83.5	102	6.39	26.6	14.1	12
Copper	80	830	6.83	12.9	**858**	74.6	**1,060**	34.2	**713**	**1,470**	**1,290**	57.2	**153**	**196**	53.2
Iron	nsa	nsa	11,400	15,600	49,500	37,900	64,000	12,500	274,000	150,000	84,000	23,100	40,600	26,400	18,900
Lead	340	430	7.32	12.7	**1,760**	181	**4,060**	182	**362**	**3,070**	**2,710**	62.4	281	338	121
Magnesium	nsa	nsa	1,840 J	3,330 J	4,340 J	2,680 J	4,900 J	1,670 J	8,410 J	6,410 J	5,080 J	3,210 J	4,450 J	4,520 J	2,830 J
Manganese	nsa	nsa	305	565	1,850	1,460	3,950	477	153,000	32,400	25,000	801	12,000	1,360	963
Mercury	0.28	0.75	0.0167 UJ	0.019 UJ	**0.632**	0.0312 J	**1.65**	0.0164 U	0.212	**0.352**	**1.58**	0.0594	0.121	0.172	0.0326 J
Nickel	60	70	7.87	12.6	49.7	17.9	**89.2**	10.4	**1,400**	**259**	**330**	22.2	49.3	28.8	20.8
Potassium	nsa	nsa	841 J	1,260 J	576 J	432 J	852 J	478 J	1,860 J	1,820 U	1,070 J	346 J	1,170 J	1,980 J	1,420 J
Selenium	nsa	nsa	5.55	7.12	24.7	19.5	43.2 U	6	215	94.4	53.2	11.3	26.7	12.5	9.06
Silver	2.0	2.5	0.729 U	0.868 U	**86.1**	**3.32**	**113**	0.653 U	**37.7**	**41.6**	**81.4**	1.34	**9.75**	**24**	**3.88**
Sodium	nsa	nsa	119	137	57.9 U	63.9	74.4	99.4	167 U	36.4 U	76.5	31.6 U	118	164	118
Thallium	nsa	nsa	2.92 U	3.47 U	4.63 U	2.28 U	28.8 U	2.61 U	667 U	146 U	43.9 U	2.53 U	45.2 U	4.68 U	2.52 U
Vanadium	nsa	nsa	14.9	21.2	15.3	17.3	17.8	11.3	33.3 U	7.42	19.4	7.51	18.5	25.5	19.9
Zinc	130	400	28.6	40.3	**590**	**151**	**1,040**	83.2	**1,580**	**716**	**1,030**	**132**	**206**	**192**	89.9

Notes: A **BOLD** value indicates that the result exceeds SL1.
A highlighted value indicates that the result exceeds SL2.
(1) RSET = Northwest Regional Sediment Evaluation Framework, Interim Final, September 2006
(2) SL1 = no adverse effects expected for benthic organisms
(3) SL2 = minor adverse effects may be observed in more sensitive groups of benthic organisms

Key:
ID = identification
J = estimated value
mg/kg = milligrams per kilogram
nsa = no screening level available
RSET = Regional Sediment Evaluation Team
TAL = target analyte list
U = not detected at indicated reporting limit
UJ = not detected at indicated reporting limit; reporting limit is estimated

Appendix B
Discharge Measurements and Results

GW-1 was measured by the volumetric method and the time to fill a 1400 mL container.

GW-2 was measured using the volumetric method filling a 2000 mL container.

GW-1

Trial	Time (sec)
1	2.03
2	1.82
3	1.69
4	1.57
5	1.78
Average time (sec)	1.778
Discharge (L/s)	**0.79**

GW-2

Trial	Time (sec)
1	32.9
2	33.56
3	32.09
4	32.21
5	31.94
Average time (sec)	32.54
Discharge (L/s)	**0.06**

GW-3 was measured using a wading rod and flow meter

GW-3

Distance (ft)	Depth (ft)	Velocity (ft/s)	Area (ft^2)	Discharge (ft^3/s)
1.3	0.5	2.73	0.325	0.89
	Total cross sectional area		0.325	
			Discharge (L/s)	**25.13**

SW-1 measured using wading rod and flow meter.

SW-1

Distance (ft)	Depth (ft)	Velocity (ft/s)	Average velocity (ft/s)	Area (ft^2)	Discharge (ft^3/s)
1	1	2.65	1.32	0.5	0.66
2	0.9	2.65	2.16	0.95	2.05
3	0.9	1.67	2.16	0.90	1.94
4	0.7	1.12	1.88	0.80	1.51
4.83	0.6	1.13	1.12	0.54	0.60
6	0.4	1.17	1.15	0.59	0.67
7	0.5	0.72	0.94	0.45	0.42
8	0.4	0.66	0.69	0.45	0.31
10	0	0	0.33	0.40	0.13
			Total:	5.6	8.29
				Discharge (L/s)	**234.91**

SW-2 and **SW-3** measured by the volumetric method. Times to fill a 5-gallon bucket and 1400 mL container, respectively, are listed.

SW-2

Trial	Time
1	3.06
2	3
3	3.22
4	2.97
5	2.97
Average time (sec)	3.044
Discharge (gps)	1.64
Discharge (L/s)	6.22

SW-3

Trial	Time
1	13.07
2	13.06
3	13.44
4	13.25
5	13.47
Average time (sec	13.258
Discharge (gps)	0.03
Discharge (L/s)	0.11

SW-5 was measured using a wading rod and flow meter.

SW-5

Distance (ft)	Depth (ft)	Velocity (ft/s)	Average velocity (ft/s)	Area (ft^2)	Discharge (ft^3/s)
1	0.3	2.16	1.08	0.15	0.16
2	0.3	1.98	2.07	0.3	0.62
3	0.4	0.98	1.48	0.35	0.52
4	0.5	3.12	2.05	0.45	0.92
5	0.4	2.19	2.65	0.45	1.19
6	0.7	2.16	2.18	0.55	1.20
7	0.5	3.87	3.01	0.6	1.81
8	0.7	0.80	2.33	0.6	1.40
9	0.5	0.95	0.87	0.6	0.52
10	0.2	0.66	0.80	0.35	0.28
11	0	0	0.33	0.1	0.03
			Total:	4.5	8.65
				Discharge (L/s)	**244.98**

SW-6 was measured using a wading rod and flow meter.

SW-6

Distance (ft)	Depth (ft)	Velocity (ft/s)	Average velocity (ft/s)	Area (ft^2)	Discharge (ft^3/s)
2	0.9	0.49	0.25	0.45	0.11
3	0.8	4.16	2.32	0.85	1.97
4	1	4.30	4.23	0.9	3.80
5	1.1	1.56	2.93	1.05	3.07
6	1	1.13	1.34	1.05	1.41
7	0.8	0	0.56	0.9	0.51
8	1	1.17	0.59	0.9	0.53
9	1	0.94	1.06	1	1.06
10	1	0.20	0.57	1	0.57
11	0.6	0.46	0.33	0.8	0.26
12	0.9	0.00	0.23	0.45	0.10
13.5	0	0	0	0.675	0
			Total:	10.03	13.40
				Discharge (L/s)	**379.36**

SW-7 was measured using a wading rod and flow meter.

SW-7

Distance (ft)	Depth (ft)	Velocity (ft/s)	Average velocity (ft/s)	Area (ft^2)	Discharge (ft^3/s)
1	1.1	4.53	2.26	0.55	1.24
2	0.5	3.41	3.97	0.8	3.17
3	0.3	5.39	4.40	0.4	1.76
4	0.4	0.91	3.15	0.35	1.10
5	0	0	0.46	0.2	0.09
6	0.5	1.16	0.58	0.25	0.14
7	0.4	3.30	2.23	0.45	1.00
8	0.5	1.73	2.51	0.45	1.13
9	0.8	2.13	1.93	0.65	1.25
10	0.7	2.14	2.13	0.75	1.60
11	0.5	1.27	1.70	0.6	1.02
12	0.6	1.40	1.33	0.55	0.73
13	0.5	2.96	2.18	0.55	1.20
14	0.4	0.52	1.74	0.45	0.78
15	0.4	2.01	1.26	0.4	0.51
16	0.3	0.21	1.11	0.35	0.39
17	0.3	0.68	0.44	0.3	0.13
18	0.2	0.70	0.69	0.25	0.17
19	0.4	0.35	0.53	0.3	0.16
20	0.2	2.28	1.32	0.3	0.39
21	0	0	1.14	0.1	0.11
			Total	9.0	18.1
				Discharge (L/s)	**512.31**

SW-8 was measured using a wading rod and flow meter.

SW-8

Distance (ft)	Depth (ft)	Velocity (ft/s)	Average velocity (ft/s)	Area (ft^2)	Discharge (ft^3/s)
1	0.2	1.85	0.93	0.1	0.09
2	0.8	1.16	1.50	0.5	0.75
3	0.9	1.87	1.51	0.85	1.29
4	0.8	2.70	2.28	0.85	1.94
5	0.9	3.12	2.91	0.85	2.47
6	0.9	2.36	2.74	0.9	2.46
7	1.5	3.33	2.84	1.2	3.41
8	1.6	4.31	3.82	1.55	5.92
9	1.4	3.44	3.87	1.5	5.81
10	1.4	3.84	3.64	1.4	5.09
11	1.3	3.95	3.89	1.35	5.25
12	1.1	1.68	2.81	1.2	3.37
13	0.8	0.50	1.09	0.95	1.03
13.5	0	0	0.25	0.2	0.05
			Total:	13.2	38.93
				Discharge (L/s)	**1102.59**

On the second trip to the field site, the only available Flo-mate flow meter was in units of 15ths of a foot. The flows needed to be calculated into metric units in order to be comparable to measurements during the other field site visits. Below I show the raw collected figures, and the calculations that were made to transfer them to metric units.

GW-1 and **GW-2** using the volumetric method. Times to fill a 2000 mL container

GW-1

Trial	Time (s)
1	2.62
2	2.16
3	2.25
4	2.47
5	2.47
Average time	2.394
Discharge (L/s)	**0.58**

GW-2

Trial	Time (s)
1	34.72
2	32.22
3	32.22
4	33.03
5	33.12
Average time	33.062
Discharge (L/s)	**0.06**

GW-3 using a wading rod and flow meter. Calculations shown as conversion to English units.

GW-3

Distance (ft)	Depth (ft)	Velocity (ft/s)	Area (ft^2)	Discharge (ft^3/s)
1.3	0.40	2.72	0.26	0.71
		Total cross sectional area	0.26	
			Discharge (L/s)	**20.03**

SW-1 wading rod and flow meter. Metric units were converted to English units.

SW-1

Distance (ft)	Depth (ft)	Velocity (ft/s)	Average velocity (ft/s)	Area (ft^2)	Discharge (ft^3/s)
1	0.59	0.34	0.17	0.295	0.05
2	0.66	1.85	1.10	0.625	0.68
3	0.59	1.39	1.62	0.625	1.01
4	0.39	0.72	1.06	0.490	0.52
5	0.26	0.13	0.43	0.325	0.14
6.5	0.2	0.44	0.29	0.345	0.10
7.4	0.26	0.34	0.39	0.207	0.08
8.7	0	0	0.17	0.169	0.03
			Total:	3.08	2.61
				Discharge (L/s)	**73.91**

SW-5 wading rod and flow meter measurements.

SW-5

Distance (ft)	Depth (ft)	Velocity (ft/s)	Average velocity (ft/s)	Area (ft2)	Discharge (ft^3/s)
1.25	0.4	0.39	0.20	0.25	0.05
2.25	0.6	1.12	0.76	0.50	0.38
3.25	0.6	1.23	1.18	0.60	0.71
4.25	0.6	0.13	0.68	0.60	0.41
5.25	0.67	1.39	0.76	0.03	0.03
6.25	0.67	2.2	1.80	0.67	1.20
7.25	0.33	0.07	1.14	0.50	0.57
8.25	0	0	0.04	0.17	0.01
			Total:	3.32	3.33
				Discharge (L/s)	**94.44**

SW-6 using a wading rod and flow meter. Calculation showing units converted from metric to English.

SW-6

Distance (ft)	Depth (ft)	Velocity (ft/s)	Average velocity (ft/s)	Area (ft^2)	Discharge (ft^3/s)
1	0.33	0.82	0.41	0.17	0.07
2	0.40	2.08	1.45	0.37	0.53
3	0.60	2.92	2.5	0.50	1.25
4	0.53	0.93	1.925	0.57	1.09
5	0.73	1.51	1.22	0.63	0.77
6	0.47	0.72	1.115	0.60	0.67
7	0.80	0.25	0.485	0.63	0.31
11	0.00	0	0.125	1.6	0.20
	Total:			5.07	4.89
				Discharge (L/s)	**138.48**

SW-7 using a wading rod and flow meter. Calculation showing units converted from metric to English.

SW-7

Distance (ft)	Depth (ft)	Velocity (ft/s)	Average velocity (ft/s)	Area (ft^2)	Discharge (ft^3/s)
1	0.40	1.85	0.925	0.2	0.19
2	0.47	2.08	1.965	0.43	0.85
3	0.40	1.21	1.645	0.43	0.71
4	0.33	1.67	1.44	0.37	0.53
5	0.47	0.59	1.13	0.53	0.60
6	0.47	0.93	0.76	0.47	0.35
7	0.33	0	0.465	0.40	0.19
8	0.33	1.13	0.565	0.33	0.19
9	0.53	1.82	1.475	0.63	0.93
10	0.00	0	0.91	0.27	0.24
11	0.33	1.13	0.565	0.50	0.28
12	0.33	2.1	1.615	0.33	0.54
13	0.40	2.35	2.225	0.43	0.96
14	0.27	1.02	1.685	0.33	0.56
15	0	0	0.51	0.13	0.07
19	0.20	1.31	0.655	1.20	0.79
20	0.20	0.07	0.69	0.20	0.14
21	0	0	0.035	0.10	0.00
			Total:	7.30	8.13
				Discharge (L/s)	**230.18**

SW-8 using a wading rod and flow meter. Calculation showing units converted from metric to English.

SW-8

Distance (ft)	Depth (ft)	Velocity (ft/s)	Average velocity (ft/s)	Area (ft^2)	Discharge (ft^3/s)
1.1	0.33	0.00	0.00	0.18	0.00
2.1	0.33	2.07	1.04	0.33	0.35
3.1	0.40	1.49	1.78	0.37	0.65
4.1	0.33	1.12	1.31	0.37	0.48
5.1	0.53	0.18	0.65	0.43	0.28
6.1	0.80	2.77	1.48	0.67	0.98
7.1	0.87	3.39	3.08	0.83	2.57
8.1	0.87	2.82	3.11	0.87	2.69
9.1	0.67	3.39	3.11	0.77	2.38
10.1	0.73	1.98	2.69	0.70	1.88
11.1	0.73	2.13	2.06	0.73	1.51
12.4	0.00	0.00	1.07	0.48	0.51
			Total:	6.73	14.27
				Discharge (L/s)	**404.23**

GW-1 volumetric discharge using a 1400 mL container and **GW-2** using a 2000 mL container.

GW-1

Trial	Time (s)
1	3.5
2	3.25
3	3.38
4	3.87
5	3.88
Average time	3.576
Discharge (L/s)	**0.39**

GW-2

Trial	Time (s)
1	33.37
2	33.56
3	32.6
4	32.85
5	33.09
Average time	33.094
Discharge (L/s)	**0.06**

GW-3 measured using a wading rod and flow meter.

GW-3

Distance (ft)	Depth (ft)	Velocity (ft/s)	Area (ft^2)	Discharge (ft^3/s)
0.9	0.45	2.71	0.203	0.55
		Total cross sectional area:	0.2025	
			Discharge (L/s)	**15.54**

SW-1 measured using a wading rod and flow meter.

SW-1

Distance (ft)	Depth (ft)	Velocity (ft/s)	Average velocity (ft/s)	Area (ft^2)	Discharge (ft^3/s)
1.1	0.55	0.22	0.11	0.30	0.03
2.1	0.55	0.525	0.37	0.55	0.20
3.1	0.5	0.91	0.72	0.525	0.38
4.1	0.4	0.08	0.50	0.55	0.27
9.1	0	0	0.04	1	0.04
			Total:	2.93	0.93
				Discharge (L/s)	**26.26**

SW-5 measured using a wading rod and flow meter.

SW-5

Distance (ft)	Depth (ft)	Velocity (ft/s)	Average velocity (ft/s)	Area (ft2)	Discharge (ft^3/s)
1	0.25	0	0.13	0.13	0.02
2	0.3	0.06	0.03	0.28	0.01
3.1	0.65	0.68	0.37	0.52	0.19
3.9	0.5	0.13	0.41	0.46	0.19
5.5	0.6	0.325	0.23	0.88	0.20
6.5	0.5	0.965	0.65	0.55	0.35
7.5	0.3	0.08	0.52	0.40	0.21
8.9	0	0	0.00	0.21	0
			Total:	3.42	1.167
				Discharge (L/s)	**33.06**

SW-6 measured using a wading rod and flow meter.

SW-6

Distance (ft)	Depth (ft)	Velocity (ft/s)	Average velocity (ft/s)	Area (ft^2)	Discharge (ft^3/s)
1.2	0.2	0.705	0.3525	0.12	0.04
2.4	0.4	1.385	1.045	0.36	0.38
3.9	0.5	0.655	1.02	0.675	0.69
5.2	0.6	1.115	0.885	0.715	0.63
6.2	0.6	0.075	0.595	0.6	0.36
7.2	0.5	0	0.0375	0.55	0.02
8.2	0.4	0	0	0.45	0
9.4	0.5	0	0	0.54	0
10.4	0	0	0	0.25	0
			Total:	4.26	2.12
				Discharge (L/s)	**59.96**

SW-7 measured using a wading rod and flow meter.

SW-7

Distance (ft)	Depth (ft)	Velocity (ft/s)	Average velocity (ft/s)	Area (ft^2)	Discharge (ft^3/s)
6.5	0.2	0.93	0.46	0.65	0.30
7.5	0.3	0.28	0.60	0.25	0.15
10.5	0.2	0.15	0.21	0.75	0.16
11.5	0.2	0.81	0.48	0.2	0.10
11.9	0.4	1.24	1.02	0.12	0.12
13.3	0.3	0.94	1.09	0.49	0.53
15.4	0.6	0.05	0.49	0.945	0.47
16.5	0.4	0.03	0.04	0.55	0.02
17.7	0.3	1.15	0.59	0.42	0.25
18.8	0.4	1.68	1.41	0.495	0.70
19.8	0.5	0.19	0.93	0.45	0.42
21.7	0	0	0.09	0.475	0.04
			Total:	5.80	3.25
				Discharge (L/s)	**92.13**

SW-8 measured using a wading rod and flow meter.

SW-8

Distance (ft)	Depth (ft)	Velocity (ft/s)	Average velocity (ft/s)	Area (ft^2)	Discharge (ft^3/s)
1	0.3	0	0	0.15	0
2.4	0.3	0	0	0.42	0
2.9	0.3	0.025	0.1275	0.15	0.019125
3.3	0.3	0.23	0.115	0.12	0.0138
5.5	0.3	1.21	0.6175	0.66	0.40755
6.4	0.8	1.73	1.47	0.495	0.72765
7.4	0.9	1.825	1.7775	0.85	1.510875
8.4	0.5	2.015	1.92	0.7	1.344
9.4	0.7	1.515	1.765	0.6	1.059
10.4	0.7	1.56	1.5375	0.7	1.07625
11.4	0.4	1.225	1.3925	0.55	0.765875
12.4	0	0	0.6125	0.2	0.1225
			Total:	**5.60**	**7.05**
				Discharge (L/s)	**199.6**

GW-1 volumetric discharge using a 1400 mL container. **GW-2** volumetric discharge using a 2000 mL container.

GW-1

Trial	Time (s)
1	4.28
2	5.22
3	5.5
4	5.56
5	4.78
Average time (s)	5.07
Discharge (L/s)	**0.28**

GW-2

Trial	Time (s)
1	33.4
2	31.72
3	32.06
4	32.72
5	32.09
Average time (s)	32.40
Discharge (L/s)	**0.06**

GW-3 wading rod and flow meter discharge.

GW-3

Distance (ft)	Depth (ft)	Velocity (ft/s)	Area (ft^2)	Discharge (ft^3/s)
0.45	0.4	3.56	0.180	0.64
		Total cross sectional area	**0.180**	
			Discharge (L/s)	**18.15**

SW-1 wading rod and flow meter discharge.

SW-1

Distance (ft)	Depth (ft)	Velocity (ft/s)	Average velocity (ft/s)	Area (ft^2)	Discharge (ft^3/s)
1	0.65	0.40	0.20	0.33	0.07
2	0.50	0.67	0.53	0.58	0.31
3	0.30	0.39	0.53	0.40	0.21
4.8	0	0	0.19	0.27	0.05
			Total:	1.57	0.63
				Discharge (L/s)	**17.93**

SW-5 wading rod and flow meter discharge.

SW-5

Distance (ft)	Depth (ft)	Velocity (ft/s)	Average velocity (ft/s)	Area (ft^2)	Discharge (ft^3/s)
2	0.4	0.32	0.20	0.40	0.08
3	0.5	0.61	0.47	0.45	0.21
4	0.6	0.41	0.51	0.55	0.28
5	0.4	0.73	0.57	0.50	0.28
6	0.25	0.22	0.47	0.33	0.15
7.9	0	0.00	0.11	0.24	0.03
			Total:	2.46	1.03
				Discharge (L/s)	**29.15**

SW-6 wading rod and flow meter discharge.

SW-6

Distance (ft)	Depth (ft)	Velocity (ft/s)	Average velocity (ft/s)	Area (ft^2)	Discharge (ft^3/s)
2	0.3	0.83	0.415	0.3	0.12
3	0.3	1.605	1.2175	0.3	0.37
4	0.5	0.545	1.075	0.4	0.43
5	0.6	1.115	0.83	0.55	0.46
6	0.6	0.11	0.6125	0.6	0.37
7	0.5	0	0.055	0.55	0.03
10.5	0	0	0	0.88	0
			Total:	3.575	1.77
				Discharge (L/s)	**50.24**

SW-7 wading rod and flow meter discharge.

SW-7

Distance (ft)	Depth (ft)	Velocity (ft/s)	Average velocity (ft/s)	Area (ft^2)	Discharge (ft^3/s)
0	0.35	0.57	0.29	0	0
1	0.3	1.41	0.99	0.33	0.32
2	0.3	1.11	1.26	0.30	0.38
3	0.35	0.17	0.64	0.33	0.21
4	0.3	0.56	0.37	0.33	0.12
5	0.2	0.74	0.65	0.25	0.16
6	0	0.00	0.37	0.10	0.04
7	0.25	0.69	0.35	0.13	0.04
10	0.3	0.62	0.66	0.83	0.54
11	0.2	0.33	0.47	0.25	0.12
12	0.2	0.47	0.40	0.20	0.08
18.4	0	0.00	0.24	0.64	0.15
			Total:	3.67	2.15
				Discharge (L/s)	**61.01**

SW-8 wading rod and flow meter discharge.

SW-8

Distance (ft)	Depth (ft)	Velocity (ft/s)	Average velocity (ft/s)	Area (ft^2)	Discharge (ft^3/s)
1	0.3	0	0	0.45	0
2	0.2	0	0	0.25	0
3	0.3	0.065	0.03	0.25	0.01
4	0.2	1.150	0.61	0.25	0.15
5	0.7	1.325	1.24	0.45	0.56
6	0.9	1.790	1.56	0.8	1.25
7	0.4	1.925	1.86	0.65	1.21
8	0.6	1.580	1.75	0.5	0.88
9	0.7	1.265	1.42	0.65	0.92
10	0.4	0.740	1.00	0.55	0.55
11.5	0	0	0.37	0.3	0.11
			Total:	5.1	5.63
				Discharge (L/s)	**159.54**

Appendix C
Field Chemical Results

Table C.1: Chemical field analyses for July.

7.8.11	pH	Salinity (‰)	EC (µS)	Alk (mg/L)	T (ºC)	D.O. (mg/L)
GW-1	6.73	0.1	72	40	5.4	
GW-2	7.77	0.2	284	200	10.1	
GW-3	7.13	0.2	253	120	8.6	
SW-1	7.57	0.1	112	60	9	
SW-2	7.8	0.1	178	60	7.2	
SW-3	9.17	0.3	570	140	17.3	
SW-4	7.77	0.2	264	60	8.3	
SW-5	9.17	0.3	485	140	17.3	
SW-6	7.88	0.1	110	80	13.5	
SW-7	8.17	0.1	117.6	60	11.5	
SW-8	7.78	0.1	115.3	60	12.1	

Table C.2: Chemical field analyses and dissolved oxygen saturation monogram for August.

8.5.11	pH	Salinity (‰)	EC (µS)	Alk (mg/L)	T (ºC)	D.O. (mg/L)
GW-1	7.56	0	89.9	40	6.1	12.2
GW-2	8.86	0.2	388.9	180	10.6	11.3
GW-3	7.15	0.2	348.1	100	8.2	7.9
SW-1	8.29	0.1	139.9	80	11.6	10.9
SW-5	8.39	0.1	199.9	80	11.9	10.7
SW-6	8.84	0.1	175	80	10.2	11.7
SW-7	8.23	0.1	225.8	100	9.1	11.1
SW-8	8.34	0.1	204.7	80	9.1	11.3

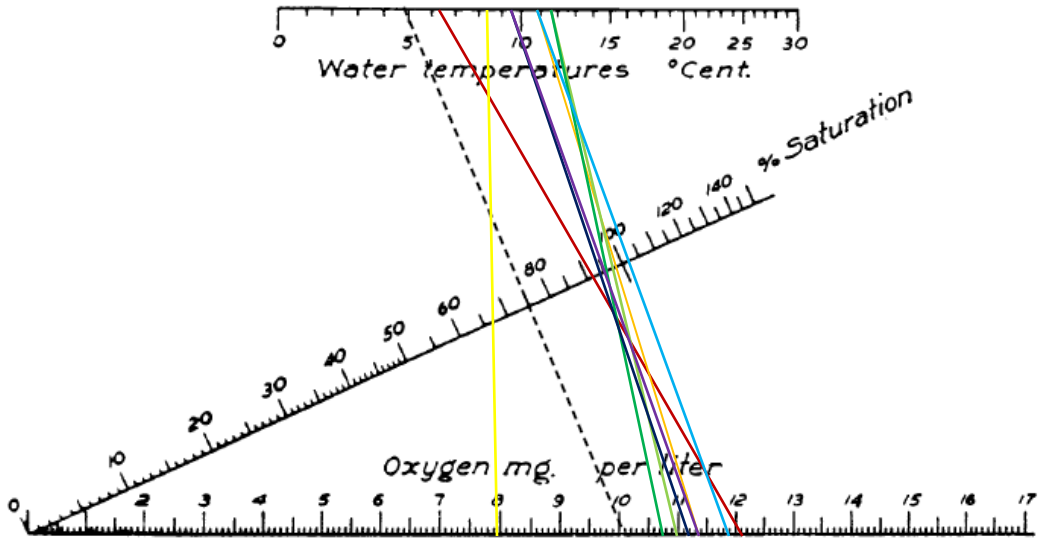

Level of oxygen saturation chart.

Table C.3: Chemical field analyses and dissolved oxygen saturation monogram for September.

9.1.11	pH	Salinity (‰)	EC (µS)	Alk (mg/L)	T (ºC)	D.O. (mg/L)
GW-1	7.26	0	81.8	40	6.7	12.9
GW-2	8.06	0.2	373	180	10.8	11.4
GW-3	6.74	0.2	333	100	8.3	7.6
SW-1	8.6	0.1	109	60	8.1	12.1
SW-5	8.02	0.1	222.8	80	9.1	11.9
SW-6	8.17	0.1	194.5	60	6.9	11.6
SW-7	8.31	0.1	251.8	100	6.3	12.9
SW-8	8.57	0.1	247.2	80	6.2	12.3

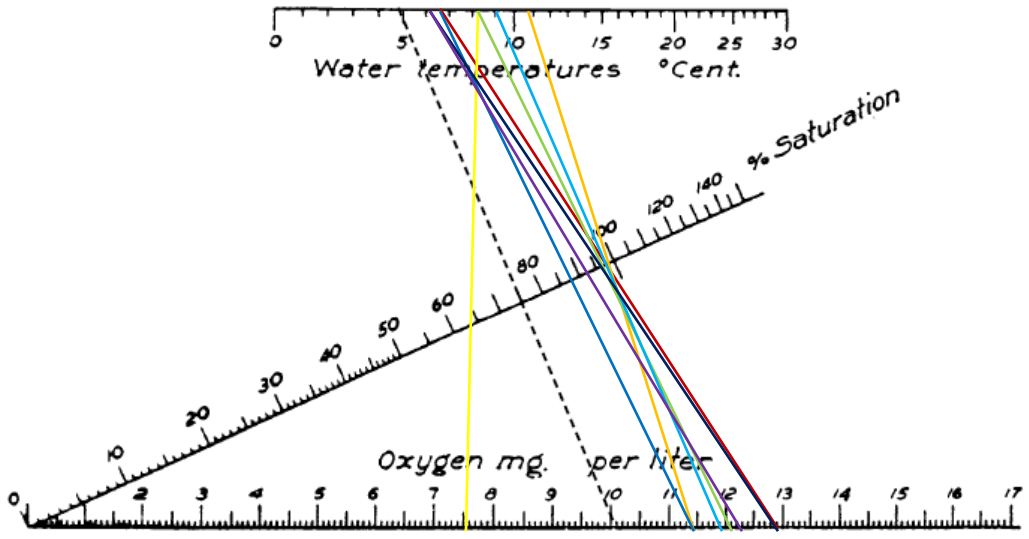

Level of oxygen saturation chart.

Table C.4: Chemical field analyses and dissolved oxygen saturation monogram for October.

10.1.11	pH	Salinity (‰)	EC (µS)	Alk (mg/L)	T (ºC)	D.O. (mg/L)
GW-1	6.97	0	75.3	40	6.7	13.2
GW-2	8.17	0.2	367	180	10.7	11.1
GW-3	6.68	0.2	326	120	8.7	6.8
SW-1	8.08	0.1	163		8.2	12.4
SW-5	8.02	0.1	223	100	9.1	8.5
SW-6	8.22	0.1	196	60	8	10.2
SW-7	8.29	0.1	258	120	7.1	13.3
SW-8	8.34	0.1	256	100	8.2	9.7

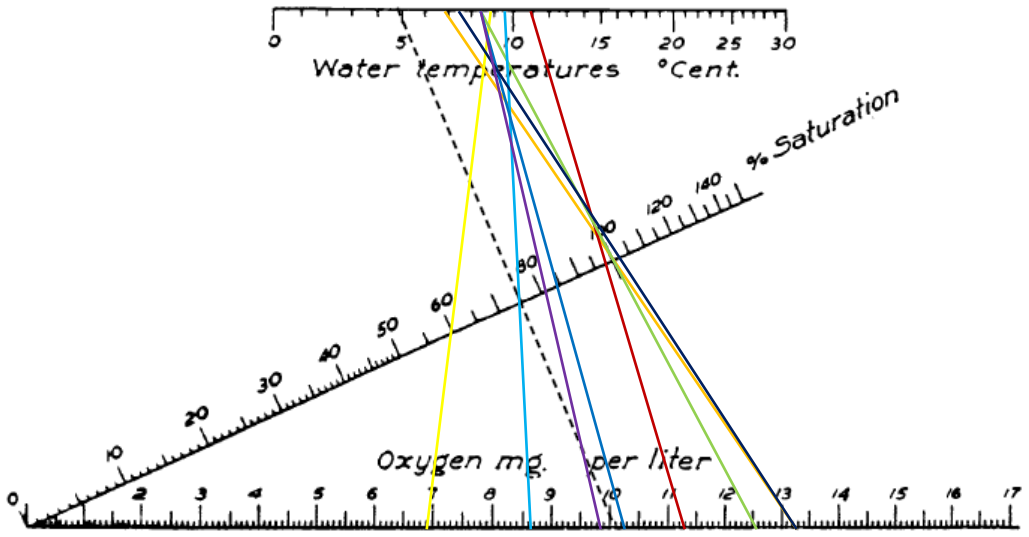

Level of oxygen saturation chart.

Appendix D
Chemical Results from UVDL and USUAL

	GW-1 F	GW-2 F	GW-3 F	GW-3 F	GW-3 U	SW-1 F	SW-1 F	SW-1 U	D.L.
Ag	N.A.	N.A.	N.A.	<0.001	<0.001	N.A.	<0.001	<0.001	0.001
Al	<0.12	<0.12	<0.12	**0.029**	**0.02**	<0.12	**0.022**	**0.101**	0.12
As	**0.07**	<0.01	<0.01	**0.026**	**0.02**	<0.01	**0.001**	**0.001**	0.01
B	<0.02	<0.02	<0.02	**0.004**	**0.005**	<0.02	**0.008**	**0.008**	0.02
Ba	**0.01**	**0.01**	**0.01**	**0.007**	**0.007**	**0.03**	**0.03**	**0.031**	0.001
Be	N.A.	N.A.	N.A.	<0.001	<0.001	N.A.	<0.001	<0.001	0.001
Ca	**3.56**	**22.2**	**7.71**	**8.419**	**8.128**	**8.07**	**8.868**	**8.396**	0.08
Cd	<0.001	<0.001	<0.001	<0.001	<0.001	<0.001	<0.001	<0.001	0.001
Co	<0.005	<0.005	<0.005	**0.001**	**0.001**	<0.005	<0.001	<0.001	0.005
Cr	<0.006	<0.006	<0.006	**0.001**	**0.001**	<0.006	<0.001	0.001	0.006
Cu	**0.03**	<0.008	**0.01**	**0.011**	**0.009**	<0.008	**0.006**	**0.006**	0.008
Fe	**0.08**	**0.93**	**3.52**	**4.236**	**1.483**	**0.04**	**0.108**	**0.178**	0.003
K	**0.66**	**2.76**	**0.68**	**0.707**	**0.774**	**0.74**	**0.783**	**0.837**	0.46
Li	N.A.	N.A.	N.A.	**0.008**	**0.009**	N.A.	**0.002**	**0.002**	0.001
Mg	**5.84**	**24.8**	**31.9**	**38.222**	**37.762**	**3.52**	**4.309**	**4.045**	0.007
Mn	**0.003**	**0.03**	**0.23**	**0.312**	**0.25**	<0.001	**0.005**	**0.006**	0.001
Mo	<0.15	<0.15	<0.15	<0.001	<0.001	<0.15	<0.001	<0.001	0.15
Na	**2.28**	**7.34**	**1.34**	**1.126**	**1.342**	**3.46**	**3.645**	**3.972**	0.08
Ni	**0.005**	<0.003	**0.004**	**0.007**	**0.007**	<0.003	**0.002**	**0.005**	0.003
P	<0.08	<0.08	<0.08	**0.051**	**0.028**	<0.08	**0.02**	**0.022**	0.08
Pb	<0.03	<0.03	<0.03	**0.008**	**0.007**	<0.03	<0.001	<0.001	0.03
S	**3.52**	**4.62**	**18.9**	N.A.	N.A.	**0.67**	N.A.	N.A.	0.07
Sb	N.A.	N.A.	N.A.	**0.007**	**0.004**	N.A.	<0.001	<0.001	0.001
Se	<0.04	<0.04	<0.04	<0.001	<0.001	<0.04	<0.001	<0.001	0.001
Si	**3.7**	**16.7**	**3.76**	**2.117**	**2.159**	**12.6**	**7.538**	**6.841**	0.15
Sn	N.A.	N.A.	N.A.	<0.001	<0.001	N.A.	<0.001	<0.001	0.001
Sr	<0.03	**0.31**	<0.03	**0.017**	**0.016**	**0.07**	**0.087**	**0.084**	0.03
Tl	N.A.	N.A.	N.A.	<0.001	<0.001	N.A.	<0.001	<0.001	0.001
V	N.A.	N.A.	N.A.	<0.001	<0.001	N.A.	<0.001	<0.001	0.001
Zn	**0.11**	**0.01**	**0.02**	**0.037**	**0.026**	**0.03**	**0.041**	**0.021**	0.005

Table D.1. Chemical results from USUAL and UVDL from July. Bold values are above the detection limit of the lab. Red and bold values indicate exceedences of EPA drinking water standards (As at 0.01 mg/L, Cu at 1.3 mg/L, Fe at 0.3 mg/L, Mn at 0.05 mg/L, Pb at 0.015 mg/L, and Zn at 5 mg/L). Calculations were made using half the detection limit. The detection limit is shown on the right. N.A. = Not Analyzed.

	SW-2 F	SW-2 F	SW-2 U	SW-3 F	SW-4 F	SW-5 F	SW-5 U	D.L.
Ag	N.A.	<0.001	<0.001	N.A.	N.A.	N.A.	<0.001	0.001
Al	<0.12	**0.017**	**0.105**	<0.12	<0.12	<0.12	**0.119**	0.12
As	<0.01	**0.013**	**0.022**	**0.06**	**0.025**	<0.01	**0.005**	0.01
B	<0.02	**0.007**	**0.006**	<0.02	<0.02	<0.02	**0.005**	0.02
Ba	**0.02**	**0.007**	**0.008**	**0.07**	**0.01**	**0.024**	**0.026**	0.001
Be	N.A.	<0.001	<0.001	N.A.	N.A.	N.A.	<0.001	0.001
Ca	**11.2**	**11.302**	**10.702**	**10.8**	**9.03**	**10.1**	**8.097**	0.08
Cd	<0.001	<0.001	<0.001	<0.001	<0.001	<0.001	<0.001	0.001
Co	<0.005	<0.001	<0.001	<0.005	<0.005	<0.005	<0.001	0.005
Cr	**0.01**	**0.001**	**0.001**	**0.01**	**0.01**	<0.006	**0.001**	0.006
Cu	<0.008	**0.006**	**0.015**	<0.008	<0.008	<0.008	**0.004**	0.008
Fe	**0.08**	**0.113**	**0.422**	**0.77**	**2.64**	**0.01**	**0.46**	0.003
K	**1.27**	**1.305**	**1.278**	**7.9**	**1.9**	**1.15**	**0.803**	0.46
Li	N.A.	**0.005**	**0.005**	N.A.	N.A.	N.A.	**0.003**	0.001
Mg	**18.5**	**18.123**	**17.424**	**62.4**	**34.9**	**12.8**	**10.348**	0.007
Mn	**0.01**	**0.008**	**0.013**	**0.08**	**0.059**	**0.014**	**0.025**	0.001
Mo	<0.15	<0.001	<0.001	<0.15	<0.15	<0.15	<0.001	0.15
Na	**2.35**	**3.164**	**2.123**	**2.72**	**2.25**	**3.48**	**2.791**	0.08
Ni	<0.003	**0.005**	**0.004**	<0.003	<0.003	<0.003	**0.001**	0.003
P	<0.08	**0.088**	**0.062**	<0.08	<0.08	**0.23**	**0.027**	0.08
Pb	<0.03	**0.003**	**0.026**	<0.03	<0.03	<0.03	**0.003**	0.03
S	20.3	N.A.	N.A.	**52.4**	**32.5**	**5.85**	N.A.	0.07
Sb	N.A.	**0.004**	**0.005**	N.A.	N.A.	N.A.	**0.001**	0.001
Se	<0.04	<0.001	<0.001	<0.04	<0.04	<0.04	<0.001	0.001
Si	**8.96**	**4.775**	**4.808**	**3.93**	**11.4**	**9.22**	**6.104**	0.15
Sn	N.A.	<0.001	<0.001	N.A.	N.A.	N.A.	<0.001	0.001
Sr	**0.05**	**0.059**	**0.054**	**0.03**	**<0.03**	**0.08**	**0.069**	0.03
Tl	N.A.	<0.001	<0.001	N.A.	N.A.	N.A.	<0.001	0.001
V	N.A.	<0.001	<0.001	N.A.	N.A.	N.A.	<0.001	0.001
Zn	**0.02**	**0.026**	**0.024**	**0.01**	**0.02**	**0.04**	**0.015**	0.005

Table D.1. Chemical results from USUAL and UVDL from July. Bold values are above the detection limit of the lab. Red and bold values indicate exceedences of EPA drinking water standards (As at 0.01 mg/L, Cu at 1.3 mg/L, Fe at 0.3 mg/L, Mn at 0.05 mg/L, Pb at 0.015 mg/L, and Zn at 5 mg/L). Calculations were made using half the detection limit. The detection limit is shown on the right. N.A. = Not Analyzed.

	SW-6 F	SW-6 U	SW-7 F	SW-7 U	SW-8 F	SW-8 U	D.L.
Ag	N.A.	<0.001	N.A.	<0.001	N.A.	<0.001	0.001
Al	<0.12	**0.126**	<0.12	**0.154**	<0.12	**0.128**	0.12
As	<0.01	**0.005**	<0.01	**0.004**	<0.01	**0.003**	0.01
B	<0.02	**0.005**	<0.02	**0.006**	<0.02	**0.01**	0.02
Ba	**0.04**	**0.028**	**0.05**	**0.02**	**0.02**	**0.02**	0.001
Be	N.A.	<0.001	N.A.	<0.001	N.A.	<0.001	0.001
Ca	**8.18**	**8.258**	**12.5**	**12.107**	**11.1**	**10.854**	0.08
Cd	<0.001	<0.001	<0.001	<0.001	<0.001	<0.001	0.001
Co	<0.005	<0.001	<0.005	<0.001	<0.005	<0.001	0.005
Cr	**0.01**	**0.001**	**0.01**	**0.001**	<0.006	**0.001**	0.006
Cu	<0.008	**0.005**	<0.008	**0.004**	<0.008	**0.006**	0.008
Fe	**0.19**	**0.509**	**0.37**	**0.612**	**0.19**	**0.411**	0.003
K	**0.74**	**0.837**	**0.55**	**0.678**	**0.65**	**0.712**	0.46
Li	N.A.	**0.003**	N.A.	**0.003**	N.A.	**0.003**	0.001
Mg	**7.39**	**7.044**	**7.47**	**7.347**	**6.74**	**6.657**	0.007
Mn	**0.01**	**0.021**	**0.01**	**0.019**	**0.01**	**0.018**	0.001
Mo	<0.15	<0.001	<0.15	<0.001	<0.15	<0.001	0.15
Na	**2.91**	**2.784**	**2.86**	**2.768**	**3.26**	**3.186**	0.08
Ni	<0.003	**0.003**	<0.003	**0.004**	<0.003	**0.002**	0.003
P	<0.08	**0.029**	<0.08	**0.026**	<0.08	**0.027**	0.08
Pb	<0.03	**0.003**	<0.03	**0.003**	<0.03	**0.003**	0.03
S	**3.17**	N.A.	**2.86**	N.A.	**3.09**	N.A.	0.07
Sb	N.A.	**0.001**	N.A.	<0.001	N.A.	<0.001	0.001
Se	<0.04	<0.001	<0.04	<0.001	<0.04	<0.001	0.001
Si	**12.4**	**6.553**	**9.5**	**4.972**	**9.6**	**4.901**	0.15
Sn	N.A.	**0.001**	N.A.	<0.001	N.A.	<0.001	0.001
Sr	**0.07**	**0.074**	**0.07**	**0.075**	**0.07**	**0.073**	0.03
Tl	N.A.	<0.001	N.A.	<0.001	N.A.	<0.001	0.001
V	N.A.	<0.001	N.A.	<0.001	N.A.	<0.001	0.001
Zn	**0.01**	**0.017**	**0.01**	**0.016**	**0.01**	**0.019**	0.005

Table D.1. Chemical results from USUAL and UVDL from July. Bold values are above the detection limit of the lab. Red and bold values indicate exceedences of EPA drinking water standards (As at 0.01 mg/L, Cu at 1.3 mg/L, Fe at 0.3 mg/L, Mn at 0.05 mg/L, Pb at 0.015 mg/L, and Zn at 5 mg/L). Calculations were made using half the detection limit. The detection limit is shown on the right. N.A. = Not Analyzed.

	GW-1 F	GW-2 F	GW-3 F	GW-3 U	SW-1 F	SW-1 U	SW-5 F	D.L.
Ag	N.A.	N.A.	N.A.	<0.001	N.A.	<0.001	N.A.	0.001
Al	<0.12	<0.12	<0.12	**0.011**	<0.12	**0.109**	<0.12	0.12
As	**0.04**	<0.01	<0.01	**0.013**	<0.01	**0.001**	<0.01	0.01
B	<0.02	<0.02	<0.02	**0.004**	<0.02	**0.005**	<0.02	0.02
Ba	**0.001**	**0.006**	**0.007**	**0.007**	**0.029**	**0.036**	**0.022**	0.001
Be	N.A.	N.A.	N.A.	<0.001	N.A.	<0.001	N.A.	0.001
Ca	**2.27**	**24.4**	**7.64**	**7.886**	**10.5**	**10.126**	**8.58**	0.08
Cd	<0.001	<0.001	<0.001	<0.001	<0.001	<0.001	<0.001	0.001
Co	<0.005	<0.005	<0.005	0.001	<0.005	<0.001	<0.005	0.005
Cr	0.0093	<0.006	<0.006	<0.001	<0.006	0.001	<0.006	0.006
Cu	<0.008	<0.008	<0.008	0.003	<0.008	0.004	<0.008	0.008
Fe	**0.03**	**1.12**	**0.15**	**0.53**	**0.02**	**0.25**	**0.54**	0.003
K	**0.29**	**2.93**	**0.66**	**0.685**	**0.85**	**0.937**	**0.73**	0.46
Li	N.A.	N.A.	N.A.	**0.009**	N.A.	**0.002**	N.A.	0.001
Mg	**5.77**	**28.7**	**34.3**	**35.013**	**5.53**	**5.361**	**10.3**	0.007
Mn	0.001	**0.041**	**0.255**	**0.271**	**0.001**	**0.01**	**0.015**	0.001
Mo	<0.15	<0.15	<0.15	<0.001	<0.15	<0.001	<0.15	0.15
Na	**0.64**	**7.1**	**0.86**	**0.937**	**3.81**	**3.564**	**2.85**	0.08
Ni	<0.003	<0.003	0.004	**0.004**	<0.003	**0.002**	<0.003	0.003
P	<0.08	<0.08	<0.08	**0.014**	<0.08	**0.032**	<0.08	0.08
Pb	<0.03	<0.03	<0.03	<0.001	<0.03	**0.002**	<0.03	0.03
S	**3.28**	**5.34**	**19.4**	N.A.	**1.06**	N.A.	**4.82**	0.07
Sb	N.A.	N.A.	N.A.	**0.002**	N.A.	<0.001	N.A.	0.001
Se	<0.04	<0.04	<0.04	<0.001	<0.04	<0.001	<0.04	0.001
Si	**4.01**	**17.3**	**3.98**	**2.18**	**11**	**5.803**	**11.6**	0.15
Sn	N.A.	N.A.	N.A.	<0.001	N.A.	<0.001	N.A.	0.001
Sr	<0.03	**0.32**	<0.03	**0.015**	**0.1**	**0.108**	**0.06**	0.03
Tl	N.A.	N.A.	N.A.	<0.001	N.A.	<0.001	N.A.	0.001
V	N.A.	N.A.	N.A.	<0.001	N.A.	<0.001	N.A.	0.001
Zn	**0.01**	<0.005	**0.01**	**0.015**	<0.005	**0.014**	<0.005	0.005

Table D.2. Chemical results from USUAL and UVDL from August. Bold values are above the detection limit of the lab. Red and bold values indicate exceedences of EPA drinking water standards (As at 0.01 mg/L, Cu at 1.3 mg/L, Fe at 0.3 mg/L, Mn at 0.05 mg/L, Pb at 0.015 mg/L, and Zn at 5 mg/L). Calculations were made using half the detection limit. The detection limit is shown on the right.

	SW-5 U	SW-6 F	SW-6 U	SW-7 F	SW-7 U	SW-8 F	SW-8 U	D.L.
Ag	<0.001	N.A.	<0.001	N.A.	<0.001	N.A.	<0.001	0.001
Al	**0.05**	<0.12	**0.033**	<0.12	**0.056**	<0.12	**0.049**	0.12
As	**0.004**	<0.01	**0.004**	<0.01	**0.003**	<0.01	**0.002**	0.01
B	**0.006**	<0.02	**0.006**	<0.02	**0.019**	<0.02	**0.007**	0.02
Ba	**0.028**	**0.022**	**0.025**	**0.021**	**0.022**	**0.019**	**0.024**	0.001
Be	<0.001	N.A.	<0.001	N.A.	<0.001	N.A.	<0.001	0.001
Ca	**10.319**	**9.9**	**9.627**	**17.7**	**15.033**	**16**	**17.203**	0.08
Cd	<0.001	<0.001	<0.001	<0.001	<0.001	<0.001	<0.001	0.001
Co	<0.001	<0.005	<0.001	<0.005	<0.001	<0.005	<0.001	0.005
Cr	0.001	<0.006	<0.001	<0.006	<0.001	<0.006	<0.001	0.006
Cu	0.005	<0.008	**0.004**	<0.008	**0.009**	<0.008	<0.002	0.008
Fe	**0.148**	**0.04**	**0.099**	**0.01**	**0.123**	**0.03**	**0.12**	0.003
K	**1.051**	**0.82**	**0.824**	**0.75**	**1.019**	**1.19**	**0.761**	0.46
Li	**0.004**	N.A.	**0.004**	N.A.	**0.01**	N.A.	**0.003**	0.001
Mg	**11.981**	**10.1**	**10.183**	**11.8**	**10.298**	**10.1**	**11.598**	0.007
Mn	**0.028**	**0.004**	**0.009**	**0.001**	**0.008**	**0.003**	**0.003**	0.001
Mo	<0.001	<0.15	<0.001	<0.15	<0.001	<0.15	<0.001	0.15
Na	**3.099**	**3.15**	**3.084**	**3.65**	**5.011**	**6.58**	**3.624**	0.08
Ni	**0.002**	<0.003	**0.002**	<0.003	**0.002**	**0.003**	**0.001**	0.003
P	**0.049**	<0.08	**0.028**	<0.08	**0.064**	<0.08	**0.027**	0.08
Pb	<0.001	<0.03	**0.001**	<0.03	**0.002**	<0.03	**0.001**	0.03
S	N.A.	**4.69**	N.A.	**4.31**	N.A.	**5.42**	N.A.	0.07
Sb	<0.001	N.A.	**0.002**	N.A.	<0.001	N.A.	<0.001	0.001
Se	<0.001	<0.04	<0.001	<0.04	<0.001	<0.04	<0.001	0.001
Si	**5.002**	**9.53**	**5.121**	**8.9**	**4.689**	**8.94**	**4.811**	0.15
Sn	<0.001	N.A.	<0.001	N.A.	<0.001	N.A.	<0.001	0.001
Sr	**0.085**	**0.07**	**0.08**	**0.09**	**0.106**	**0.1**	**0.105**	0.03
Tl	<0.001	N.A.	<0.001	N.A.	<0.001	N.A.	<0.001	0.001
V	<0.001	N.A.	<0.001	N.A.	<0.001	N.A.	<0.001	0.001
Zn	**0.021**	**0.02**	**0.015**	**0.01**	**0.023**	**0.01**	**0.012**	0.005

Table D.2. Chemical results from USUAL and UVDL from August. Bold values are above the detection limit of the lab. Red and bold values indicate exceedences of EPA drinking water standards (As at 0.01 mg/L, Cu at 1.3 mg/L, Fe at 0.3 mg/L, Mn at 0.05 mg/L, Pb at 0.015 mg/L, and Zn at 5 mg/L). Calculations were made using half the detection limit. The detection limit is shown on the right.

	GW-1 F	GW-2 F	GW-3 F	SW-1 F	SW-5 F	SW-6 F	SW-7 F	SW-8 F	D.L.
Ag	N.A.	N.A.	N.A.	N.A.	N.A.	N.A.	N.A.	N.A.	0.001
Al	<0.12	<0.12	<0.12	<0.12	<0.12	<0.12	<0.12	<0.12	0.12
As	**0.02**	<0.01	0.01	<0.01	<0.01	<0.01	<0.01	<0.01	0.01
B	<0.02	<0.02	<0.02	<0.02	<0.02	<0.02	<0.02	**0.02**	0.02
Ba	<0.001	0.01	0.01	**0.03**	**0.02**	**0.02**	**0.02**	**0.02**	0.001
Be	N.A.	N.A.	N.A.	N.A.	N.A.	N.A.	N.A.	N.A.	0.001
Ca	2.15	24.3	7.69	**12**	**10.6**	**10.1**	**20.6**	**17.5**	0.08
Cd	<0.001	<0.001	<0.001	<0.001	<0.001	<0.001	<0.001	<0.001	0.001
Co	<0.005	<0.005	<0.005	<0.005	<0.005	<0.005	<0.005	<0.005	0.005
Cr	<0.006	<0.006	<0.006	<0.006	<0.006	<0.006	<0.006	<0.006	0.006
Cu	<0.008	<0.008	<0.008	<0.008	<0.008	<0.008	<0.008	<0.008	0.008
Fe	0.02	**0.96**	0.17	**0.02**	0	**0.11**	**0.03**	**0.02**	0.003
K	0.78	3.06	0.99	**1.17**	**1.04**	**1.12**	**1.05**	**2.15**	0.46
Li	N.A.	N.A.	N.A.	N.A.	N.A.	N.A.	N.A.	N.A.	0.001
Mg	4.53	27.8	33.2	**6.29**	**15.7**	**12.4**	**13.8**	**11.9**	0.007
Mn	<0.001	0.044	**0.308**	<0.001	**0.011**	**0.003**	**0.003**	**0.002**	0.001
Mo	<0.15	<0.15	<0.15	<0.15	<0.15	<0.15	<0.15	<0.15	0.15
Na	0.67	7.32	1.04	**4.21**	**3.23**	**3.11**	**3.26**	**6.36**	0.08
Ni	<0.003	<0.003	<0.003	<0.003	<0.003	<0.003	<0.003	<0.003	0.003
P	<0.08	<0.08	<0.08	<0.08	<0.08	<0.08	<0.08	<0.08	0.08
Pb	<0.03	<0.03	<0.03	<0.03	<0.03	<0.03	<0.03	<0.03	0.03
S	2.66	5.25	18.8	**1.68**	**8.03**	**6.58**	**5.75**	**6.88**	0.07
Sb	N.A.	N.A.	N.A.	N.A.	N.A.	N.A.	N.A.	N.A.	0.001
Se	<0.04	<0.04	<0.04	<0.04	<0.04	<0.04	<0.04	<0.04	0.001
Si	4.18	17.6	4.3	**11**	**8.77**	**8.8**	**8.29**	**8.38**	0.15
Sn	N.A.	N.A.	N.A.	N.A.	N.A.	N.A.	N.A.	N.A.	0.001
Sr	<0.03	0.33	<0.03	**0.11**	**0.07**	**0.07**	**0.11**	**0.11**	0.03
Tl	N.A.	N.A.	N.A.	N.A.	N.A.	N.A.	N.A.	N.A.	0.001
V	N.A.	N.A.	N.A.	N.A.	N.A.	N.A.	N.A.	N.A.	0.001
Zn	0.01	0.01	0.02	**0.01**	**0.01**	**0.04**	**0.01**	**0.02**	0.005

Table D.3. Chemical results from USUAL from September. Bold values are above the detection limit of the lab. Red and bold values indicate exceedences of EPA drinking water standards (As at 0.01 mg/L, Cu at 1.3 mg/L, Fe at 0.3 mg/L, Mn at 0.05 mg/L, Pb at 0.015 mg/L, and Zn at 5 mg/L). Calculations were made using half the detection limit. The detection limit is shown on the right.

	SW-1 SS-1	SW-2a	SW-5 SS-2	GW-1 Rock
Ag	0.66	20.72	173.35	0.27
Al	5187.49	5548.56	6168.6	14315.04
As	13	2868.38	714.47	3.27
B	1.01	1.09	1.39	0.4
Ba	73.25	20.28	103.78	19.76
Be	0.52	0.63	0.67	0.47
Ca	1394.01	1138.62	1612.78	73.19
Cd	0.08	3.41	1.61	0.01
Co	17.74	36	28.25	19.99
Cr	14.09	21.27	15.18	31.07
Cu	10.95	328.3	1898.08	8.83
Fe	19516.49	64307.72	38797.34	24340.61
K	1757.32	1275.16	1755.69	1041.38
Li	7.25	6.9	7.77	36.77
Mg	1829.48	6197.56	4922.11	7264.37
Mn	299.99	4233.93	2470.02	219.7
Mo	0.45	0.52	0.64	0.1
Na	150.26	332.28	317.44	401.44
Ni	14.82	47.35	15.18	14.66
P	418.49	370.79	425.58	222.02
Pb	17.97	1383.41	278.25	2.09
Sb	0.05	2.19	159.84	0.02
Se	0.22	0.2	0.23	0.32
Si	223.63	218.01	311.24	236.03
Sn	0.06	0.32	0.05	0.01
Sr	14.16	5.71	13.89	6.57
Tl	0.15	0.13	0.17	0.07
V	18.38	14.57	14.72	10.01
Zn	46.74	510.23	227.78	42.88

Table D.2. Chemical results from UVDL sediment and rock samples from September. Bold values are above the detection limit of the lab. Red and bold values indicate exceedences of EPA drinking water standards (As at 0.01 mg/L, Cu at 1.3 mg/L, Fe at 0.3 mg/L, Mn at 0.05 mg/L, Pb at 0.015 mg/L, and Zn at 5 mg/L). Calculations were made using half the detection limit. The detection limit is shown on the right.

	GW-1 F	GW-2 F	GW-3 F	GW-3 U	SW-1 F	SW-1 U	D.L.
Ag	N.A.	N.A.	N.A.	<0.001	N.A.	<0.001	0.001
Al	<0.12	<0.12	<0.12	0.016	<0.12	**0.059**	0.12
As	**0.02**	<0.01	<0.01	**0.015**	<0.01	**0.002**	0.01
B	<0.02	<0.02	<0.02	0.006	<0.02	**0.008**	0.02
Ba	<0.001	**0.01**	**0.01**	0.01	**0.03**	**0.039**	0.001
Be	N.A.	N.A.	N.A.	<0.001	N.A.	<0.001	0.001
Ca	**2.31**	**23.6**	**7.61**	7.958	**11.6**	**12.022**	0.08
Cd	<0.001	<0.001	<0.001	<0.001	<0.001	<0.001	0.001
Co	<0.005	<0.005	<0.005	0.002	<0.005	<0.001	0.005
Cr	<0.006	<0.006	<0.006	<0.001	<0.006	0.001	0.006
Cu	<0.008	<0.008	<0.008	0.003	<0.008	**0.003**	0.008
Fe	**0.02**	**0.93**	<0.20	**0.68**	<0.02	**0.187**	0.003
K	**0.79**	**3.2**	**0.9**	0.816	**2.11**	**2.085**	0.46
Li	N.A.	N.A.	N.A.	0.01	N.A.	**0.003**	0.001
Mg	**3.88**	**29.3**	**33.9**	34.699	**6.8**	**7.063**	0.007
Mn	<0.001	**0.042**	**0.378**	**0.396**	**0.002**	**0.024**	0.001
Mo	<0.15	<0.15	<0.15	<0.001	<0.15	<0.001	0.15
Na	**0.69**	**7.67**	**0.99**	0.961	**4.48**	**4.206**	0.08
Ni	<0.003	<0.003	<0.003	0.006	<0.003	**0.002**	0.003
P	<0.08	<0.08	<0.08	0.013	<0.08	**0.032**	0.08
Pb	<0.03	<0.03	<0.03	0.002	<0.03	**0.002**	0.03
S	**2.23**	**5.26**	**18.7**	N.A.	**1.72**	N.A.	0.07
Sb	N.A.	N.A.	N.A.	0.002	N.A.	<0.001	0.001
Se	<0.04	<0.04	<0.04	<0.001	<0.04	<0.001	0.001
Si	**4.1**	**17.2**	**4.26**	2.356	**10.1**	**5.553**	0.15
Sn	N.A.	N.A.	N.A.	<0.001	N.A.	<0.001	0.001
Sr	<0.03	**0.35**	<0.03	0.015	**0.11**	**0.123**	0.03
Tl	N.A.	N.A.	N.A.	<0.001	N.A.	<0.001	0.001
V	N.A.	N.A.	N.A.	<0.001	N.A.	<0.001	0.001
Zn	**0.02**	**0.02**	**0.03**	0.03	**0.02**	**0.034**	0.005

Table D.5. Chemical results from USUAL and UVDL from October. Bold values are above the detection limit of the lab. Red and bold values indicate exceedences of EPA drinking water standards (As at 0.01 mg/L, Cu at 1.3 mg/L, Fe at 0.3 mg/L, Mn at 0.05 mg/L, Pb at 0.015 mg/L, and Zn at 5 mg/L). Calculations were made using half the detection limit. The detection limit is shown on the right.

	SW-5 F	SW-5 U	SW-6 F	SW-6 U	SW-7 F	SW-7 U	D.L.
Ag	N.A.	<0.001	N.A.	**0.001**	N.A.	<0.001	0.001
Al	<0.12	**0.078**	<0.12	**0.029**	<0.12	**0.014**	0.12
As	<0.01	**0.011**	<0.01	**0.006**	<0.01	**0.002**	0.01
B	<0.02	**0.013**	<0.02	**0.009**	<0.02	**0.005**	0.02
Ba	**0.02**	**0.027**	**0.02**	**0.026**	**0.02**	**0.024**	0.001
Be	N.A.	<0.001	N.A.	<0.001	N.A.	<0.001	0.001
Ca	**10.8**	**11.29**	**10.2**	**10.668**	**21.2**	**21.534**	0.08
Cd	<0.001	<0.001	<0.001	<0.001	<0.001	<0.001	0.001
Co	<0.005	0.001	<0.005	<0.001	<0.005	<0.001	0.005
Cr	<0.006	<0.001	<0.006	<0.001	<0.006	<0.001	0.006
Cu	<0.008	**0.007**	<0.008	**0.003**	<0.008	**0.001**	0.008
Fe	<0.003	**0.384**	<0.01	**0.107**	<0.003	**0.081**	0.003
K	**1.17**	**1.528**	**1.18**	**1.372**	**1.01**	**1.08**	0.46
Li	N.A.	**0.005**	N.A.	**0.004**	N.A.	**0.004**	0.001
Mg	**15.7**	**15.236**	**12.7**	**12.129**	**15.1**	**14.781**	0.007
Mn	**0.003**	**0.121**	<0.001	**0.009**	<0.001	**0.002**	0.001
Mo	<0.15	<0.001	<0.15	<0.001	<0.15	<0.001	0.15
Na	**3.27**	**3.184**	**3**	**2.864**	**3.34**	**3.138**	0.08
Ni	<0.003	**0.003**	<0.003	**0.002**	<0.003	**0.001**	0.003
P	<0.08	**0.025**	<0.08	**0.02**	<0.08	**0.014**	0.08
Pb	<0.03	**0.006**	<0.03	**0.002**	<0.03	**0.001**	0.03
S	**7.81**	N.A.	**6.54**	N.A.	**6.23**	N.A.	0.07
Sb	N.A.	**0.002**	N.A.	**0.002**	N.A.	<0.001	0.001
Se	<0.04	<0.001	<0.04	<0.001	<0.04	<0.001	0.001
Si	**8.59**	**4.805**	**8.47**	**4.678**	**7.88**	**4.291**	0.15
Sn	N.A.	<0.001	N.A.	<0.001	N.A.	<0.001	0.001
Sr	**0.08**	**0.088**	**0.07**	**0.079**	**0.11**	**0.118**	0.03
Tl	N.A.	<0.001	N.A.	<0.001	N.A.	<0.001	0.001
V	N.A.	<0.001	N.A.	<0.001	N.A.	<0.001	0.001
Zn	**0.02**	**0.024**	**0.01**	**0.025**	**0.01**	**0.016**	0.005

Table D.5. Chemical results from USUAL and UVDL from October. Bold values are above the detection limit of the lab. Red and bold values indicate exceedences of EPA drinking water standards (As at 0.01 mg/L, Cu at 1.3 mg/L, Fe at 0.3 mg/L, Mn at 0.05 mg/L, Pb at 0.015 mg/L, and Zn at 5 mg/L). Calculations were made using half the detection limit. The detection limit is shown on the right.

	SW-8 F	SW-8 U	D.L.
Ag	N.A.	**0.002**	0.001
Al	<0.12	**0.024**	0.12
As	<0.01	**0.003**	0.01
B	<0.02	**0.03**	0.02
Ba	**0.02**	**0.021**	0.001
Be	N.A.	<0.001	0.001
Ca	**18.5**	**19.106**	0.08
Cd	<0.001	<0.001	0.001
Co	<0.005	<0.001	0.005
Cr	<0.006	<0.001	0.006
Cu	<0.008	**0.003**	0.008
Fe	<0.003	**0.117**	0.003
K	**3.91**	**2.782**	0.46
Li	N.A.	**0.009**	0.001
Mg	**12.9**	**12.596**	0.007
Mn	0.002	**0.008**	0.001
Mo	<0.15	<0.001	0.15
Na	**7.21**	**6.564**	0.08
Ni	<0.003	**0.001**	0.003
P	<0.08	**0.036**	0.08
Pb	<0.03	**0.003**	0.03
S	**7.71**	N.A.	0.07
Sb	N.A.	<0.001	0.001
Se	<0.04	<0.001	0.001
Si	**8.5**	**4.688**	0.15
Sn	N.A.	<0.001	0.001
Sr	**0.13**	**0.131**	0.03
Tl	N.A.	<0.001	0.001
V	N.A.	<0.001	0.001
Zn	**0.02**	**0.025**	0.005

Table D.5. Chemical results from USUAL and UVDL from October. Bold values are above the detection limit of the lab. Red and bold values indicate exceedences of EPA drinking water standards (As at 0.01 mg/L, Cu at 1.3 mg/L, Fe at 0.3 mg/L, Mn at 0.05 mg/L, Pb at 0.015 mg/L, and Zn at 5 mg/L). Calculations were made using half the detection limit. The detection limit is shown on the right.

Appendix E
XRD Results

Table E.1: Height and theta values for peak results for tailings sample.

Pos. [°2Th.]	Height [cts]	FWHM [°2Th.]	d-spacing [Å]	Rel. Int. [%]
2.0220	**1997.84**	**0.0590**	**43.69315**	**62.02**
2.2037	849.31	0.0787	40.09023	26.36
8.8694	**948.71**	**0.0984**	**9.97039**	**29.45**
12.4107	148.90	0.3149	7.13221	4.62
17.8044	295.49	0.1181	4.98187	9.17
19.9214	185.36	0.2362	4.45699	5.75
20.8603	673.77	0.1181	4.25846	20.91
22.9749	79.37	0.1968	3.87108	2.46
23.8826	81.09	0.1574	3.72596	2.52
24.8447	111.87	0.2362	3.58382	3.47
25.5693	135.53	0.1574	3.48388	4.21
26.6456	**3221.50**	**0.1181**	**3.34555**	**100.00**
26.8850	528.12	0.0787	3.31629	16.39
27.9287	163.82	0.1968	3.19470	5.09
29.9756	149.88	0.2362	2.98105	4.65
31.3258	100.16	0.1968	2.85557	3.11
32.0418	419.56	0.1378	2.79337	13.02
33.2215	25.67	0.4723	2.69683	0.80
35.0925	235.44	0.1968	2.55721	7.31
36.5558	296.26	0.1378	2.45814	9.20
37.7354	51.87	0.4723	2.38397	1.61
38.4087	41.90	0.2362	2.34371	1.30
39.4665	180.79	0.0984	2.28330	5.61
40.2982	117.68	0.1574	2.23807	3.65
42.4781	196.81	0.2362	2.12813	6.11
45.5404	157.73	0.1574	1.99190	4.90
50.1321	319.65	0.0984	1.81969	9.92
52.9802	67.82	0.7085	1.72839	2.11
54.8717	98.23	0.1574	1.67320	3.05
59.9537	283.42	0.1200	1.54168	8.80
60.1136	163.75	0.0960	1.54178	5.08
61.9595	89.40	0.2880	1.49650	2.78
64.1106	40.65	0.3840	1.45138	1.26
65.6293	19.33	0.7680	1.42142	0.60
67.7344	158.43	0.0960	1.38227	4.92
68.1320	168.95	0.0960	1.37517	5.24
68.3150	210.25	0.1200	1.37193	6.53
69.6612	38.23	0.5760	1.34868	1.19
73.4566	39.07	0.5760	1.28808	1.21

Table E.2: Height and peak results for sediment sample 2 (SS-2), re-run of tailings sample.

Pos. [°2Th.]	Height [cts]	FWHM [°2Th.]	d-spacing [Å]	Rel. Int. [%]
2.0300	**5310.76**	**0.0394**	**43.52094**	**77.07**
2.2051	2297.34	0.0787	40.06600	33.34
6.2360	129.09	0.1181	14.17361	1.87
8.8754	**2372.43**	**0.0984**	**9.96367**	**34.43**
12.3585	568.94	0.0984	7.16224	8.26
12.5124	543.54	0.0787	7.07450	7.89
17.8045	1122.18	0.1181	4.98185	16.29
18.8273	129.56	0.1181	4.71345	1.88
19.9195	320.72	0.2558	4.45741	4.65
20.8503	1492.08	0.1181	4.26047	21.65
22.9680	154.43	0.1574	3.87223	2.24
23.8874	158.32	0.1574	3.72523	2.30
24.8788	533.12	0.2165	3.57898	7.74
25.1945	364.96	0.1181	3.53484	5.30
25.5510	266.78	0.1574	3.48632	3.87
26.6377	**6890.75**	**0.1181**	**3.34652**	**100.00**
26.8554	2345.70	0.0984	3.31988	34.04
27.9047	382.41	0.1968	3.19739	5.55
29.9511	342.21	0.1574	2.98342	4.97
31.3213	261.71	0.1968	2.85597	3.80
32.0471	1077.62	0.1574	2.79292	15.64
33.6134	118.04	0.1181	2.66628	1.71
35.0852	426.93	0.1771	2.55773	6.20
36.0647	218.04	0.1574	2.49048	3.16
36.5401	597.37	0.1378	2.45916	8.67
37.7778	113.14	0.3149	2.38139	1.64
38.4095	69.59	0.2362	2.34366	1.01
39.4595	405.44	0.0984	2.28369	5.88
40.2785	220.77	0.0984	2.23912	3.20
42.4459	484.28	0.0984	2.12967	7.03
45.5427	666.10	0.1574	1.99180	9.67
50.1268	716.06	0.1200	1.81837	10.39
50.2803	341.20	0.0720	1.81768	4.95
53.1234	183.05	0.2880	1.72264	2.66
54.8624	232.76	0.0960	1.67208	3.38
55.9712	119.62	0.3840	1.64155	1.74
59.9432	487.51	0.1200	1.54192	7.07
60.1064	289.72	0.0960	1.54195	4.20
60.9527	66.84	0.4800	1.51878	0.97
61.9552	139.48	0.3840	1.49659	2.02
64.0360	122.06	0.1440	1.45289	1.77
65.6186	47.95	0.7680	1.42162	0.70
67.7334	279.91	0.0960	1.38229	4.06
68.1386	404.74	0.0960	1.37505	5.87
68.3119	387.48	0.1200	1.37199	5.62
69.7111	102.36	0.4800	1.34783	1.49
70.4596	65.72	0.3840	1.33534	0.95
73.5170	66.46	0.2880	1.28717	0.96

Appendix F
PHREEQC Results

----------Solution composition----------

pH 8.29
pe 4
redox O(0)/O(-2)
temp 11.6
units mg/L

Alkalinity	80
Al	0.008
As	0.001
B	0.006
Ca	10.981
Cd	0.0005
Cu	0.001
Fe	0.045
K	0.846
Mg	5.389
Mn	0.002
Na	3.725
P	0.021
Pb	0.0005
S	1.06
Si	4.727
Sr	0.107
Zn	0.011
O(0)	10.9

Elements	Molality	Moles
Al	2.97E-07	2.97E-07
Alkalinity	1.31E-03	1.31E-03
As	1.34E-08	1.34E-08
B	5.55E-07	5.55E-07
Ca	2.74E-04	2.74E-04
Cd	4.45E-09	4.45E-09
Cu	1.57E-08	1.57E-08
Fe	8.06E-07	8.06E-07
K	2.16E-05	2.16E-05
Mg	2.22E-04	2.22E-04
Mn	3.64E-08	3.64E-08
Na	1.62E-04	1.62E-04
O(0)	6.81E-04	6.81E-04
P	6.78E-07	6.78E-07
Pb	2.41E-09	2.41E-09
S	1.10E-05	1.10E-05
Si	7.87E-05	7.87E-05
Sr	1.22E-06	1.22E-06
Zn	1.68E-07	1.68E-07

----------Description of solution----------

pH = 8.290
pe = 4.000
Activity of water = 1.000
Ionic strength = 1.750e-03
Mass of water (kg) = 1.000e+00
Total carbon (mol/kg) = 1.310e-03
Total CO2 (mol/kg) = 1.310e-03
Temperature (deg C) = 11.600
Electrical balance (eq) = -1.542e-04
Percent error, 100*(Cat-|An|)/(Cat+|An|) = -6.21
Iterations = 9
Total H = 1.110153e+02
Total O = 5.551181e+01

----------Redox couples----------

Redox couple	pe	Eh (volts)
O(-2)/O(0)	13.3334	0.7533

Phase	SI	log IAP	log KT	Chemical Composition
Hematite	**13.45**	**13.10**	**-0.35**	**Fe2O3**
Cupricferrite	**12.39**	**20.11**	**7.72**	**CuFe2O4**
Pyrolusite	**8.66**	**52.29**	**43.62**	**MnO2**
Nsutite	**8.54**	**26.05**	**17.50**	**MnO2**
Bixbyite	**8.47**	**8.85**	**0.38**	**Mn2O3**
Birnessite	**7.96**	**26.05**	**18.09**	**MnO2**
Magnesioferrite	**6.78**	**25.94**	**19.16**	**Fe2MgO4**
Maghemite	**6.71**	**13.10**	**6.39**	**Fe2O3**
Magnetite	**6.29**	**11.41**	**5.12**	**Fe3O4**
Hausmannite	5.86	70.36	64.50	Mn3O4
Goethite	5.56	6.55	0.99	FeOOH
Manganite	5.32	30.66	25.34	MnOOH
Lepidocrocite	5.18	6.55	1.37	FeOOH
Cuprousferrite	3.36	-5.43	-8.79	CuFeO2
Ferrihydrite	2.75	6.55	3.80	Fe(OH)3
Hydroxylapatite	2.71	-41.62	-44.33	Ca5(PO4)3OH
Kaolinite	1.59	10.24	8.66	Al2Si2O5(OH)4
Diaspore	1.51	9.23	7.72	AlOOH
Gibbsite	0.16	9.23	9.08	Al(OH)3
Quartz	0.07	-4.11	-4.18	SiO2

----------Solution composition----------

pH	8.86
pe	4
redox	O(0)/O(-2)
temp	10.6
units	mg/L
Alkalinity	180
O(0)	11.3

Al	0.006
As	0.0005
B	0.005
Ca	24.571
Cd	0.0005
Cu	0.001
Fe	1.323
K	3.011
Mg	26.782
Mn	0.053
Na	6.788
P	0.024
Pb	0.0005
S	5.34
Si	8.116
Sr	0.379
Zn	0.017

Elements	Molality	Moles
Al	2.22E-07	2.22E-07
Alkalinity	2.95E-03	2.95E-03
As	6.68E-09	6.68E-09
B	4.63E-07	4.63E-07
Ca	6.13E-04	6.13E-04
Cd	4.45E-09	4.45E-09
Cu	1.57E-08	1.57E-08
Fe	2.37E-05	2.37E-05
K	7.70E-05	7.70E-05
Mg	1.10E-03	1.10E-03
Mn	9.65E-07	9.65E-07
Na	2.95E-04	2.95E-04
O(0)	7.06E-04	7.06E-04
P	7.75E-07	7.75E-07
Pb	2.41E-09	2.41E-09
S	5.56E-05	5.56E-05
Si	1.35E-04	1.35E-04
Sr	4.33E-06	4.33E-06
Zn	2.60E-07	2.60E-07

----------Description of solution----------

pH = 8.860
pe = 4.000
Activity of water = 1.000
Ionic strength = 5.009e-03
Mass of water (kg) = 1.000e+00
Total carbon (mol/kg) = 2.765e-03
Total CO2 (mol/kg) = 2.765e-03
Temperature (deg C) = 10.600
Electrical balance (eq) = 7.749e-04
Percent error, 100*(Cat-|An|)/(Cat+|An|) = 11.89
Iterations = 11
Total H = 1.110169e+02
Total O = 5.551669e+01

Phase	SI	log IAP	log KT	Chemical Composition
Hematite	**16.15**	**15.88**	**-0.27**	**Fe2O3**
Cupricferrite	**15.26**	**23.11**	**7.86**	**CuFe2O4**
Bixbyite	**12.94**	**13.4**	**0.46**	**Mn2O3**
Hausmannite	**12.55**	**77.32**	**64.77**	**Mn3O4**
Magnesioferrite	**11.15**	**30.49**	**19.34**	**Fe2MgO4**
Pyrolusite	**10.92**	**54.71**	**43.8**	**MnO2**
Nsutite	**10.9**	**28.4**	**17.5**	**MnO2**
Birnessite	**10.31**	**28.4**	**18.09**	**MnO2**
Magnetite	**10.27**	**15.53**	**5.26**	**Fe3O4**
Maghemite	**9.5**	**15.88**	**6.39**	**Fe2O3**
Manganite	7.67	33.01	25.34	MnOOH
Goethite	6.91	7.94	1.03	FeOOH
Lepidocrocite	6.57	7.94	1.37	FeOOH
Hydroxylapatite	6.05	-38.28	-44.33	Ca5(PO4)3OH
Cuprousferrite	4.87	-3.9	-8.78	CuFeO2
Ferrihydrite	4.1	7.94	3.84	Fe(OH)3
Chrysotile	2.09	36.03	33.94	Mg3Si2O5(OH)4
Dolomite(ordered)	1.82	-14.92	-16.74	CaMg(CO3)2
Dolomite(disordered)	1.21	-14.92	-16.13	.13 CaMg(CO3)2
Diaspore	0.88	8.67	7.79	AlOOH
Calcite	0.82	-7.59	-8.41	CaCO3
Kaolinite	0.79	9.54	8.75	Al2Si2O5(OH)4
Sepiolite	0.75	17.52	16.77	Mg2Si3O7.5OH:3H2O
Aragonite	0.6	-7.59	-8.19	CaCO3
Magnesite	0.31	-7.33	-7.64	MgCO3
Quartz	0.3	-3.9	-4.2	SiO2
MnHPO4	0.03	-25.37	-25.4	MnHPO4

----------Solution composition----------

pH 7.15
pe 4
redox O(0)/O(-2)
temp 8.2
units mg/L

Alkalinity	100
Al	0.004
As	0.009
B	0.004
Ca	8.22
Cd	0.0005
Cu	0.003
Fe	0.169
K	0.694
Mg	31.423
Mn	0.314
Na	0.98
P	0.018
Pb	0.0005
S	19.4
Si	1.918
Sr	0.017
Zn	0.025
O(0)	7.9

Elements	Molality	Moles
Al	1.48E-07	1.48E-07
Alkalinity	1.64E-03	1.64E-03
As	1.20E-07	1.20E-07
B	3.70E-07	3.70E-07
Ca	2.05E-04	2.05E-04
Cd	4.45E-09	4.45E-09
Cu	4.72E-08	4.72E-08
Fe	3.03E-06	3.03E-06
K	1.78E-05	1.78E-05
Mg	1.29E-03	1.29E-03
Mn	5.72E-06	5.72E-06
Na	4.26E-05	4.26E-05
O(0)	4.94E-04	4.94E-04
P	5.81E-07	5.81E-07
Pb	2.41E-09	2.41E-09
S	2.02E-04	2.02E-04
Si	3.19E-05	3.19E-05
Sr	1.94E-07	1.94E-07
Zn	3.82E-07	3.82E-07

----------Description of solution----------

pH = 7.150
pe = 4.000
Activity of water = 1.000
Ionic strength = 4.130e-03
Mass of water (kg) = 1.000e+00
Total carbon (mol/kg) = 1.937e-03
Total CO2 (mol/kg) = 1.937e-03
Temperature (deg C) = 8.200
Electrical balance (eq) = 1.029e-03
Percent error, 100*(Cat-|An|)/(Cat+|An|) = 20.67
Iterations = 11
Total H = 1.110160e+02
Total O = 5.551408e+01

Redox couple	pe	Eh (volts)
O(-2)/O(0)	14.7048	0.8209

Phase	SI	log IAP	log KT	Chemical Composition
Hematite	**12.45**	**12.38**	**-0.07**	**Fe2O3**
Cupricferrite	**10.41**	**18.59**	**8.19**	**CuFe2O4**
Nsutite	**8.64**	**26.15**	**17.5**	**MnO2**
Pyrolusite	**8.4**	**52.62**	**44.23**	**MnO2**
Birnessite	**8.05**	**26.15**	**18.09**	**MnO2**
Bixbyite	**7.92**	**8.58**	**0.66**	**Mn2O3**
Maghemite	**5.99**	**12.38**	**6.39**	**Fe2O3**
Manganite	**5.43**	**30.77**	**25.34**	**MnOOH**
Goethite	5.07	6.19	1.12	FeOOH
Hausmannite	5.02	70.45	65.43	Mn3O4
Lepidocrocite	4.82	6.19	1.37	FeOOH
Magnetite	4.61	10.2	5.58	Fe3O4
Magnesioferrite	3.89	23.66	19.78	Fe2MgO4
Ferrihydrite	2.23	6.19	3.96	Fe(OH)3
Cuprousferrite	1.92	-6.84	-8.75	CuFeO2
Diaspore	1.79	9.74	7.95	AlOOH
Kaolinite	1.5	10.49	8.98	Al2Si2O5(OH)4
MnHPO4	0.75	-24.65	-25.4	MnHPO4
Gibbsite	0.45	9.74	9.29	Al(OH)3

9.000e-01 Solution 1
1.000e-01 Solution 2

----------Solution composition----------

Elements	Molality	Moles
Al	2.89E-07	2.89E-07
As	1.27E-08	1.27E-08
B	5.46E-07	5.46E-07
C	1.46E-03	1.46E-03
Ca	3.08E-04	3.08E-04
Cd	4.45E-09	4.45E-09
Cu	1.57E-08	1.57E-08
Fe	3.10E-06	3.10E-06
K	2.72E-05	2.72E-05
Mg	3.10E-04	3.10E-04
Mn	1.29E-07	1.29E-07
Na	1.75E-04	1.75E-04
P	6.88E-07	6.88E-07
Pb	2.41E-09	2.41E-09
S	1.55E-05	1.55E-05
Si	8.43E-05	8.43E-05
Sr	1.53E-06	1.53E-06
Zn	1.77E-07	1.77E-07

----------Description of solution----------

pH = 8.470 Charge balance
pe = 13.162 Adjusted to redox equilibrium
Activity of water = 1.000
Ionic strength = 2.087e-03
Mass of water (kg) = 1.000e+00
Total alkalinity (eq/kg) = 1.475e-03
Total CO2 (mol/kg) = 1.455e-03
Temperature (deg C) = 11.500
Electrical balance (eq) = -6.126e-05
Percent error, 100*(Cat-|An|)/(Cat+|An|) = -2.11
Iterations = 16
Total H = 1.110155e+02
Total O = 5.551230e+01

Phase	SI	log IAP	log KT	Chemical Composition
Hematite	**14.69**	**14.34**	**-0.35**	**Fe2O3**
Cupricferrite	**13.75**	**21.49**	**7.73**	**CuFe2O4**
Bixbyite	**10.22**	**10.61**	**0.39**	**Mn2O3**
Pyrolusite	**9.54**	**53.18**	**43.64**	**MnO2**
Nsutite	**9.43**	**26.94**	**17.5**	**MnO2**
Birnessite	**8.84**	**26.94**	**18.09**	**MnO2**
Magnesioferrite	**8.5**	**27.68**	**19.18**	**Fe2MgO4**
Hausmannite	**8.49**	**73.02**	**64.53**	**Mn3O4**
Magnetite	**8.14**	**13.27**	**5.14**	**Fe3O4**
Maghemite	**7.96**	**14.34**	**6.39**	**Fe2O3**
Manganite	6.21	31.55	25.34	MnOOH
Goethite	6.18	7.17	0.99	FeOOH
Lepidocrocite	5.8	7.17	1.37	FeOOH
Cuprousferrite	4.1	-4.68	-8.79	CuFeO2
Hydroxylapatite	3.6	-40.73	-44.33	Ca5(PO4)3OH
Ferrihydrite	3.37	7.17	3.8	Fe(OH)3
Diaspore	1.34	9.07	7.73	AlOOH
Kaolinite	1.3	9.96	8.66	Al2Si2O5(OH)4
Quartz	0.1	-4.09	-4.19	SiO2

7.900e-01 Solution 2
2.100e-01 Solution 3

----------Solution composition----------

Elements	Molality	Moles
Al	2.07E-07	2.07E-07
As	3.05E-08	3.05E-08
B	4.43E-07	4.43E-07
C	2.59E-03	2.59E-03
Ca	5.28E-04	5.28E-04
Cd	4.45E-09	4.45E-09
Cu	2.24E-08	2.24E-08
Fe	1.94E-05	1.94E-05
K	6.46E-05	6.46E-05
Mg	1.14E-03	1.14E-03
Mn	1.96E-06	1.96E-06
Na	2.42E-04	2.42E-04
P	7.34E-07	7.34E-07
Pb	2.41E-09	2.41E-09
S	8.63E-05	8.63E-05
Si	1.13E-04	1.13E-04
Sr	3.46E-06	3.46E-06
Zn	2.86E-07	2.86E-07

----------Description of solution----------

pH = 8.586 Charge balance
pe = 13.151 Adjusted to redox equilibrium
Activity of water = 1.000
Ionic strength = 4.856e-03
Mass of water (kg) = 1.000e+00
Total alkalinity (eq/kg) = 2.676e-03
Total CO2 (mol/kg) = 2.591e-03
Temperature (deg C) = 10.096
Electrical balance (eq) = 8.283e-04
Percent error, 100*(Cat-|An|)/(Cat+|An|) = 13.20
Iterations = 18
Total H = 1.110167e+02
Total O = 5.551615e+01

Phase	SI	log IAP	log KT	Chemical Composition
Hematite	**16.17**	**15.94**	**-0.23**	**Fe2O3**
Cupricferrite	**15.19**	**23.12**	**7.93**	**CuFe2O4**
Bixbyite	**12.83**	**13.33**	**0.5**	**Mn2O3**
Hausmannite	**12.38**	**77.29**	**64.91**	**Mn3O4**
Nsutite	**10.9**	**28.4**	**17.5**	**MnO2**
Pyrolusite	**10.86**	**54.75**	**43.89**	**MnO2**
Magnesioferrite	**10.59**	**30.02**	**19.43**	**Fe2MgO4**
Birnessite	**10.31**	**28.4**	**18.09**	**MnO2**
Magnetite	**10.27**	**15.59**	**5.33**	**Fe3O4**
Maghemite	**9.55**	**15.94**	**6.39**	**Fe2O3**
Manganite	**7.67**	**33.01**	**25.34**	**MnOOH**
Goethite	6.92	7.97	1.05	FeOOH
Lepidocrocite	6.6	7.97	1.37	FeOOH
Cuprousferrite	4.81	-3.96	-8.77	CuFeO2
Hydroxylapatite	4.67	-39.66	-44.33	Ca5(PO4)3OH
Ferrihydrite	4.1	7.97	3.87	Fe(OH)3
Dolomite(ordered)	1.18	-15.54	-16.73	CaMg(CO3)2
Kaolinite	1.18	9.98	8.8	Al2Si2O5(OH)4
Diaspore	1.13	8.95	7.82	AlOOH
Dolomite(disordered)	0.57	-15.54	-16.11	CaMg(CO3)2
MnHPO4	0.55	-24.85	-25.4	MnHPO4
Calcite	0.46	-7.94	-8.41	CaCO3
Chrysotile	0.33	34.34	34.01	Mg3Si2O5(OH)4
Aragonite	0.25	-7.94	-8.19	CaCO3
Quartz	0.24	-3.96	-4.21	SiO2
Rhodochrosite	0.15	-10.42	-10.56	MnCO3
Magnesite	0.04	-7.6	-7.64	MgCO3

Appendix G
PHREEQC Species Distribution

	Species	Molality	Activity	Log Molality	Log Activity	Log Gamma
	OH-	7.13E-07	6.81E-07	-6.147	-6.167	-0.02
	H+	5.37E-09	5.13E-09	-8.27	-8.29	-0.02
	H2O	5.55E+01	1.00E+00	1.744	0	0
Al		2.97E-07				
	Al(OH)4-	2.68E-07	2.56E-07	-6.572	-6.591	-0.02
	Al(OH)3	2.78E-08	2.78E-08	-7.556	-7.556	0
	As(5)	1.34E-08				
	HAsO4-2	1.28E-08	1.06E-08	-7.893	-7.976	-0.083
B		5.55E-07				
	H3BO3	5.07E-07	5.07E-07	-6.295	-6.295	0
	H2BO3-	4.70E-08	4.49E-08	-7.328	-7.348	-0.02
C(4)		1.31E-03				
	HCO3-	1.27E-03	1.22E-03	-2.895	-2.914	-0.019
	H2CO3	1.67E-05	1.67E-05	-4.777	-4.777	0
	CO3-2	1.01E-05	8.44E-06	-4.995	-5.074	-0.079
	CaHCO3+	3.62E-06	3.46E-06	-5.441	-5.461	-0.019
	CaCO3	2.20E-06	2.20E-06	-5.657	-5.657	0
	MgHCO3+	2.20E-06	2.10E-06	-5.658	-5.678	-0.02
	MgCO3	1.02E-06	1.02E-06	-5.993	-5.993	0
	NaHCO3	1.38E-07	1.38E-07	-6.862	-6.862	0
	ZnCO3	4.41E-08	4.41E-08	-7.355	-7.355	0
	NaCO3-	3.74E-08	3.58E-08	-7.427	-7.447	-0.019
	CuCO3	1.35E-08	1.35E-08	-7.871	-7.871	0
	SrHCO3+	1.29E-08	1.23E-08	-7.89	-7.909	-0.019
	SrCO3	3.74E-09	3.74E-09	-8.427	-8.427	0
	ZnHCO3+	2.78E-09	2.65E-09	-8.555	-8.576	-0.021
	PbCO3	1.83E-09	1.83E-09	-8.738	-8.738	0
	MnHCO3+	6.78E-10	6.48E-10	-9.169	-9.188	-0.02
Ca		2.74E-04				
	Ca+2	2.68E-04	2.23E-04	-3.572	-3.651	-0.079
	CaHCO3+	3.62E-06	3.46E-06	-5.441	-5.461	-0.019
	CaCO3	2.20E-06	2.20E-06	-5.657	-5.657	0
	CaSO4	3.87E-07	3.87E-07	-6.413	-6.413	0
	CaHPO4	3.69E-08	3.69E-08	-7.434	-7.434	0
	CaPO4-	1.48E-08	1.41E-08	-7.831	-7.85	-0.019
	CaOH+	2.71E-09	2.59E-09	-8.568	-8.587	-0.019
Cd		4.45E-09				
	Cd+2	3.80E-09	3.17E-09	-8.42	-8.499	-0.079
Cu(2)		1.57E-08				
	CuCO3	1.35E-08	1.35E-08	-7.871	-7.871	0
Fe(3)		8.06E-07				
	Fe(OH)2+	4.84E-07	4.62E-07	-6.316	-6.335	-0.019
	Fe(OH)4-	1.86E-07	1.78E-07	-6.73	-6.749	-0.019
	Fe(OH)3	1.36E-07	1.36E-07	-6.867	-6.867	0
K		2.16E-05				
	K+	2.16E-05	2.07E-05	-4.665	-4.685	-0.02
	KSO4-	1.23E-09	1.17E-09	-8.912	-8.931	-0.019

	Species	Molality	Activity	Log Molality	Log Activity	Log Gamma
Mg		2.22E-04				
	Mg+2	2.18E-04	1.82E-04	-3.661	-3.74	-0.079
	MgHCO3+	2.20E-06	2.10E-06	-5.658	-5.678	-0.02
	MgCO3	1.02E-06	1.02E-06	-5.993	-5.993	0
	MgSO4	2.57E-07	2.57E-07	-6.591	-6.591	0
	MgHPO4	4.15E-08	4.15E-08	-7.383	-7.383	0
	MgOH+	4.10E-08	3.92E-08	-7.387	-7.406	-0.019
Mn(2)		3.56E-08				
	Mn+2	3.49E-08	2.88E-08	-7.458	-7.541	-0.083
Na		1.62E-04				
	Na+	1.62E-04	1.55E-04	-3.791	-3.811	-0.02
	NaHCO3	1.38E-07	1.38E-07	-6.862	-6.862	0
	NaCO3-	3.74E-08	3.58E-08	-7.427	-7.447	-0.019
	NaSO4-	7.38E-09	7.05E-09	-8.132	-8.152	-0.019
O(0)		6.81E-04				
	O2	3.41E-04	3.41E-04	-3.468	-3.467	0
P		6.78E-07				
	HPO4-2	5.43E-07	4.54E-07	-6.265	-6.343	-0.078
	MgHPO4	4.15E-08	4.15E-08	-7.383	-7.383	0
	H2PO4-	4.06E-08	3.89E-08	-7.391	-7.411	-0.019
	CaHPO4	3.69E-08	3.69E-08	-7.434	-7.434	0
	CaPO4-	1.48E-08	1.41E-08	-7.831	-7.85	-0.019
Pb		2.41E-09				
	PbCO3	1.83E-09	1.83E-09	-8.738	-8.738	0
S(6)		1.10E-05				
	SO4-2	1.04E-05	8.65E-06	-4.984	-5.063	-0.079
	CaSO4	3.87E-07	3.87E-07	-6.413	-6.413	0
	MgSO4	2.57E-07	2.57E-07	-6.591	-6.591	0
	NaSO4-	7.38E-09	7.05E-09	-8.132	-8.152	-0.019
	SrSO4	1.49E-09	1.49E-09	-8.827	-8.827	0
	KSO4-	1.23E-09	1.17E-09	-8.912	-8.931	-0.019
Si		7.87E-05				
	H4SiO4	7.71E-05	7.72E-05	-4.113	-4.113	0
	H3SiO4-	1.56E-06	1.49E-06	-5.808	-5.828	-0.02
Sr		1.22E-06				
	Sr+2	1.20E-06	1.00E-06	-5.92	-5.999	-0.079
	SrHCO3+	1.29E-08	1.23E-08	-7.89	-7.909	-0.019
	SrCO3	3.74E-09	3.74E-09	-8.427	-8.427	0
	SrSO4	1.49E-09	1.49E-09	-8.827	-8.827	0
Zn		1.68E-07				
	Zn+2	1.09E-07	9.09E-08	-6.962	-7.041	-0.079
	ZnCO3	4.41E-08	4.41E-08	-7.355	-7.355	0
	ZnOH+	6.49E-09	6.19E-09	-8.188	-8.209	-0.021
	Zn(OH)2	5.55E-09	5.55E-09	-8.255	-8.255	0
	ZnHCO3+	2.78E-09	2.65E-09	-8.555	-8.576	-0.021

	Species	Molality	Activity	Log Molality	Log Activity	Log Gamma
	OH-	2.51E-06	2.33E-06	-5.601	-5.633	-0.033
	H+	1.49E-09	1.38E-09	-8.828	-8.86	-0.032
	H2O	5.55E+01	1.00E+00	1.744	0	0
Al	2.22E-07					
	Al(OH)4-	2.15E-07	2.00E-07	-6.668	-6.7	-0.032
	Al(OH)3	7.54E-09	7.54E-09	-8.123	-8.123	0
As(3)	0.00E+00					
As(5)	6.68E-09					
	HAsO4-2	6.59E-09	4.76E-09	-8.181	-8.322	-0.141
B	4.63E-07					
	H3BO3	3.39E-07	3.39E-07	-6.47	-6.47	0.001
	H2BO3-	1.18E-07	1.09E-07	-6.928	-6.961	-0.033
	MgH2BO3+	3.19E-09	2.95E-09	-8.497	-8.53	-0.033
	CaH2BO3+	2.64E-09	2.45E-09	-8.578	-8.612	-0.033
C(4)	2.77E-03					
	HCO3-	2.58E-03	2.40E-03	-2.588	-2.619	-0.031
	CO3-2	8.14E-05	6.05E-05	-4.09	-4.218	-0.129
	MgCO3	3.07E-05	3.07E-05	-4.514	-4.514	0
	CaCO3	2.92E-05	2.92E-05	-4.535	-4.535	0
	MgHCO3+	1.90E-05	1.76E-05	-4.721	-4.754	-0.032
	CaHCO3+	1.35E-05	1.25E-05	-4.871	-4.902	-0.031
	H2CO3	8.99E-06	8.99E-06	-5.046	-5.046	0
	NaCO3-	5.02E-07	4.67E-07	-6.299	-6.331	-0.031
	NaHCO3	4.89E-07	4.89E-07	-6.311	-6.311	0
	ZnCO3	1.50E-07	1.50E-07	-6.823	-6.823	0
	SrCO3	8.00E-08	8.00E-08	-7.097	-7.097	0
	SrHCO3+	7.74E-08	7.21E-08	-7.111	-7.142	-0.031
	MnHCO3+	1.82E-08	1.69E-08	-7.74	-7.772	-0.032
	CuCO3	1.16E-08	1.16E-08	-7.936	-7.936	0
	ZnHCO3+	2.64E-09	2.43E-09	-8.579	-8.614	-0.035
	Cu(CO3)2-2	2.61E-09	1.89E-09	-8.583	-8.724	-0.141
	CdCO3	2.16E-09	2.16E-09	-8.666	-8.666	0
	PbCO3	1.74E-09	1.74E-09	-8.76	-8.76	0
	Pb(CO3)2-2	4.19E-10	3.03E-10	-9.377	-9.518	-0.141
	Cd(CO3)2-2	1.34E-10	9.67E-11	-9.873	-10.014	-0.141
Ca	6.13E-04					
	Ca+2	5.68E-04	4.22E-04	-3.246	-3.375	-0.129
	CaCO3	2.92E-05	2.92E-05	-4.535	-4.535	0
	CaHCO3+	1.35E-05	1.25E-05	-4.871	-4.902	-0.031
	CaSO4	2.99E-06	2.99E-06	-5.525	-5.525	0
	CaPO4-	8.18E-08	7.61E-08	-7.087	-7.118	-0.031
	CaHPO4	5.48E-08	5.48E-08	-7.261	-7.261	0
	CaOH+	1.78E-08	1.65E-08	-7.751	-7.782	-0.031
	CaH2BO3+	2.64E-09	2.45E-09	-8.578	-8.612	-0.033
Cd	4.45E-09					
	CdCO3	2.16E-09	2.16E-09	-8.666	-8.666	0
	Cd+2	2.10E-09	1.57E-09	-8.677	-8.806	-0.129
Cu(2)	1.57E-08					
	CuCO3	1.16E-08	1.16E-08	-7.936	-7.936	0
	Cu(CO3)2-2	2.61E-09	1.89E-09	-8.583	-8.724	-0.141
	Cu(OH)2	1.09E-09	1.09E-09	-8.962	-8.962	0
	CuOH+	3.88E-10	3.60E-10	-9.411	-9.443	-0.032
Fe(2)	1.28E-18					
	Fe+2	1.17E-18	8.46E-19	-17.932	-18.073	-0.141
Fe(3)	2.37E-05					
	Fe(OH)4-	1.75E-05	1.63E-05	-4.756	-4.788	-0.031
	Fe(OH)2+	3.30E-06	3.07E-06	-5.482	-5.513	-0.031
	Fe(OH)3	2.87E-06	2.87E-06	-5.542	-5.542	0
K	7.70E-05					
	K+	7.70E-05	7.15E-05	-4.113	-4.146	-0.032
	KSO4-	1.79E-08	1.66E-08	-7.748	-7.779	-0.031
	KHPO4-	1.56E-10	1.45E-10	-9.808	-9.839	-0.031

	Species	Molality	Activity	Log Molality	Log Activity	Log Gamma
Mg	1.10E-03					
	Mg+2	1.05E-03	7.79E-04	-2.98	-3.109	-0.129
	MgCO3	3.07E-05	3.07E-05	-4.514	-4.514	0
	MgHCO3+	1.90E-05	1.76E-05	-4.721	-4.754	-0.032
	MgSO4	4.50E-06	4.50E-06	-5.347	-5.347	0
	MgOH+	6.06E-07	5.64E-07	-6.218	-6.248	-0.031
	MgHPO4	1.40E-07	1.40E-07	-6.855	-6.855	0
	MgH2BO3+	3.19E-09	2.95E-09	-8.497	-8.53	-0.033
	MgPO4-	2.36E-09	2.20E-09	-8.627	-8.658	-0.031
	MgH2PO4+	2.58E-10	2.40E-10	-9.588	-9.619	-0.031
Mn(2)	5.53E-07					
	Mn+2	5.30E-07	3.83E-07	-6.276	-6.417	-0.141
	MnHCO3+	1.82E-08	1.69E-08	-7.74	-7.772	-0.032
	MnOH+	2.41E-09	2.24E-09	-8.618	-8.65	-0.032
	MnSO4	2.04E-09	2.04E-09	-8.691	-8.691	0
Mn(6)	1.68E-09					
	MnO4-2	1.68E-09	1.26E-09	-8.774	-8.9	-0.126
Mn(7)	4.11E-07					
	MnO4-	4.11E-07	3.81E-07	-6.387	-6.42	-0.033
Na	2.95E-04					
	Na+	2.94E-04	2.73E-04	-3.531	-3.563	-0.032
	NaCO3-	5.02E-07	4.67E-07	-6.299	-6.331	-0.031
	NaHCO3	4.89E-07	4.89E-07	-6.311	-6.311	0
	NaSO4-	5.52E-08	5.14E-08	-7.258	-7.289	-0.031
	NaHPO4-	9.22E-10	8.58E-10	-9.035	-9.067	-0.031
O(0)	7.06E-04					
	O2	3.53E-04	3.54E-04	-3.452	-3.451	0.001
P	7.75E-07					
	HPO4-2	4.86E-07	3.63E-07	-6.314	-6.44	-0.126
	MgHPO4	1.40E-07	1.40E-07	-6.855	-6.855	0
	CaPO4-	8.18E-08	7.61E-08	-7.087	-7.118	-0.031
	CaHPO4	5.48E-08	5.48E-08	-7.261	-7.261	0
	H2PO4-	9.04E-09	8.41E-09	-8.044	-8.075	-0.031
	MgPO4-	2.36E-09	2.20E-09	-8.627	-8.658	-0.031
	NaHPO4-	9.22E-10	8.58E-10	-9.035	-9.067	-0.031
	SrHPO4	2.59E-10	2.59E-10	-9.586	-9.586	0
	MgH2PO4+	2.58E-10	2.40E-10	-9.588	-9.619	-0.031
	PO4-3	1.59E-10	8.16E-11	-9.799	-10.088	-0.289
	KHPO4-	1.56E-10	1.45E-10	-9.808	-9.839	-0.031
Pb	2.41E-09					
	PbCO3	1.74E-09	1.74E-09	-8.76	-8.76	0
	Pb(CO3)2-2	4.19E-10	3.03E-10	-9.377	-9.518	-0.141
	PbOH+	1.90E-10	1.75E-10	-9.722	-9.757	-0.035
S(6)	5.56E-05					
	SO4-2	4.80E-05	3.57E-05	-4.319	-4.447	-0.129
	MgSO4	4.50E-06	4.50E-06	-5.347	-5.347	0
	CaSO4	2.99E-06	2.99E-06	-5.525	-5.525	0
	NaSO4-	5.52E-08	5.14E-08	-7.258	-7.289	-0.031
	SrSO4	1.87E-08	1.87E-08	-7.729	-7.729	0
	KSO4-	1.79E-08	1.66E-08	-7.748	-7.779	-0.031
	MnSO4	2.04E-09	2.04E-09	-8.691	-8.691	0
	ZnSO4	2.97E-10	2.97E-10	-9.527	-9.527	0
Si	1.35E-04					
	H4SiO4	1.26E-04	1.26E-04	-3.901	-3.9	0.001
	H3SiO4-	9.42E-06	8.75E-06	-5.026	-5.058	-0.032
	H2SiO4-2	2.31E-10	1.73E-10	-9.637	-9.763	-0.125
Sr	4.33E-06					
	Sr+2	4.15E-06	3.09E-06	-5.382	-5.511	-0.129
	SrCO3	8.00E-08	8.00E-08	-7.097	-7.097	0
	SrHCO3+	7.74E-08	7.21E-08	-7.111	-7.142	-0.031
	SrSO4	1.87E-08	1.87E-08	-7.729	-7.729	0
	SrHPO4	2.59E-10	2.59E-10	-9.586	-9.586	0
Zn	2.60E-07					
	ZnCO3	1.50E-07	1.50E-07	-6.823	-6.823	0
	Zn+2	5.81E-08	4.32E-08	-7.236	-7.365	-0.129
	Zn(OH)2	3.64E-08	3.64E-08	-7.439	-7.439	0
	ZnOH+	1.09E-08	1.01E-08	-7.963	-7.998	-0.035
	ZnHCO3+	2.64E-09	2.43E-09	-8.579	-8.614	-0.035
	Zn(OH)3-	1.44E-09	1.33E-09	-8.841	-8.876	-0.035
	ZnSO4	2.97E-10	2.97E-10	-9.527	-9.527	0

				Log	Log	Log
	Species	Molality	Activity	Molality	Activity	Gamma
	H+	7.58E-08	7.08E-08	-7.121	-7.15	-0.029
	OH-	3.97E-08	3.71E-08	-7.401	-7.431	-0.03
	H2O	5.55E+01	1.00E+00	1.744	0	0
Al		1.48E-07				
	Al(OH)3	8.86E-08	8.86E-08	-7.052	-7.052	0
	Al(OH)2+	3.34E-08	3.12E-08	-7.477	-7.505	-0.029
	Al(OH)4-	2.62E-08	2.45E-08	-7.582	-7.612	-0.029
	AlOH+2	1.14E-10	8.74E-11	-9.944	-10.058	-0.115
As(5)		1.20E-07				
	HAsO4-2	7.72E-08	5.75E-08	-7.113	-7.24	-0.128
	H2AsO4-	4.30E-08	3.99E-08	-7.367	-7.399	-0.032
B		3.70E-07				
	H3BO3	3.68E-07	3.68E-07	-6.435	-6.434	0
	H2BO3-	2.37E-09	2.21E-09	-8.626	-8.656	-0.03
C(4)		1.94E-03				
	HCO3-	1.62E-03	1.51E-03	-2.791	-2.82	-0.029
	H2CO3	3.01E-04	3.01E-04	-3.522	-3.522	0
	MgHCO3+	1.45E-05	1.35E-05	-4.84	-4.869	-0.029
	CaHCO3+	2.81E-06	2.64E-06	-5.551	-5.579	-0.028
	CO3-2	9.25E-07	7.06E-07	-6.034	-6.151	-0.117
	MgCO3	4.22E-07	4.22E-07	-6.375	-6.375	0
	MnHCO3+	1.21E-07	1.13E-07	-6.919	-6.948	-0.029
	CaCO3	1.15E-07	1.15E-07	-6.939	-6.939	0
	NaHCO3	4.72E-08	4.72E-08	-7.327	-7.327	0
	CuCO3	3.39E-08	3.39E-08	-7.47	-7.47	0
	ZnCO3	1.10E-08	1.10E-08	-7.96	-7.96	0
	ZnHCO3+	9.78E-09	9.09E-09	-8.009	-8.041	-0.032
	SrHCO3+	2.07E-09	1.94E-09	-8.685	-8.713	-0.028
	PbCO3	1.08E-09	1.08E-09	-8.967	-8.967	0
	NaCO3-	9.11E-10	8.53E-10	-9.04	-9.069	-0.029
	CuHCO3+	5.90E-10	5.48E-10	-9.229	-9.261	-0.032
	PbHCO3+	4.34E-10	4.03E-10	-9.363	-9.395	-0.032
Ca		2.05E-04				
	Ca+2	1.98E-04	1.51E-04	-3.703	-3.82	-0.117
	CaSO4	3.95E-06	3.95E-06	-5.403	-5.403	0
	CaHCO3+	2.81E-06	2.64E-06	-5.551	-5.579	-0.028
	CaCO3	1.15E-07	1.15E-07	-6.939	-6.939	0
	CaHPO4	9.59E-09	9.59E-09	-8.018	-8.018	0
	CaH2PO4+	6.02E-10	5.64E-10	-9.22	-9.249	-0.029
	CaPO4-	2.62E-10	2.45E-10	-9.582	-9.61	-0.029
Cd		4.45E-09				
	Cd+2	4.30E-09	3.28E-09	-8.366	-8.484	-0.117
	Cu(2)	4.72E-08				
	CuCO3	3.39E-08	3.39E-08	-7.47	-7.47	0
Cu+2		1.07E-08	8.16E-09	-7.971	-8.088	-0.117
	CuOH+	1.66E-09	1.55E-09	-8.781	-8.81	-0.029
	CuHCO3+	5.90E-10	5.48E-10	-9.229	-9.261	-0.032
	CuSO4	2.05E-10	2.05E-10	-9.688	-9.688	0
	Cu(OH)2	1.04E-10	1.04E-10	-9.983	-9.983	0
Fe(3)		3.03E-06				
	Fe(OH)2+	2.99E-06	2.80E-06	-5.525	-5.554	-0.029
	Fe(OH)3	3.50E-08	3.50E-08	-7.455	-7.455	0
	Fe(OH)4-	6.04E-09	5.65E-09	-8.219	-8.248	-0.029
K		1.78E-05				
	K+	1.77E-05	1.66E-05	-4.751	-4.78	-0.029
	KSO4-	1.54E-08	1.44E-08	-7.813	-7.842	-0.029

				Log	Log	Log
	Species	Molality	Activity	Molality	Activity	Gamma
Mg		1.29E-03				
	Mg+2	1.26E-03	9.60E-04	-2.9	-3.018	-0.117
	MgSO4	2.06E-05	2.06E-05	-4.687	-4.687	0
	MgHCO3+	1.45E-05	1.35E-05	-4.84	-4.869	-0.029
	MgCO3	4.22E-07	4.22E-07	-6.375	-6.375	0
	MgHPO4	8.39E-08	8.39E-08	-7.076	-7.076	0
	MgOH+	1.13E-08	1.06E-08	-7.946	-7.974	-0.028
	MgH2PO4+	7.97E-09	7.46E-09	-8.099	-8.127	-0.029
Mn(2)		5.72E-06				
	Mn+2	5.52E-06	4.11E-06	-5.258	-5.386	-0.128
	MnHCO3+	1.21E-07	1.13E-07	-6.919	-6.948	-0.029
	MnSO4	8.02E-08	8.02E-08	-7.096	-7.096	0
	MnOH+	4.09E-10	3.83E-10	-9.388	-9.417	-0.029
Na		4.26E-05				
	Na+	4.26E-05	3.98E-05	-4.371	-4.4	-0.029
	NaHCO3	4.72E-08	4.72E-08	-7.327	-7.327	0
	NaSO4-	3.01E-08	2.82E-08	-7.521	-7.549	-0.029
	NaCO3-	9.11E-10	8.53E-10	-9.04	-9.069	-0.029
O(0)		4.94E-04				
	O2	2.47E-04	2.47E-04	-3.607	-3.607	0
P		5.81E-07				
	HPO4-2	2.41E-07	1.85E-07	-6.617	-6.733	-0.115
	H2PO4-	2.37E-07	2.22E-07	-6.625	-6.653	-0.029
	MgHPO4	8.39E-08	8.39E-08	-7.076	-7.076	0
	CaHPO4	9.59E-09	9.59E-09	-8.018	-8.018	0
	MgH2PO4+	7.97E-09	7.46E-09	-8.099	-8.127	-0.029
	CaH2PO4+	6.02E-10	5.64E-10	-9.22	-9.249	-0.029
	CaPO4-	2.62E-10	2.45E-10	-9.582	-9.61	-0.029
Pb		2.41E-09				
	PbCO3	1.08E-09	1.08E-09	-8.967	-8.967	0
	Pb+2	6.67E-10	5.09E-10	-9.176	-9.293	-0.117
	PbHCO3+	4.34E-10	4.03E-10	-9.363	-9.395	-0.032
	PbOH+	1.96E-10	1.82E-10	-9.708	-9.74	-0.032
S(6)		2.02E-04				
	SO4-2	1.77E-04	1.35E-04	-3.751	-3.869	-0.117
	MgSO4	2.06E-05	2.06E-05	-4.687	-4.687	0
	CaSO4	3.95E-06	3.95E-06	-5.403	-5.403	0
	MnSO4	8.02E-08	8.02E-08	-7.096	-7.096	0
	NaSO4-	3.01E-08	2.82E-08	-7.521	-7.549	-0.029
	KSO4-	1.54E-08	1.44E-08	-7.813	-7.842	-0.029
	ZnSO4	6.88E-09	6.88E-09	-8.162	-8.162	0
	SrSO4	3.21E-09	3.21E-09	-8.494	-8.494	0
	HSO4-	5.89E-10	5.51E-10	-9.23	-9.259	-0.029
	CuSO4	2.05E-10	2.05E-10	-9.688	-9.688	0
Si		3.19E-05				
	H4SiO4	3.19E-05	3.19E-05	-4.496	-4.496	0
	H3SiO4-	4.31E-08	4.03E-08	-7.366	-7.395	-0.029
Sr		1.94E-07				
	Sr+2	1.89E-07	1.44E-07	-6.724	-6.842	-0.117
	SrSO4	3.21E-09	3.21E-09	-8.494	-8.494	0
	SrHCO3+	2.07E-09	1.94E-09	-8.685	-8.713	-0.028
Zn		3.82E-07				
	Zn+2	3.54E-07	2.70E-07	-6.451	-6.569	-0.117
	ZnCO3	1.10E-08	1.10E-08	-7.96	-7.96	0
	ZnHCO3+	9.78E-09	9.09E-09	-8.009	-8.041	-0.032
	ZnSO4	6.88E-09	6.88E-09	-8.162	-8.162	0
	ZnOH+	1.08E-09	1.00E-09	-8.968	-9	-0.032

	Species	Molality	Activity	Log Molality	Log Activity	Log Gamma
	OH-	1.07E-06	1.02E-06	-5.97	-5.991	-0.022
	H+	3.56E-09	3.39E-09	-8.448	-8.47	-0.021
	H2O	5.55E+01	1.00E+00	1.744	0	0
Al		2.89E-07				
	Al(OH)4-	2.70E-07	2.57E-07	-6.569	-6.59	-0.021
	Al(OH)3	1.89E-08	1.89E-08	-7.723	-7.723	0
	As(5)	1.27E-08				
	HAsO4-2	1.23E-08	9.99E-09	-7.909	-8	-0.091
B		5.46E-07				
	H3BO3	4.77E-07	4.78E-07	-6.321	-6.321	0
	H2BO3-	6.71E-08	6.38E-08	-7.173	-7.195	-0.022
C(4)		1.46E-03				
	HCO3-	1.41E-03	1.35E-03	-2.85	-2.871	-0.021
	CO3-2	1.71E-05	1.41E-05	-4.766	-4.852	-0.086
	H2CO3	1.22E-05	1.22E-05	-4.913	-4.913	0
	CaHCO3+	4.40E-06	4.19E-06	-5.357	-5.378	-0.021
	CaCO3	4.02E-06	4.02E-06	-5.395	-5.395	0
	MgHCO3+	3.34E-06	3.18E-06	-5.477	-5.498	-0.021
	MgCO3	2.32E-06	2.32E-06	-5.636	-5.636	0
	NaHCO3	1.64E-07	1.64E-07	-6.785	-6.785	0
	NaCO3-	6.76E-08	6.44E-08	-7.17	-7.191	-0.021
	ZnCO3	6.20E-08	6.20E-08	-7.207	-7.207	0
	SrHCO3+	1.75E-08	1.67E-08	-7.757	-7.778	-0.021
	CuCO3	1.32E-08	1.32E-08	-7.879	-7.879	0
	SrCO3	7.64E-09	7.64E-09	-8.117	-8.117	0
	ZnHCO3+	2.60E-09	2.47E-09	-8.585	-8.608	-0.023
	MnHCO3+	2.49E-09	2.37E-09	-8.604	-8.625	-0.021
	PbCO3	1.86E-09	1.86E-09	-8.731	-8.731	0
Ca		3.08E-04				
	Ca+2	2.99E-04	2.45E-04	-3.525	-3.61	-0.086
	CaHCO3+	4.40E-06	4.19E-06	-5.357	-5.378	-0.021
	CaCO3	4.02E-06	4.02E-06	-5.395	-5.395	0
	CaSO4	5.80E-07	5.80E-07	-6.236	-6.236	0
	CaHPO4	3.96E-08	3.96E-08	-7.402	-7.402	0
	CaPO4-	2.40E-08	2.29E-08	-7.619	-7.64	-0.021
	CaOH+	4.47E-09	4.26E-09	-8.35	-8.371	-0.021
Cd		4.45E-09				
	Cd+2	3.48E-09	2.86E-09	-8.458	-8.544	-0.086
	Cu(2)	1.57E-08				
	CuCO3	1.32E-08	1.32E-08	-7.879	-7.879	0
	Fe(3)	3.10E-06				
	Fe(OH)2+	1.35E-06	1.28E-06	-5.871	-5.892	-0.021
	Fe(OH)4-	1.19E-06	1.13E-06	-5.926	-5.947	-0.021
	Fe(OH)3	5.61E-07	5.61E-07	-6.251	-6.251	0
K		2.72E-05				
	K+	2.72E-05	2.59E-05	-4.566	-4.587	-0.021
	KSO4-	2.10E-09	2.00E-09	-8.677	-8.698	-0.021

	Species	Molality	Activity	Log Molality	Log Activity	Log Gamma
Mg		3.10E-04				
	Mg+2	3.04E-04	2.49E-04	-3.518	-3.604	-0.086
	MgHCO3+	3.34E-06	3.18E-06	-5.477	-5.498	-0.021
	MgCO3	2.32E-06	2.32E-06	-5.636	-5.636	0
	MgSO4	4.80E-07	4.80E-07	-6.319	-6.319	0
	MgOH+	8.44E-08	8.04E-08	-7.074	-7.095	-0.021
	MgHPO4	5.55E-08	5.55E-08	-7.255	-7.255	0
Mn(2)		1.21E-07				
	Mn+2	1.18E-07	9.54E-08	-6.929	-7.02	-0.091
	MnHCO3+	2.49E-09	2.37E-09	-8.604	-8.625	-0.021
Mn(7)		8.68E-09				
	MnO4-	8.68E-09	8.25E-09	-8.062	-8.084	-0.022
Na		1.75E-04				
	Na+	1.75E-04	1.67E-04	-3.757	-3.778	-0.021
	NaHCO3	1.64E-07	1.64E-07	-6.785	-6.785	0
	NaCO3-	6.76E-08	6.44E-08	-7.17	-7.191	-0.021
	NaSO4-	1.09E-08	1.04E-08	-7.962	-7.983	-0.021
O(0)		6.84E-04				
	O2	3.42E-04	3.42E-04	-3.466	-3.466	0
P		6.88E-07				
	HPO4-2	5.40E-07	4.45E-07	-6.267	-6.352	-0.085
	MgHPO4	5.55E-08	5.55E-08	-7.255	-7.255	0
	CaHPO4	3.96E-08	3.96E-08	-7.402	-7.402	0
	H2PO4-	2.65E-08	2.52E-08	-7.578	-7.599	-0.021
	CaPO4-	2.40E-08	2.29E-08	-7.619	-7.64	-0.021
Pb		2.41E-09				
	PbCO3	1.86E-09	1.86E-09	-8.731	-8.731	0
S(6)		1.55E-05				
	SO4-2	1.44E-05	1.18E-05	-4.841	-4.927	-0.086
	CaSO4	5.80E-07	5.80E-07	-6.236	-6.236	0
	MgSO4	4.80E-07	4.80E-07	-6.319	-6.319	0
	NaSO4-	1.09E-08	1.04E-08	-7.962	-7.983	-0.021
	SrSO4	2.50E-09	2.50E-09	-8.602	-8.602	0
	KSO4-	2.10E-09	2.00E-09	-8.677	-8.698	-0.021
Si		8.43E-05				
	H4SiO4	8.18E-05	8.19E-05	-4.087	-4.087	0
	H3SiO4-	2.50E-06	2.38E-06	-5.602	-5.624	-0.021
Sr		1.53E-06				
	Sr+2	1.50E-06	1.23E-06	-5.823	-5.909	-0.086
	SrHCO3+	1.75E-08	1.67E-08	-7.757	-7.778	-0.021
	SrCO3	7.64E-09	7.64E-09	-8.117	-8.117	0
	SrSO4	2.50E-09	2.50E-09	-8.602	-8.602	0
Zn		1.77E-07				
	Zn+2	9.35E-08	7.67E-08	-7.029	-7.115	-0.086
	ZnCO3	6.20E-08	6.20E-08	-7.207	-7.207	0
	Zn(OH)2	1.07E-08	1.07E-08	-7.97	-7.97	0
	ZnOH+	8.25E-09	7.83E-09	-8.084	-8.106	-0.023
	ZnHCO3+	2.60E-09	2.47E-09	-8.585	-8.608	-0.023

	Species	Molality	Activity	Log Molality	Log Activity	Log Gamma
	OH-	1.28E-06	1.19E-06	-5.893	-5.925	-0.032
	H+	2.79E-09	2.59E-09	-8.554	-8.586	-0.032
	H2O	5.55E+01	1.00E+00	1.744	0	0
Al		2.07E-07				
	Al(OH)4-	1.92E-07	1.79E-07	-6.716	-6.748	-0.031
	Al(OH)3	1.45E-08	1.45E-08	-7.84	-7.84	0
	Al(OH)2+	2.01E-10	1.87E-10	-9.698	-9.729	-0.031
	As(5)	3.05E-08				
	HAsO4-2	2.99E-08	2.17E-08	-7.525	-7.663	-0.139
	H2AsO4-	5.93E-10	5.47E-10	-9.227	-9.262	-0.035
B		4.43E-07				
	H3BO3	3.72E-07	3.72E-07	-6.43	-6.429	0
	H2BO3-	6.82E-08	6.32E-08	-7.166	-7.199	-0.033
	MgH2BO3+	1.94E-09	1.80E-09	-8.712	-8.745	-0.033
	CaH2BO3+	1.34E-09	1.25E-09	-8.872	-8.904	-0.033
		2.59E-03				
	HCO3-	2.47E-03	2.30E-03	-2.607	-2.638	-0.031
	CO3-2	4.09E-05	3.05E-05	-4.388	-4.515	-0.127
	MgHCO3+	1.91E-05	1.78E-05	-4.718	-4.75	-0.032
	H2CO3	1.63E-05	1.63E-05	-4.787	-4.787	0
	MgCO3	1.62E-05	1.62E-05	-4.791	-4.791	0
	CaCO3	1.29E-05	1.29E-05	-4.891	-4.891	0
	CaHCO3+	1.12E-05	1.05E-05	-4.95	-4.98	-0.031
	NaHCO3	3.90E-07	3.90E-07	-6.41	-6.41	0
	NaCO3-	2.11E-07	1.97E-07	-6.675	-6.706	-0.031
	ZnCO3	1.42E-07	1.42E-07	-6.848	-6.848	0
	SrHCO3+	5.89E-08	5.49E-08	-7.23	-7.26	-0.031
	MnHCO3+	5.71E-08	5.32E-08	-7.243	-7.274	-0.031
	SrCO3	3.22E-08	3.22E-08	-7.492	-7.492	0
	CuCO3	1.85E-08	1.85E-08	-7.733	-7.733	0
Ca	ZnHCO3+	4.68E-09	4.32E-09	-8.33	-8.365	-0.035
	Cu(CO3)2-2	2.09E-09	1.52E-09	-8.679	-8.818	-0.139
	PbCO3	1.89E-09	1.89E-09	-8.724	-8.724	0
	CdCO3	1.49E-09	1.49E-09	-8.828	-8.828	0
	Pb(CO3)2-2	2.29E-10	1.66E-10	-9.641	-9.779	-0.139
Ca		5.28E-04				
	Ca+2	4.99E-04	3.73E-04	-3.302	-3.428	-0.127
	CaCO3	1.29E-05	1.29E-05	-4.891	-4.891	0
	CaHCO3+	1.12E-05	1.05E-05	-4.95	-4.98	-0.031
	CaSO4	4.10E-06	4.10E-06	-5.387	-5.387	0
	CaHPO4	4.79E-08	4.79E-08	-7.32	-7.32	0
	CaPO4-	3.76E-08	3.50E-08	-7.425	-7.456	-0.031
	CaOH+	7.95E-09	7.41E-09	-8.1	-8.13	-0.031
	CaH2BO3+	1.34E-09	1.25E-09	-8.872	-8.904	-0.033
	CaH2PO4+	1.10E-10	1.02E-10	-9.959	-9.99	-0.031
Cd		4.45E-09				
	Cd+2	2.86E-09	2.14E-09	-8.544	-8.67	-0.127
	CdCO3	1.49E-09	1.49E-09	-8.828	-8.828	0
	Cu(2)	2.24E-08				
	CuCO3	1.85E-08	1.85E-08	-7.733	-7.733	0
	Cu(CO3)2-2	2.09E-09	1.52E-09	-8.679	-8.818	-0.139
	Cu(OH)2	9.77E-10	9.77E-10	-9.01	-9.01	0
	CuOH+	6.35E-10	5.90E-10	-9.197	-9.229	-0.032
	Cu+2	1.38E-10	1.03E-10	-9.861	-9.988	-0.127
Fe(3)		1.94E-05				
	Fe(OH)4-	9.93E-06	9.25E-06	-5.003	-5.034	-0.031
	Fe(OH)2+	6.59E-06	6.14E-06	-5.181	-5.212	-0.031
	Fe(OH)3	2.83E-06	2.83E-06	-5.549	-5.549	0
K		6.46E-05				
	K+	6.46E-05	6.00E-05	-4.19	-4.222	-0.032
	KSO4-	2.33E-08	2.17E-08	-7.632	-7.663	-0.031
	KHPO4-	1.29E-10	1.20E-10	-9.89	-9.92	-0.031

	Species	Molality	Activity	Log Molality	Log Activity	Log Gamma
Mg		1.14E-03				
	Mg+2	1.10E-03	8.21E-04	-2.959	-3.086	-0.127
	MgHCO3+	1.91E-05	1.78E-05	-4.718	-4.75	-0.032
	MgCO3	1.62E-05	1.62E-05	-4.791	-4.791	0
	MgSO4	7.37E-06	7.37E-06	-5.132	-5.132	0
	MgOH+	3.22E-07	3.01E-07	-6.492	-6.522	-0.03
	MgHPO4	1.46E-07	1.46E-07	-6.837	-6.837	0
	MgH2BO3+	1.94E-09	1.80E-09	-8.712	-8.745	-0.033
	MgPO4-	1.29E-09	1.21E-09	-8.888	-8.919	-0.031
	MgH2PO4+	5.07E-10	4.72E-10	-9.295	-9.326	-0.031
Mn(2)		1.80E-06				
	Mn+2	1.73E-06	1.26E-06	-5.761	-5.9	-0.139
	MnHCO3+	5.71E-08	5.32E-08	-7.243	-7.274	-0.031
	MnSO4	1.04E-08	1.04E-08	-7.983	-7.983	0
	MnOH+	4.03E-09	3.75E-09	-8.394	-8.426	-0.031
	Mn(6)	3.48E-10				
	MnO4-2	3.48E-10	2.61E-10	-9.459	-9.583	-0.125
Mn(7)		1.58E-07				
	MnO4-	1.58E-07	1.47E-07	-6.8	-6.833	-0.032
Na		2.42E-04				
	Na+	2.42E-04	2.25E-04	-3.617	-3.649	-0.032
	NaHCO3	3.90E-07	3.90E-07	-6.41	-6.41	0
	NaCO3-	2.11E-07	1.97E-07	-6.675	-6.706	-0.031
	NaSO4-	7.08E-08	6.59E-08	-7.15	-7.181	-0.031
	NaHPO4-	7.47E-10	6.96E-10	-9.126	-9.157	-0.031
	NaH2BO3	2.97E-11	2.97E-11	-10.528	-10.528	0
O(0)		6.62E-04				
	O2	3.31E-04	3.32E-04	-3.48	-3.48	0
P		7.34E-07				
	HPO4-2	4.83E-07	3.63E-07	-6.316	-6.44	-0.125
	MgHPO4	1.46E-07	1.46E-07	-6.837	-6.837	0
	CaHPO4	4.79E-08	4.79E-08	-7.32	-7.32	0
	CaPO4-	3.76E-08	3.50E-08	-7.425	-7.456	-0.031
	H2PO4-	1.70E-08	1.58E-08	-7.77	-7.801	-0.031
	MgPO4-	1.29E-09	1.21E-09	-8.888	-8.919	-0.031
	NaHPO4-	7.47E-10	6.96E-10	-9.126	-9.157	-0.031
	MgH2PO4+	5.07E-10	4.72E-10	-9.295	-9.326	-0.031
	SrHPO4	2.07E-10	2.07E-10	-9.683	-9.683	0
	KHPO4-	1.29E-10	1.20E-10	-9.89	-9.92	-0.031
	CaH2PO4+	1.10E-10	1.02E-10	-9.959	-9.99	-0.031
Pb		2.41E-09				
	PbCO3	1.89E-09	1.89E-09	-8.724	-8.724	0
	Pb(CO3)2-2	2.29E-10	1.66E-10	-9.641	-9.779	-0.139
	PbOH+	2.17E-10	2.00E-10	-9.663	-9.698	-0.035
S(6)		8.63E-05				
	SO4-2	7.47E-05	5.58E-05	-4.126	-4.253	-0.127
	MgSO4	7.37E-06	7.37E-06	-5.132	-5.132	0
	CaSO4	4.10E-06	4.10E-06	-5.387	-5.387	0
	NaSO4-	7.08E-08	6.59E-08	-7.15	-7.181	-0.031
	SrSO4	2.35E-08	2.35E-08	-7.629	-7.629	0
	KSO4-	2.33E-08	2.17E-08	-7.632	-7.663	-0.031
	MnSO4	1.04E-08	1.04E-08	-7.983	-7.983	0
	ZnSO4	8.65E-10	8.65E-10	-9.063	-9.063	0
Si		1.13E-04				
	H4SiO4	1.09E-04	1.09E-04	-3.962	-3.961	0
	H3SiO4-	4.29E-06	3.98E-06	-5.368	-5.4	-0.032
Sr		3.46E-06				
	Sr+2	3.34E-06	2.50E-06	-5.476	-5.603	-0.127
	SrHCO3+	5.89E-08	5.49E-08	-7.23	-7.26	-0.031
	SrCO3	3.22E-08	3.22E-08	-7.492	-7.492	0
	SrSO4	2.35E-08	2.35E-08	-7.629	-7.629	0
	SrHPO4	2.07E-10	2.07E-10	-9.683	-9.683	0
Zn		2.86E-07				
	ZnCO3	1.42E-07	1.42E-07	-6.848	-6.848	0
	Zn+2	1.08E-07	8.08E-08	-6.966	-7.093	-0.127
	Zn(OH)2	1.93E-08	1.93E-08	-7.715	-7.715	0
	ZnOH+	1.04E-08	9.59E-09	-7.984	-8.018	-0.035
	ZnHCO3+	4.68E-09	4.32E-09	-8.33	-8.365	-0.035
	ZnSO4	8.65E-10	8.65E-10	-9.063	-9.063	0
	Zn(OH)3-	4.06E-10	3.75E-10	-9.391	-9.426	-0.035

Appendix H
HFO Surface Composition

[a] HFO surface composition for mix .99 1 and .01 solution 1. Hfo_s shows the species complexed to the strong sites of HFO. Hfo_w shows the species complexed to the weak sites of HFO.

equilibrate 5 # equilibrate with solution number 5
Hfo_w 0.005 600 89
Hfo_s 0.2

Hfo 3.217e-03 Surface charge, eq
5.813e-03 sigma, C/m**2
3.301e-02 psi, V
-1.352e+00 -F*psi/RT
2.586e-01 exp(-F*psi/RT)
6.000e+02 specific area, m**2/g
5.340e+04 m**2 for 8.900e+01 g

Hfo_s 2.000e-01 moles

Species	Moles	Mole Fraction	Molality	Log Molality
Hfo_sOPb+	7.69E-02	0.384	7.69E-02	-1.114
Hfo_sOZn+	6.61E-02	0.331	6.61E-02	-1.18
Hfo_sOHAsO4-3	4.48E-02	0.224	4.48E-02	-1.349
Hfo_sOCu+	6.68E-03	0.033	6.68E-03	-2.175
Hfo_sOHCa+2	1.96E-03	0.01	1.96E-03	-2.709
Hfo_sO-	1.47E-03	0.007	1.47E-03	-2.832
Hfo_sOH	8.40E-04	0.004	8.40E-04	-3.076
Hfo_sPO4-2	7.33E-04	0.004	7.33E-04	-3.135
Hfo_sOCd+	5.28E-04	0.003	5.28E-04	-3.278
Hfo_sHPO4-	2.30E-05	0	2.30E-05	-4.638
Hfo_sOH2+	1.10E-05	0	1.10E-05	-4.959
Hfo_sOHSO4-2	4.32E-06	0	4.32E-06	-5.364
Hfo_sHAsO4-	1.72E-07	0	1.72E-07	-6.766
Hfo_sSO4-	2.83E-08	0	2.83E-08	-7.548
Hfo_sH2PO4	1.23E-08	0	1.23E-08	-7.911
Hfo_sH2BO3	1.30E-09	0	1.30E-09	-8.885
Hfo_sH2AsO4	7.26E-11	0	7.26E-11	-10.139

Hfo_w 5.000e-03 moles

Species	Moles	Mole Fraction	Molality	Log Molality
Hfo_wOHAsO4-3	4.50E-03	0.9	4.50E-03	-2.347
Hfo_wOMg+	1.74E-04	0.035	1.74E-04	-3.76
Hfo_wO-	1.48E-04	0.03	1.48E-04	-3.83
Hfo_wOH	8.45E-05	0.017	8.45E-05	-4.073
Hfo_wPO4-2	7.37E-05	0.015	7.37E-05	-4.132
Hfo_wOZn+	6.96E-06	0.001	6.96E-06	-5.157
Hfo_wOCa+	4.43E-06	0.001	4.43E-06	-5.353
Hfo_wOCu+	3.45E-06	0.001	3.45E-06	-5.463
Hfo_wHPO4-	2.31E-06	0	2.31E-06	-5.636
Hfo_wOH2+	1.11E-06	0	1.11E-06	-5.957
Hfo_wOHSO4-2	4.35E-07	0	4.35E-07	-6.362
Hfo_wOPb+	3.45E-07	0	3.45E-07	-6.462
Hfo_wOCd+	2.26E-08	0	2.26E-08	-7.645
Hfo_wHAsO4-	1.73E-08	0	1.73E-08	-7.763
Hfo_wSO4-	2.85E-09	0	2.85E-09	-8.545
Hfo_wH2PO4	1.23E-09	0	1.23E-09	-8.909
Hfo_wH2BO3	1.31E-10	0	1.31E-10	-9.883
Hfo_wH2AsO4	7.30E-12	0	7.30E-12	-11.137

[b] HFO surface composition for mix .99 1 and .01 solution 2. Hfo_s shows the species complexed to the strong sites of HFO. Hfo_w shows the species complexed to the weak sites of HFO.

equilibrate 4 # equilibrate with solution 4
Hfo_w 0.005 600 89
Hfo_s 0.2

Hfo 2.675e-03 Surface charge, eq
4.833e-03 sigma, C/m**2
4.049e-02 psi, V
-1.651e+00 -F*psi/RT
1.919e-01 exp(-F*psi/RT)
6.000e+02 specific area, m**2/g
5.340e+04 m**2 for 8.900e+01 g

Hfo_s 2.000e-01 moles

Species	Moles	Mole Fraction	Molality	Log Molality
Hfo_sOPb+	1.04E-01	0.521	1.04E-01	-0.982
Hfo_sOHAsO4-3	4.35E-02	0.218	4.35E-02	-1.361
Hfo_sOZn+	3.98E-02	0.199	3.98E-02	-1.4
Hfo_sOCu+	6.59E-03	0.033	6.59E-03	-2.181
Hfo_sPO4-2	1.88E-03	0.009	1.88E-03	-2.725
Hfo_sO-	1.70E-03	0.008	1.70E-03	-2.771
Hfo_sOH	9.39E-04	0.005	9.39E-04	-3.027
Hfo_sOHCa+2	7.92E-04	0.004	7.92E-04	-3.101
Hfo_sOCd+	4.48E-04	0.002	4.48E-04	-3.349
Hfo_sHPO4-	5.73E-05	0	5.73E-05	-4.242
Hfo_sOH2+	1.19E-05	0	1.19E-05	-4.924
Hfo_sOHSO4-2	1.86E-06	0	1.86E-06	-5.731
Hfo_sHAsO4-	1.57E-07	0	1.57E-07	-6.804
Hfo_sH2PO4	2.97E-08	0	2.97E-08	-7.528
Hfo_sSO4-	1.18E-08	0	1.18E-08	-7.927
Hfo_sH2BO3	1.87E-09	0	1.87E-09	-8.728
Hfo_sH2AsO4	6.45E-11	0	6.45E-11	-10.191

Hfo_w 5.000e-03 moles

Species	Moles	Mole Fraction	Molality	Log Molality
Hfo_wOHAsO4-3	4.48E-03	0.897	4.48E-03	-2.348
Hfo_wPO4-2	1.94E-04	0.039	1.94E-04	-3.712
Hfo_wO-	1.75E-04	0.035	1.75E-04	-3.758
Hfo_wOH	9.68E-05	0.019	9.68E-05	-4.014
Hfo_wOMg+	3.43E-05	0.007	3.43E-05	-4.465
Hfo_wHPO4-	5.91E-06	0.001	5.91E-06	-5.229
Hfo_wOZn+	4.30E-06	0.001	4.30E-06	-5.367
Hfo_wOCu+	3.48E-06	0.001	3.48E-06	-5.458
Hfo_wOCa+	1.90E-06	0	1.90E-06	-5.722
Hfo_wOH2+	1.23E-06	0	1.23E-06	-5.911
Hfo_wOPb+	4.80E-07	0	4.80E-07	-6.319
Hfo_wOHSO4-2	1.92E-07	0	1.92E-07	-6.718
Hfo_wOCd+	1.97E-08	0	1.97E-08	-7.706
Hfo_wHAsO4-	1.62E-08	0	1.62E-08	-7.791
Hfo_wH2PO4	3.05E-09	0	3.05E-09	-8.515
Hfo_wSO4-	1.22E-09	0	1.22E-09	-8.914
Hfo_wH2BO3	1.93E-10	0	1.93E-10	-9.715
Hfo_wH2AsO4	6.64E-12	0	6.64E-12	-11.178